The Dissertation Committee for Mark Thomas Harnett certifies that this is the approved version of the following dissertation:

BURST TIMING-DEPENDENT PLASTICITY OF NMDA RECEPTOR-MEDIATED TRANSMISSION IN MIDBRAIN DOPAMINE NEURONS: A PUTATIVE CELLULAR SUBSTRATE FOR REWARD LEARNING

Committee:

Hitoshi Morikawa, Supervisor

Daniel Johnston

R. Adron Harris

Rueben Gonzales

Nace L. Golding

BURST TIMING-DEPENDENT PLASTICITY OF NMDA RECEPTOR-MEDIATED TRANSMISSION IN MIDBRAIN DOPAMINE NEURONS: A PUTATIVE CELLULAR SUBSTRATE FOR REWARD LEARNING

by

Mark Thomas Harnett, B.A.

Dissertation

Presented to the Faculty of the Graduate School of

The University of Texas at Austin

in Partial Fulfillment

of the Requirements

for the Degree of

Doctor of Philosophy

The University of Texas at Austin

August, 2009

Dedication

To my parents

for their constant support, humor, and encouragement in all my endeavors.

Acknowledgements

I must first acknowledge my Ph.D. supervisor: Hitoshi Morikawa, M.D.-Ph.D. Graduate students and their mentors rarely escape conflict, controversy and quarrel; however, I suspect the dialectical process that so characterized our interactions has produced better science and a more intense learning experience than would have occurred had our relationship been more prosaic.

I would also like to thank my thesis committee for guidance, constructive criticism, and gentle nudges in the right direction. Also for their availability in the face of numerous and weighty responsibilities and their ability to see right to the quick of things:

Daniel Johnston, Ph.D.
R. Adron Harris, Ph.D.
Nace L. Golding, Ph.D.
Rueben Gonzales, Ph.D.

I must gratefully acknowledge the experimental contributions to this thesis of my Morikawa lab collaborators Brian Bernier, who performed the flash photolysis recordings to address the roles of PKA and PKC in Aim 1, and Dr. Kee-Chan Ahn, who executed numerous DHPG perfusion experiments in support of the PKA v. PKC story in Aim 1 and carried out all the *in vivo* animal treatment presented in Aim 2. I would also like to thank Dr. Nikolai Dembrow of the Johnston lab for his assistance in creating the 2-photon morphological reconstructions of DA neurons.

The members of the Morikawa lab (past and present) deserve a vast amount of credit both for their scientific assistance in terms of stimulating discussions, refinement of experimental ideas, critically reviewing text, data, and hypotheses, as well as their (almost) infinite patience in putting up with my antics, listening to my ranting and raving, and offering a foil for some of my more bizarre laboratory idiosyncrasies. Thanks in particular go to Guohong "The Destroyer" Cui, Takashi "The Runner" Okamoto, Matt "Tan-Man" Sullivan, Brian "Orca" Bernier, Kee-Chan "Beluga" Ahn, Simona Perra and Leslie "The Ballerina" Ramsey.

I would also like to thank Professors Jon Mihic and Rick Aldrich for being so extremely collegial and supportive during my Ph.D. They were available when I needed them and were always helpful, encouraging, and insightful (though in very different ways).

I am indebted to members of the Johnston laboratory for listening to my crazy ideas, reviewing manuscripts, giving me advice, loaning me reagents, troubleshooting, supplying me with great experimental and technical ideas, and providing a fantastic resource for electrophysiology of the highest quality right across the street. I would in particular like to thank Drs. Rishi Narayanan, Nikolai "Molly" Dembrow, Randy Chitwood, Darren Brager and Rick Gray for all their help over the past few years.

Dr. Michael Roberts, formerly a graduate student in Jon Mihic's lab, now a postdoc with my former undergraduate thesis advisor Larry Trussell, also deserves significant recognition for his support over the years: reading manuscripts, reviewing posters and abstracts, helping me to sharpen experimental concepts and design, sharing ideas, listening to the tremendous amount of verbiage (some good, most bad) that accompanies a Ph.D., and generally being an excellent scientific colleague. His calm, grace, and focus while doing science is something I wish I could better emulate. Thanks Michael.

I must also acknowledge my numerous previous mentors; the PIs who took me in to their labs and taught me the basics of day-to-day science and gave me my first tastes of a research life before coming to grad school. Professor Thomas F. J. Martin at the University of Wisconsin Madison took a gamble on an inexperienced summer undergraduate intern for which I will be forever grateful. Professor Laurence O. Trussell at Oregon Health & Science University upped the ante by taking an only slightly more experienced undergraduate into his lab for a whole year's senior thesis project. Larry introduced me to patch-clamping, kindling my obsession, and though it may pain me slightly to say, was right, and continues to be right, about everything (shamelessly brilliant punning aside). Professor Stephen M. Smith at Oregon Health & Science University rescued me when I was a failing post-baccalaureate researcher in Minnesota and reinvigorated my love for electrophysiology with a heady concoction of browbeating, beer and Britishisms. Steve deserves a great deal of thanks for teaching me just how fantastically exciting science can be, for all his support over the years, and for being a great friend and colleague (despite his infuriating inability to speak English properly).

I would be remiss if I did not acknowledge the very generous financial support that made this thesis work possible. The National Science Foundation's Graduate Research Fellowship Program funded me for three years. The Waggoner Center for Alcohol and Addiction Research's Bruce & Jones Fellowship also contributed significantly to my support, as did a UT Institute for Neuroscience Fellowship and the UT School of Biological Science's Continuing Fellowship. I am very grateful for their munificence.

Finally, and most importantly, I would like to thank my partner Grace Mitchell.

BURST TIMING-DEPENDENT PLASTICITY OF NMDA RECEPTOR-MEDIATED TRANSMISSION IN MIDBRAIN DOPAMINE NEURONS: A PUTATIVE CELLULAR SUBSTRATE FOR REWARD LEARNING

Publication No._____

Mark Thomas Harnett, Ph.D.

The University of Texas at Austin, 2009

Supervisor: Hitoshi Morikawa

The neurotransmitter dopamine (DA) represents a neural substrate for positive motivation as its spatiotemporal distribution across the brain is responsible for goal-directed behavior and learning reward associations. The critical determinant of DA release throughout the brain is the firing pattern of DA-producing neurons. Synchronized bursts of spikes can be triggered by sensory stimuli in these neurons, evoking phasic release of DA in target brain areas to drive reward-based reinforcement learning and behavior. These bursts are generated by NMDA-type glutamate receptors (NMDARs). This dissertation reports a novel form of long-term potentiation (LTP) of NMDAR-mediated excitatory transmission at DA neurons as a putative cellular substrate for changes in DA neuron firing during reward learning.

Patch-clamp electrophysiological recording from DA neurons in acute brain slices from young adult rats demonstrated that synaptic NMDARs exhibit LTP in an associative

manner, requiring coordinated pre- and postsynaptic burst firing. Ca^{2+} signals produced by postsynaptic burst firing needed to be amplified by preceding metabotropic neurotransmitter inputs to effectively drive plasticity. Activation of NMDARs themselves was also necessary. These two coincidence detectors governed the timing-dependence of NMDAR plasticity in a manner analogous to the timing rule for cue-reward learning paradigms in behaving animals. Further mechanistic study revealed that PKA, but not PKC, activity gated LTP induction by regulating the magnitude of Ca^{2+} signal amplification via the inositol 1,4,5-triphospate (IP_3) receptor and release of Ca^{2+} from intracellular stores. Plasticity of NMDARs was input specific and appeared to be expressed postsynaptically, but was not associated with a change in NMDAR subunit stoichiometry. LTP of NDMARs was DA-independent, and was specific for NMDARs: the same induction protocol produced long-term depression of AMPA receptors. NMDARs that had undergone LTP could be depotentiated in a spike-conditional manner, consistent with active unlearning. Finally, repeated, *in vivo* amphetamine experience dramatically increased facilitation of spike-evoked Ca^{2+} signals, which in turn drove enhanced plasticity.

NMDAR plasticity thus represents a potential neural substrate for conditioned DA neuron burst responses to environmental stimuli acquired during reward-based learning as well a novel therapeutic target for intervention-based therapy of addictive disorders.

Table of Contents

List of Tables

List of Figures

CHAPTER 1: INTRODUCTION

The appropriate association between environmental cues and motivational valence is crucial for the brain to accurately guide behavior. Dopamine (DA) neurons located in the substantia nigra pars compacta (SNc) and ventral tegmental area (VTA) of the midbrain are thought to assign positive values to objects and experiences in order to effectively influence decision-making strategies (Dayan and Niv, 2008; Doya, 2008; Floresco et al., 2008; Montague, 2007; Montague and Berns, 2002; Montague et al., 2004; Montague et al., 2006; Niv et al., 2006; Rangel et al., 2008; Roesch et al., 2007; St Onge and Floresco, 2009). *In vivo* electrophysiological experiments in humans, non-human primates, and rodents, coupled with human functional imaging and computational modeling studies, have suggested that this occurs through changes in DA neuron firing rate, which encode reward prediction errors (D'Ardenne et al., 2008; Montague et al., 1996; Montague et al., 2004; Morris et al., 2004; Nakahara et al., 2004; Pan et al., 2005; Roesch et al., 2007; Schultz, 1998; Schultz et al., 1997; Zaghloul et al., 2009). As such, DA neurons transition from tonic single-spike firing (1-5 Hz) to burst firing (2-10 spikes at 10-50 Hz) in response to the unexpected presentation of primary rewards. Intriguingly, the burst response shifts in time to respond to environmental cues that reliably predict reward delivery after repeated cue-reward pairing. The locus of neural plasticity responsible for this conditioned DA neuron response is unknown.

Release of phasic DA in target areas of the striatum, prefrontal cortex, and/or other structures in response to burst firing influences synaptic integration, plasticity, and network output (Bao et al., 2001; Costa, 2007; Floresco and Magyar, 2006; Gonzalez-Islas and Hablitz, 2003; Gurden et al., 1999; Hassani et al., 2001; Ito et al., 2002; Nicola et al., 2000; Otani et al., 1998; Otani et al., 2003; Reynolds et al., 2001; Reynolds and Wickens, 2000, 2002; Sawaguchi and Goldman-Rakic, 1991; Schultz, 2006; Vijayraghavan et al., 2007; Wang et al., 2004; Wickens et al., 2007). These structures either directly or indirectly feedback onto DA neurons, and thus represent a putative substrate for the plasticity associated with DA neuron activity during learning. However,

plasticity of synaptic transmission and/or intrinsic excitability (*i.e.* ion channels) at DA neurons themselves has recently emerged as a candidate mechanism for changes in DA neuron responsiveness (Bonci and Malenka, 1999; Liu et al., 2005; Mameli et al., 2007; Nugent et al., 2007; Thomas and Malenka, 2003; Thomas et al., 2000). A compelling argument in support of this hypothesis comes from the study of drug addiction. All addictive drugs elevate DA in target regions (Di Chiara and Imperato, 1988), either through changes in terminal efflux or changes in DA neuron firing. More recent neurobiological evidence shows that drug experience either drives or influences various forms of cellular plasticity at DA neurons (Bellone and Luscher, 2006; Berke and Hyman, 2000; Borgland et al., 2006; Engblom et al., 2008; Hyman, 2005; Hyman et al., 2006; Jones and Bonci, 2005; Jones et al., 2000; Kauer and Malenka, 2007; Liu et al., 2005; Saal et al., 2003; Schilstrom et al., 2006; Thomas et al., 2001; Ungless et al., 2001; Zweifel et al., 2008). AMPA-type glutamate receptors, the main arbiters of excitatory synaptic transmission throughout the brain, have received significant attention as a substrate for changes in DA neuron excitability associated with learning and drug experience. However, it is NMDA-type glutamate receptors (NMDARs) that drive the transition from slow, tonic firing to burst firing in DA neurons (Chergui et al., 1994a; Morikawa et al., 2003; Overton and Clark, 1997; Tong et al., 1996a). Thus, potentiation of NMDAR-dependent excitation of DA neurons should preferentially control the development of the conditioned burst response. It is therefore likely that drugs of abuse influence NMDARs, resulting in the profound behavioral alterations that accompany drug abuse, including motivational dysfunction and overlearning of stimuli associated with drug experience. Despite numerous studies describing the plasticity of AMPARs in DA neurons in both naïve and drug-experienced animals (Jones and Bonci, 2005; Kauer and Malenka, 2007), synaptic activity-dependent plasticity of NMDAR-mediated transmission has yet to be demonstrated.

This dissertation investigates the plasticity of NMDARs at DA neurons in acute slices prepared from young adult rats using whole-cell patch-clamp electrophysiology, Ca^{2+} imaging, and electrical synaptic stimulation in a manner designed to mimic the

neural activity that occurs during reward learning in the behaving animal. The data presented here show for the first time NMDARs at DA neurons are plastic in an activity dependent manner consistent with *in vivo* learning rules. This novel form of plasticity exhibits a number of interesting cellular features and represents one of the few instances of burst timing-dependent synaptic plasticity described in the brain. In addition, the induction of this form of plasticity can be altered by repeated *in vivo* amphetamine experience via changes in intracellular Ca^{2+} signaling. These results demonstrate that synaptic plasticity of NMDARs at DA neurons may represent a novel cellular substrate for reward learning that is modulated by drug experience.

This introduction will summarize the theories, hypotheses, and background studies in the fields of reward learning and DA neuron physiology and synaptic plasticity necessary to contextualize the data presented and the interpretations made in this dissertation.

1.1 DA and Reward Learning

1.1.1 WHAT IS THE FUNCTION OF DOPAMINE?

Dopamine was "discovered" as a neurotransmitter in its own right, not a precursor to epinephrine and norepinephrine, in the late 1950s by Arvid Carlsson (Carlsson et al., 1957), see also (Benes, 2001). Since that time, experimental manipulations of DA have been shown to produce profound behavioral changes, yet defining the specific role(s) of DA in brain function has proven remarkably challenging (Berridge, 2006; Redgrave et al., 2008; Schultz, 2007). Anatomical lesion studies, pharmacological intervention, disease-based dysfunction of dopamine systems, exogenous electrical stimulation of dopaminergic pathways, genetic and optical manipulation, and functional brain imaging all implicate DA in positive motivated behavior; that is, appetitive goal-directed movement (as opposed to avoidance of aversive outcomes, which is negative motivated behavior). However, depending on the many details of the experimental paradigms

employed, DA appears to influence and/or control a whole host of neural functions, resulting in no specific set of "DA behaviors" (Schultz, 2007). DA is clearly involved in motor output (shown most dramatically in cases of Parkinson's disease) (Baik et al., 1995; Carlsson et al., 1957; Schultz, 2007; Wickens et al., 2007; Wickens et al., 2003), but it is also a (if not the) major factor in reward learning (Day et al., 2007; Delamater and Oakeshott, 2007; Ljungberg et al., 1992; Mirenowicz and Schultz, 1996; Montague et al., 1996; Morris et al., 2004; Niv et al., 2005; Pan et al., 2005; Reynolds et al., 2001; Roesch et al., 2007; Schultz, 1998, 2002; Waelti et al., 2001; Wise, 2004; Zweifel et al., 2009) and addiction (Berke and Hyman, 2000; Everitt and Robbins, 2005; Hyman, 2005; Hyman et al., 2006a; Kalivas and Volkow, 2005; Melis et al., 2005; Phillips et al., 2003; Volkow et al., 2009); plays a significant role in habit formation (Costa, 2007; Everitt and Robbins, 2005; Ito et al., 2002; Wickens et al., 2007) and the modulation of memory by both novelty and emotional context (Adcock et al., 2006; Amico et al., 2007; Li et al., 2003; Lisman and Grace, 2005; Schott et al., 2006; Shohamy and Wagner, 2008; Wittmann et al., 2005); is critical for working memory (Aleman et al., 2000; Amico et al., 2007; Castner et al., 2000; Sawaguchi and Goldman-Rakic, 1991; Vijayraghavan et al., 2007; Wang et al., 2004; Williams and Goldman-Rakic, 1995); influences cognition, decision making and higher order brain function (Dayan and Niv, 2008; Doya, 2008; Floresco and Magyar, 2006; Floresco et al., 2008; Montague, 2007; Montague and Berns, 2002; Montague et al., 2004; Montague et al., 2006; Niv et al., 2006; Niv et al., 2005; Rangel et al., 2008; St Onge and Floresco, 2009); and is implicated in a wide range of neurological diseases including obsessive compulsive disorder (Denys et al., 2004), attention deficit hyperactivity disorder (Arnsten, 2006a, b; Leo et al., 2003), psychosis, and schizophrenia (Aleman et al., 2000; Guillin et al., 2007; Toda and Abi-Dargham, 2007). The various subtleties and wide-ranging effects of DA in the CNS have so far prevented a single, comprehensive DA theory from unifying these diverse processes.

Recently, one particular function of DA has been the subject of intense investigation, and as such, significant insight has been gained into a neural process that had previously been underappreciated. Through a combination of *in vivo*

electrophysiology in awake, behaving animals, computational modeling, and functional imaging, it has been shown that DA neuron firing, the critical determinant of spatiotemporal DA concentration throughout the brain, is sensitive to environmental reward contingency in a manner consistent with theoretical models of reinforcement-based machine learning. This has significant implications for how the brain interprets its surroundings in order to guide behavior in a way to maximize positive outcomes. In addition, this finding is supported by recent evidence suggesting that drug addiction may represent a disease of reward learning: a computational reinforcement process gone awry (Redish, 2004).

1.1.2 REINFORCEMENT LEARNING

Reinforcement learning was originally developed in the field of machine learning to train artificial systems (computational models) to learn based on their interactions with the environment rather than on an *a priori* instruction set. The theoretical framework was built on the psychological concept of reinforcement first demonstrated experimentally by Ivan Pavlov in the late 19th century and further refined by B. F. Skinner in the middle of the 20th. Reinforcement is the process by which the outcome, either positive or negative, of behavior influences subsequent behavior. Recent neurobiological investigations have begun to address the circuit and cellular substrates of reinforcement, thus providing neural loci for processes that were previously only either abstract psychological concepts or implemented solely in computational models. Thus the concept of reinforcement learning has recently been heavily applied to learning in animals, particularly within a systems-level framework. The effects of reinforcement can be dramatic (as in the case of a foot-shock paired with an operant level press) or subtle (an increase in the rate of response for maze running after a food reward). Learning occurs in both scenarios, and although the neuronal processes underlying the learning are currently under intense scrutiny, they remain unclear.

Reinforcers - those stimuli that alter behavior - can be categorized into two groups: positive and negative. Positive reinforcers are usually rewards and are often

termed appetitive stimuli, while negative reinforcers are usually punishments and are referred to as aversive stimuli. The valence, positive or negative, of a particular stimulus is not static; reinforcers are conditional in that what was once positive may become negative and vice versa. There is no small amount of controversy about the correct nomenclature for these concepts, but for the sake of clarity and brevity this dissertation will assume all rewards are positive reinforcers and appetitive while all punishments are negative reinforcers and aversive. In terms of behavioral consequences, animals tend to repeat behaviors that lead to the delivery of rewards and to eliminate behaviors that result in punishment.

DA has been shown to play a critical role in reward-based reinforcement learning - that is, the learning associated with appetitive stimuli and positive reinforcers (Mirenowicz and Schultz, 1996) (but see (Rosenkranz and Grace, 2002)). The most compelling explanation for how DA influences this process has emerged primarily from the laboratory of Wolfram Schultz and is termed the reward prediction error hypothesis (Contreras-Vidal and Schultz, 1999; Ljungberg et al., 1992; Schultz, 1998, 2006; Waelti et al., 2001). A competing, though not necessarily mutually exclusive, hypothesis, incentive salience, has also been proposed to explain what DA does in the brain (Berridge, 2006; Berridge and Robinson, 1998, 2003; Berridge et al., 2009; Robinson and Berridge, 1993).

1.1.2.1 Reward Prediction

While recording single unit spikes extracellularly in awake, behaving primates, Schultz and colleagues discovered that DA neurons in the midbrain regions of the SNc and VTA robustly and phasically increased their firing rate in response to the presentation of an unexpected reward (in this case a small amount of juice delivered near the mouth through a tube) (Ljungberg et al., 1992). An unexpected reward is one that the animal had no way of accurately predicting and thus cannot expect. Numerous subsequent studies have confirmed this original finding, demonstrating that in awake (and anesthetized) animals, the majority of DA neurons fire in a slow, tonic pattern,

approximately 2-5 Hz. However, when animals are presented with an unexpected reward, a large population of DA neurons (~50 to 80%) transiently increase their firing to 10-50 Hz for 100-500 ms, approximately 2-10 spikes, in what is termed a burst. Interestingly, DA neurons do not respond to neutral sensory cues presented in the same manner as primary rewards (either tones or lights), demonstrating that DA neurons selectively detect primary rewards (though DA do respond to high intensity neutral sensory cues, which will be discussed below). What is even more interesting is that the response pattern of DA neurons can be altered by repetitively pairing a neutral cue with a primary reward at a set time interval. If the cue accurately predicts the delivery of the reward, the DA neurons "learn" to respond with a burst to the reward-predicting cue and stop responding at the time of predicted reward delivery. This process can be forward conditioned, in that a new, earlier cue can be paired with the first reward-predicting cue and subsequent reward delivery, resulting in DA neurons changing their response to burst selectively to the earliest reliable reward predictor, and then not responding to any of the previously learned cues or predicted reward delivery (Schultz, 1998). This indicates that DA neurons, and thus animals themselves, are always "looking" for the earliest reward predicting cues, in order to have the most accurate positive valence map for reference in planning and executing behaviors. In addition, after conditioning animals to a certain cue-reward pairing, omitting the predicted reward causes a transient suppression of DA neuron firing to or near 0 Hz for 100 to 500 ms at exactly the time of predicted, but omitted, reward delivery. Based on these results, Schultz and colleagues posited that DA neuron firing rate coded for error in the animals' internal reward prediction model. Thus, when the reward contingency of the environment is exactly as predicted (according to some undefined internal model), DA neuron firing rate is stable (tonic firing at 1-5 Hz). However, when things are "better than predicted," as when an unexpected reward is presented, DA neurons transiently increased their firing rate. When things are "worse than expected," *i.e.* a reward that is predicted is omitted, DA neurons transiently decrease their firing rate. It is important to note that these contingency changes are only for positive valence events – although it is currently a subject of contention, there is limited

evidence supporting the idea that DA neurons respond to aversive outcomes or their predictors (Brischoux et al., 2009; Mirenowicz and Schultz, 1996; Ungless et al., 2004); they selectively signal changes in reward delivery. Thus "worse than expected," coded by decreases in DA neuron activity, is only in terms of rewards that were omitted or not obtained.

Efficient reward learning is of obvious adaptive value – the more accurate the internal model of environmental reward contingency, the better the decisions about which options to pursue in a complex world, and the higher the chances of survival and reproductive success (Doya, 2008; Floresco et al., 2008; Montague, 2007; Montague and Berns, 2002; Montague et al., 2006; Niv et al., 2006; Rangel et al., 2008; St Onge and Floresco, 2009). Thus, even honeybees express associative reward learning (Hammer, 1997; Hammer and Menzel, 1995), with reinforcement provided by an octopaminergic neuron that operates in a similar manner to that hypothesized for DA neurons in mammals (Hammer, 1993). Single cell analogues for operant reward learning have been described in Aplysia (Lorenzetti et al., 2008), underscoring the importance and prevalence of reward learning.

1.1.2.2 Neural Error Signals and the Temporal Difference Model

Changes in DA neuron population firing rate drive changes in the spatiotemporal distribution of DA in target areas (Aragona et al., 2008; Sombers et al., 2009). It is hypothesized that these changes in DA concentration are read out by downstream brain structures like the striatum and prefrontal cortex and used to update internal reward contingency models to more accurately guide decision-making and action selection in a complex and dynamic environment. One way this may occur is through temporal difference (TD) learning (Brown et al., 1999; Nakahara et al., 2004; Niv et al., 2005; Pan et al., 2005, 2008; Suri and Schultz, 1999), a supervised form of learning by which predictions are refined through an iterative process of comparison between an internal model and immediate experience. The difference between the model and the outcome for each time-step is compared, in an effort to update to a more accurate set of predictions

about the environment. Thus, the fluctuations in postsynaptic DA produced by changes in DA neuron firing rate during reward experience are the error signals exploited by the brain to teach the TD model to alter its predictions about the future appropriately. Under certain conditions, these phasic DA signals in target regions may be sufficient to directly drive behavioral output (Cheer et al., 2007; Phillips et al., 2003; Roitman et al., 2004; Talwar et al., 2002), though it is unclear how much of these effects is a result of learning vs. a direct consequence of DA release.

Changes in DA neuron firing during reward learning and the basic tenets of the TD model have been confirmed by other laboratories in both primates (Morris et al., 2004; Nakahara et al., 2004) and rodents (Pan et al., 2005; Roesch et al., 2007). These results have been extended by fMRI studies that have detected reward prediction error signals in other parts of the brain (McClure et al., 2003; O'Doherty et al., 2003) and recently in the midbrain (D'Ardenne et al., 2008). Finally, *in vivo* single unit recordings in human beings have also detected TD-type error signals at DA neurons, confirming the initial observations of Schultz et al (Zaghloul et al., 2009).

1.1.2.3 The Competing Hypothesis: Incentive Salience

The incentive salience hypothesis seeks to explain the role of DA in the nervous system based on behavioral observations and parses reward into separable components of "liking" vs. "wanting." This hypothesis was developed by Robinson and Berridge after they observed that despite inhibition of DA via a variety of approaches, rats still displayed behavioral measures of "liking" rewards and drugs of abuse (Berridge, 2006; Berridge and Robinson, 1998, 2003; Berridge et al., 2009; Berridge et al., 1989; Robinson and Berridge, 1993, 2000, 2001, 2008). This is in contrast to the overwhelming majority of literature showing that DA inhibition decreased reward. Robinson and Berridge resolved this conflict by suggesting that it is difficult for an animal to express "liking" in the absence of "wanting," as "wanting" seems to mediate the motivational component of reward and is what DA is encoding. This makes it very challenging to experimentally measure "liking," necessitating approaches like measuring

facial expressions in response to administered sucrose after DA inhibition (Berridge et al., 1989). This is one of the weaknesses of this hypothesis; it is particularly hard to measure experimentally, and the assays that have been employed are often difficult to interpret (*i.e.* quantifying rat facial expressions).

A point of support put forward by advocates of this hypothesis is the results from work on dopamine deficient (DD) mice, which have had the tyrosine hydroxylase gene knocked out and are thus unable to synthesize L-dopa, the precusor to DA (Zhou and Palmiter, 1995; Zhou et al., 1995), conducted by Richard Palmiter's group. Though these studies show limited differences between DD mice and controls for "liking" sucrose (Cannon and Palmiter, 2003) and drug-induced conditioned place preference (CPP) (Hnasko et al., 2005), they are again difficult to interpret in light of the fact that this is an extreme transgenic phenotype, which must be kept alive through supplemental L-dopa. As is always the concern with non-conditional, non-specific knockouts, off target or compensatory effects may be more significant than the knockout itself in accounting for experimental results. Indeed, DD mice exhibit CPP in response to cocaine via serotonin (Hnasko et al., 2007).

Further support for the incentive salience hypothesis comes from the unlikely source of the superior colliculus (SC). Using anesthetized animals, Peter Redgrave and colleagues have shown that a direct projection from SC to DA neurons can trigger short-latency, phasic bursts of spikes from DA neurons after disinhibition of SC in response to high-intensity visual stimuli with no presumable valence or predictive power (Comoli et al., 2003; Dommett et al., 2005). Direct electrical stimulation of SC could recapitulate this effect. This result has been used to argue in favor of DA neuron responses not being necessarily selective to reward, but instead sensitive to "biological salience" in that important, significant, surprising, or novel stimuli activate DA neurons, not just rewards and reward contingencies (Redgrave and Gurney, 2006; Redgrave et al., 2008; Redgrave et al., 1999; Ungless, 2004). This idea that DA neurons are not slaves to the reward prediction error model is congruent with studies reporting the effects of novelty on DA signals (Horvitz et al., 1997; Legault and Wise, 2001), as well as the effects of aversive

stimuli on DA neuron activity (Brischoux et al., 2009; Ungless et al., 2004). However, both SC and aversion experiments were all performed in anesthetized rats, and are thus subject to speculation with regards as to how important these processes are in behaving animals.

1.2 Anatomical and Functional Input/Output of DA neurons

1.2.1 CONNECTIVITY OF DA NEURONS

1.2.1.1 Inputs

DA neurons are thought to construct a dynamic representation of reward for objects, events, experiences, or environments. One simple strategy that may contribute to this process is integration of information across a broad range of brain structures including sensory, memory, and internal state processing areas. This is generally consistent with what is known from DA neuron anatomy as they are innervated by glutamatergic projections from the prefrontal cortex (PFC) (Carr and Sesack, 2000; Tong et al., 1996a, b), subthalamic nuclei (STN) (Chergui et al., 1994; Iribe et al., 1999; Kitai et al., 1999; Smith and Grace, 1992), SC (Coizet et al., 2003; Comoli et al., 2003; Dommett et al., 2005; McHaffie et al., 2006) pedunculopontine tegmental nucleus (PPTN, which also includes a cholinergic component) (Kitai et al., 1999; Lodge and Grace, 2006b; Overton and Clark, 1997; Pan and Hyland, 2005), bed nucleus of the stria terminalis (BNST) (Dumont and Williams, 2004; Georges and Aston-Jones, 2001, 2002), amygdala (Han et al., 1997; Lee et al., 2005; Lee et al., 2006),and hippocampus, though this may be through ventral pallidum via an indirect basal ganglia loop (Floresco et al., 2003; Lisman and Grace, 2005; Lodge and Grace, 2006a, 2007, 2008). DA neurons receive strong reciprocal inhibitory feedback from the striatum in addition to GABAergic inhibition from the nearby substantia nigra pars reticulata (Celada et al., 1999; Grace and Bunney, 1979; Tepper et al., 1995) and local interneurons. Activity in the habenula is

also associated with inhibition of DA neurons *in vivo*, which is curious as it is thought to be a glutamatergic region (Hong and Hikosaka, 2008; Matsumoto and Hikosaka, 2007, 2009). Possibly, habenular neurons synapse onto local GABAergic neurons to inhibit DA neurons (Hikosaka et al., 2008). Finally, DA neurons receive serotonergic and hormonal input via the dorsal raphe and hypothalamus, respectively (Aston-Jones et al., 2009; Harris and Aston-Jones, 2006; Harris et al., 2005; Harris et al., 2007; Rodaros et al., 2007; Tagliaferro and Morales, 2008; Wanat et al., 2008; Wang et al., 2007).

1.2.1.2 Outputs

DA neurons have a highly divergent projection pattern: the ~20-40,000 DA neurons in the midbrain of rats innervate almost every one of the ~3-5 million medium spiny neurons in the striatum (Goldman-Rakic et al., 1992; Loizou, 1972; Schultz, 1998; Swanson and Hartman, 1975; Voorn et al., 1988). As well, DA neurons innervate many of the neurons in the PFC, hippocampus, amygdala, and polysensory associational cortices, resulting in a redundancy of the DA signal in various brain regions (Goldman-Rakic et al., 1992; Hyman et al., 2006b; Sawaguchi and Goldman-Rakic, 1991; Schultz, 1998; Smiley et al., 1992; Williams and Goldman-Rakic, 1993; Williams et al., 1992). DA innervation of these areas is often layer- and cell-type specific. DA neurons do not generally send significant projections to primary sensory cortices (Berger et al., 1991) (but see below).

While the basal ganglia, in particular the striatum, and the PFC are considered to be the primary targets of DA neurons, via the mesostriatal and mesocortical pathways, respectively, and appear to be most involved in effecting the behavioral consequences of DA neural activity (Hyman et al., 2006; Schultz, 1998), DA does play an important role in memory encoding in the hippocampus (Adcock et al., 2006; Gasbarri et al., 1996; Hersi et al., 1995; Li et al., 2003; Lisman and Grace, 2005; Wittmann et al., 2005) and amygdala (Bissiere et al., 2003; Everitt et al., 2003; Kroner et al., 2005; Rosenkranz and Grace, 2002). In addition, despite the limited anatomical evidence mentioned above, DA may also play a role in plasticity and/or remodeling in sensory cortex (Bao et al., 2001;

Bao et al., 2003; Gavornik et al., 2009; Shuler and Bear, 2006). The effects of DA in sensory cortex may be similar to those of other neuromodulators that have received more attention (Froemke et al., 2007; Kilgard and Merzenich, 1998).

1.2.1.3 Cellular Morphology of DA Neurons

DA neurons exhibit an atypical morphological profile, particularly when compared with the far more numerous pyramidal neurons of the hippocampus and cortex or medium spiny neurons of the striatum (Figure 1.1) (Lapish et al., 2007; Prensa and Parent, 2001; Tepper et al., 1987). DA neuron cell bodies are generally ovoid in shape and ~20-30 μm in size. From 2 to 6 primary dendrites give rise to a limited set of secondary and tertiary dendrites, the vast majority of which are smooth (*i.e.* lacking spines) and restricted to SNc and VTA, except for 1-2 large dendrites which can reach into substantia nigra pars reticulata (SNr). Dendrites generally project bilaterally from the soma, are usually oriented along the mediolateral axis, and can span over 1 mm. The axons of DA neurons often emerge not from the soma, as in "conventional" neurons, but from either a primary or even secondary dendrite, usually within 50 μm of the soma but in some cases greater than 200 μm distal (Gentet and Williams, 2007; Hausser et al., 1995; Lapish et al., 2007). The functional impact of this dramatic morphological phenotype is unclear; it may operate to "privilege" one set of dendrites over another, in either controlling axonal output or backpropagation through the rest of the arbor (Gentet and Williams, 2007; Vetter et al., 2001). An important note is that the few studies that have addressed single-cell anatomy of DA neurons have focused on SNc – relatively little is known about the cellular morphology of neurons from the VTA.

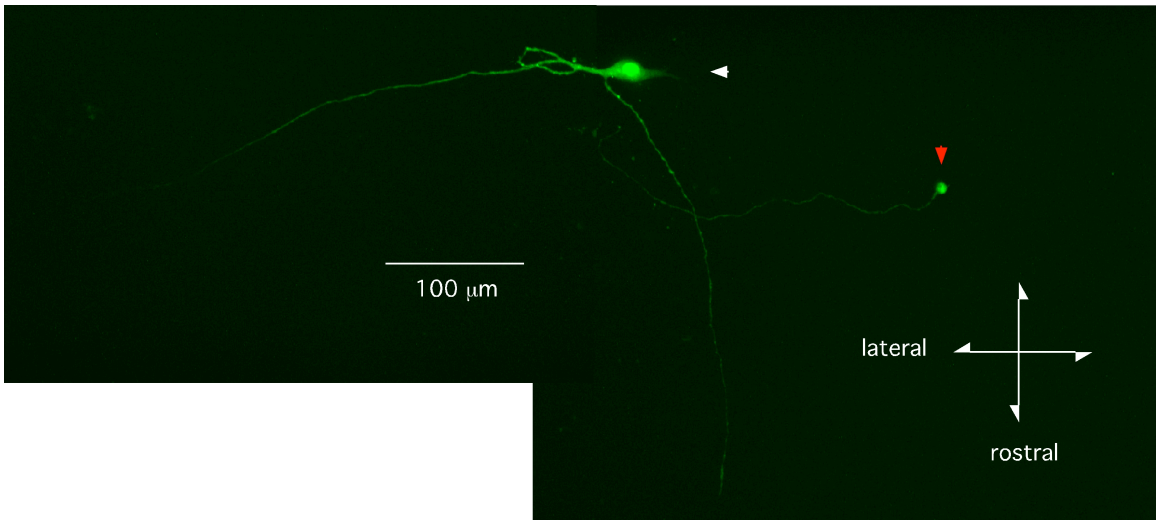

Figure 1.1. Example Morphology of a DA Neuron in the Horizontal Slice. Two-photon laser scanning microscopy image of a rosto-medial SNc DA neuron filled with 80 μM of the morphological dye Alexa594 via the patch pipette. Image is a 2-dimensional maximal intensity projection of 100 1 μm optical z-sections. Only the proximal part of the medial dendritic arbor is visible before it dives into the slice beyond the range of the imaging system (white arrowhead). Below the imaging plane, it gives rise to the axon, which resurfaces before being cut, resulting in a terminal bleb (red arrowhead).

1.2.1.4 Subpopulations

A final point regarding DA neuron anatomy is that recent reports suggest that a variety of subpopulations exist in the SNc and VTA exhibiting specific patterns of innervation and enervation, as well as physiological properties (Fadel and Deutch, 2002; Ford et al., 2006; Ikemoto, 2007; Lammel et al., 2008; Omelchenko and Sesack, 2005, 2006), in addition to the canonical segregation of DA pathways into mesolimbic, mesocortical, and nigrostriatal. There has been almost no morphological comparison across different types of DA neurons in light of the reports of these differences. These results have yet to be integrated into a unified framework for understanding the spatiotemporal regulation of DA release, but a more sophisticated and subtle understanding of DA neuron input and output based on these subpopulations is likely to be forthcoming.

1.2.2 CONTROL OF FIRING IN DA NEURONS

1.2.2.1 An Intrinsic Pacemaker Guides DA Neuron Firing

DA neurons possess an intrinsic pacemaking capability. Even when dissociated in a dish, DA neurons lacking axons and dendrites exhibit robust oscillatory spiking at 1-4 Hz (Cardozo and Bean, 1995; Puopolo et al., 2007). This same oscillation is observed in acute brain slices (Figures 1.2A-C) (Cui et al., 2007; Okamoto et al., 2006) and is thought to underlie the tonic, background firing of DA neurons observed *in vivo* (Grace and Bunney, 1980, 1983a, b, 1984b; Hyland et al., 2002). *In vivo* firing of DA neurons is usually faster and more irregular than that observed *in vitro*, due to interaction of the pacemaker with synaptic input (Brazhnik et al., 2008; Lee et al., 2004; Paladini and Tepper, 1999; Tepper and Lee, 2007; Tepper et al., 1995; Tepper et al., 1998) (Floresco et al., 2003; Grace et al., 2007; Smith and Grace, 1992). Blockade of Na^+ channels with TTX reveals a subthreshold oscillation (Figure 1.2C) mediated by a low voltage-activated isoform of L-type voltage-activated Ca^{2+} channel (VACC)

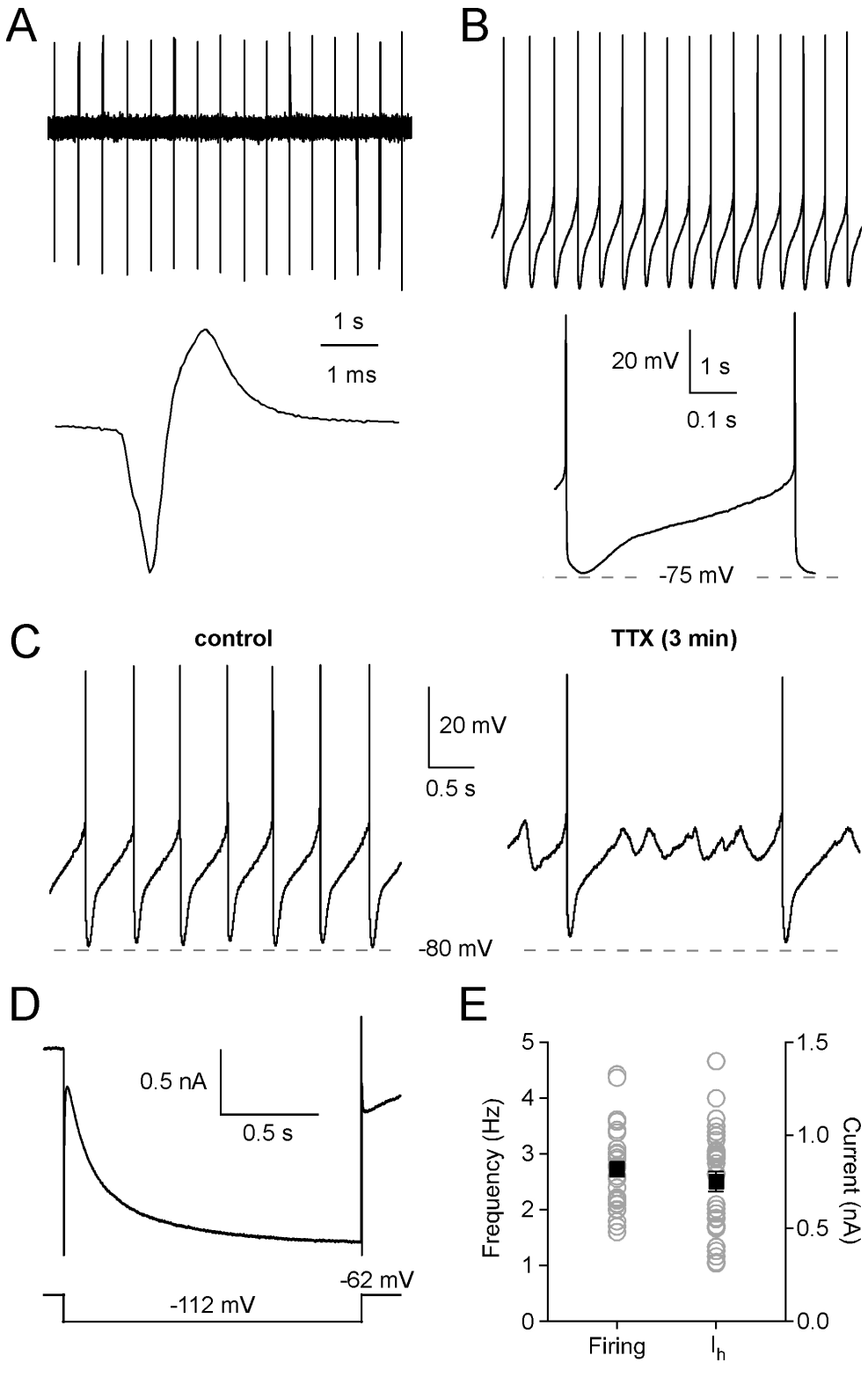
A
1 s
1 ms
B
20 mV
1 s
0.1 s
-75 mV
C
control
TTX (3 min)
20 mV
0.5 s
-80 mV
D
0.5 nA
0.5 s
-62 mV
-112 mV
E
Frequency (Hz)
Current (nA)
Firing
I_h

Figure 1.2. Distinctive physiological features of DA neurons: spontaneous firing and I_h.
(A) Example cell-attached tight-seal recording of spontaneous firing in a DA neuron in voltage-clamp mode (V_c = -55 mV). Inset below shows magnified averaged cell-attached spikes. Note broad AP waveform.
(B) Spontaneous firing in a different neuron recorded in the gramicidin perforated-patch configuration in current-clamp ($I_{injection}$ = 0 pA). Inset below shows expanded waveform. Note the large, slow AHP (which is mediated in large part by SK/$I_{K(Ca)}$) and prolonged subthreshold depolarizing phase.
(C) Partial blockade of Na^+ channels with TTX (50 nM) reveals subthreshold oscillations (right) that lack the characteristic broad and deep AHP associated with pacemaker firing (left).
(D) Representative whole-cell voltage-clamp recording of I_h. Voltage command is shown below.
(E) Distribution of firing frequencies recorded in cell-attached voltage-clamp prior to whole-cell break-in for a set of 30 neurons used for plasticity experiments (left) and maximal I_h current amplitudes for the same set of neurons immediately after break-in (right). Individual neurons are shown as gray circles; black squares represent mean ± SEM.

(Avery and Johnston, 1996; Chan et al., 2007; Durante et al., 2004; Harris et al., 1989; Helton et al., 2005; Lipscombe et al., 2004; Takada et al., 2001; Xu and Lipscombe, 2001). There is recent evidence, however, suggesting that this mechanism is specific to adult SNc DA neurons, whereas VTA and young SNc neurons employ a Ca^{2+}-independent subthreshold oscillation (Chan et al., 2007; Surmeier et al., 2007). HCN channels, the canonical "pacemaking channels" first identified in cardiac cells (Brown and Difrancesco, 1980), are expressed in DA neurons and mediate the I_h conductance gated by hyperpolarization (Figure 1.2D) (Okamoto et al., 2006; Robinson and Siegelbaum, 2003). I_h contributes to bringing the cell back to threshold following activation by the deep and broad afterhyperpolarization (AHP) of the previous spike cycle. A subthreshold, persistent Na^+ current may also contribute to the roles of L-type VACCs and I_h in driving the cell to spike (Puopolo et al., 2007). After the spike, Ca^{2+} influx via VACCs (augmented by Ca^{2+}-induced Ca^{2+} release from internal stores (CICR), see below) gates the opening of small-conductance Ca^{2+}-activated K+ channels (SK), resulting in the prolonged hyperpolarizing trajectory of the AHP, which begins the cycle again.

1.2.2.2 Burst Firing of DA Neurons

DA neurons transition from tonic single-spike firing (1-5 Hz) to phasic burst firing (>10 Hz) in response to primary rewards and reward predicting cues *in vivo*. A DA neuron burst is classically defined as a discrete event initiated by two spikes less than 80 ms apart and terminated by an interspike interval of greater than 160 ms (Grace and Bunney, 1984; Overton and Clark, 1997). Bursts commonly consist of 2-5 spikes, but bursts of up to 23 spikes have been observed in anesthetized animals (Grace and Bunney, 1984). Burst firing dramatically increases release of DA in target areas (Floresco et al., 2003) to drive learning and behavior (Cheer et al., 2007a; Day and Carelli, 2007; Day et al., 2007; Phillips et al., 2003; Redgrave et al., 2008; Roitman et al., 2004; Tsai et al., 2009). This transition in firing mode is gated by the activation of postsynaptic NMDARs and is independent of AMPARs (Chergui et al., 1993; Overton and Clark, 1992; Tong et

al., 1996a; Zweifel et al., 2009). It has been suggested that bursting results from the interaction of pacemaker oscillations with the voltage-dependence of NMDARs due to Mg^{2+} pore block (Kuznetsov et al., 2006; Wilson and Callaway, 2000). In particular, the negative slope conductance of NMDARs is in a range (-60 to -40 mV) where the DA neuron voltage dwells for an extended period of time between spikes. DA neurons also exhibit broad AP waveforms (Figures 1.2A-C) (Cardozo and Bean, 1995; Grace and Bunney, 1980, 1983a, b; Puopolo et al., 2007) which may enhance Mg^{+} unblock of NMDARs during spiking, allowing the increased voltage-dependent synaptic conductance to entrain the neuron to a transient, high firing frequency.

The anatomical source(s) of glutamatergic input activating NMDARs to trigger subsequent bursting are controversial. Previous work has suggested that specific upstream loci mediated bursting including the STN (Chergui et al., 1994a; Smith and Grace, 1992) and PFC (Tong et al., 1996a, b), though recent studies have focused on PPTN (Floresco et al., 2003; Lodge and Grace, 2006a; Lokwan et al., 1999; Zweifel et al., 2009) and SC (Comoli et al., 2003; Dommett et al., 2005; Redgrave and Gurney, 2006; Redgrave et al., 2008; Redgrave et al., 1999). However, it is unlikely that bursting is solely controlled by one of these brain areas, due to the limited nature of their inputs. More likely, different environmental or motor information is conveyed to DA neurons to activate NMDARs through the appropriate upstream circuitry. In addition, these studies were all conducted in anesthetized animals; it remains to be seen how these brain structures, and others, contribute to reward-based bursting in behaving animals.

1.2.2.3 "Information" and "Coding" in DA Neurons

Understanding how information is represented in the brain is one of the overarching goals of neuroscience. Remarkably little is known about what is actually being conveyed by neural activity, let alone how it is processed in the brain, particularly outside of primary sensory systems. Conventional theories posit that within higher order brain regions (*i.e.* cortex and hippocampus) the temporal patterning of spikes is used to convey meaning and content between and across various circuits, but exactly what a

single spike means, or if it means anything at all, is unclear. Timing, down to the order of milliseconds, however, does appear to be important in coding, particularly in the well-studied integrate-and-fire neurons such as pyramidal neurons in the hippocampus and cortex (Borst and Theunissen, 1999; Durstewitz et al., 2000; Fellous et al., 2004; Tiesinga et al., 2008). Appropriate timing of spikes is important for the induction of plasticity (Dan and Poo, 2004), perception and behavior (Houweling and Brecht, 2008; Huber et al., 2008; Voigt et al., 2008), and memory encoding (Dragoi and Buzsaki, 2006; Harris et al., 2003; Wierzynski et al., 2009). In DA neurons, however, what is being coded is reasonably well understood, at least from the reward prediction error hypothesis perspective. Information from DA neurons is read out as changes in the spatiotemporal pattern of DA release in target structures. Therefore, individual spikes and their millisecond-to-millisecond timing are insignificant: as long as tonic dopamine stays within a physiological range, downstream targets are able to perform their tasks (if this level is artificially or pathologically altered, however, performance suffers with considerable behavioral consequences). What does significantly alter the informational content of the downstream DA signal are changes in firing pattern (from tonic firing to bursting or from tonic firing to pausing) (Niv, 2007; Schultz, 2007) and recruitment of larger or smaller assemblies of DA neurons to these firing pattern transitions (Floresco et al., 2003; Grace et al., 2007; Niv et al., 2007). Thus, while timing is extremely important to DA neurons, it is on a much slower scale than conventional model neurons, requiring an altered perspective on the relative importance of action potential output and the postsynaptic strategies employed by DA neurons to regulate cellular information processing.

1.3 Intracellular Ca^{2+} signaling in DA neurons

1.3.1 FACILITATION OF SPIKE-EVOKED CA^{2+} SIGNALS BY INTRACELLULAR STORES

Ca^{2+} signaling, triggered by either postsynaptic spikes or local synaptic events, is critical for the plasticity of synapses throughout the CNS (Linden, 1999; Sjostrom and Nelson, 2002). In DA neurons, spike-evoked Ca^{2+} influx through VACCs can trigger CICR from the endoplasmic reticulum through ryanodine receptors (RyRs) and inositol 1,4,5-triphosphate receptors (IP_3Rs) (Figure 1.3) (Cui et al., 2007). IP_3Rs can also be activated independent of VACCs by PI-coupled receptors. These two processes can synergistically interact to amplify spike-evoked Ca^{2+} signals, as we have shown previously (Cui et al., 2007). After weak, persistent stimulation of PI-coupled receptors has elevated intracellular IP_3 tone, but not enough to trigger significant Ca^{2+} release from stores on its own, spike-evoked, VACC-mediated Ca^{2+} influx is more effective at mobilizing Ca^{2+} release from internal stores due to the supralinear interaction between Ca^{2+} and IP_3 in gating the IP_3R (Berridge, 1995, 1998; Ehrlich et al., 1994; Finch et al., 1991; Mak et al., 1998; Taylor and Laude, 2002). This is similar to a previous report of IP_3R facilitation of spike-evoked Ca^{2+} signals in hippocampal CA1 neurons (Nakamura et al., 1999).

1.3.2 CA^{2+} WAVES IN DA NEURONS

As mentioned above, PI-coupled receptor stimulation can directly activate IP_3Rs through increasing IP_3 via phospholipase C (PLC) even at resting cytosolic Ca^{2+} levels. When PI-coupled receptors are stimulated strongly enough to generate large increases intracellular IP_3, regenerative, propagating waves of Ca^{2+} release from stores are triggered in both DA (Fiorillo and Williams, 1998; Morikawa et al., 2003; Paladini and Williams, 2004) and other neurons (Jaffe and Brown, 1994; Larkum et al., 2003; Nakamura et al., 1999; Watanabe et al., 2006). In DA neurons, the Ca^{2+} wave manifests electrophysiologically as either a slow, SK-mediated outward current in voltage-clamp or

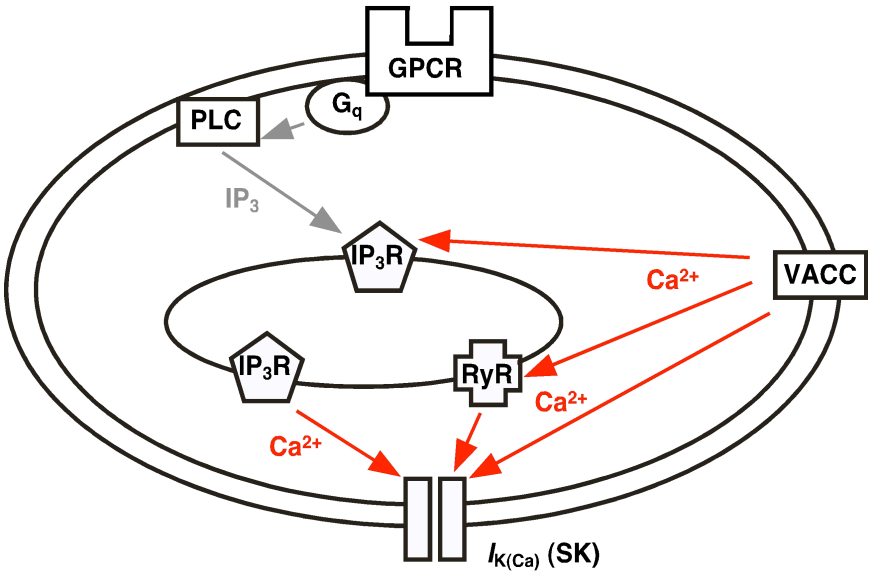

Figure 1.3. Ca^{2+} signaling pathways in DA neurons.
Small conductance Ca^{2+}-activated K^+ channels (SK) are opened directly during spikes via Ca^{2+} influx from voltage-activated Ca^{2+} channels (VACC) and indirectly by Ca^{2+}-induced Ca^{2+} release (CICR) from internal stores via both IP_3 receptors (IP_3R) and ryanodine receptors (RyR), resulting in $I_{K(Ca)}$. The IP_3R-dependent, CICR-mediated component of the spike-evoked Ca^{2+} signal can be modulated by the activity of G_q-coupled metabotropic receptors (GPCR) via phospholipase C (PLC) due to the synergistic interaction between IP_3 and Ca^{2+} at the IP_3R. In addition, strong activation of G_q-coupled receptors can generate enough IP_3 to mobilize Ca^{2+} release from stores in a VACC-independent manner, resulting in a propagating Ca^{2+} wave. Red arrows represent Ca^{2+} pathways while gray arrows indicate other 2nd messenger systems.

a prolonged (0.5-5s), hyperpolarizing pause in spontaneous firing in current clamp (Cui et al., 2007; Morikawa et al., 2000; Morikawa et al., 2003; Paladini et al., 2001).

1.3.3 CA^{2+} STORES AND PLASTICITY

Despite reports demonstrating the importance of IP_3R-mediated release from stores for synaptic plasticity in pyramidal neurons (Raymond and Redman, 2002, 2006), few studies have directly examined the role of either propagating Ca^{2+} waves or facilitation of spike-evoked Ca^{2+} signals by intracellular Ca^{2+} stores in synaptic plasticity outside of the cerebellum (but see (Fernandez de Sevilla et al., 2008)), where the role of IP_3Rs in facilitating complex spike-evoked Ca^{2+} signals for plasticity is well characterized (Augustine et al., 2003; Bosman and Konnerth, 2009; Finch and Augustine, 1998; Hartmann and Konnerth, 2005; Miyata et al., 2000; Wang et al., 2000).

1.4 Cellular Plasticity as a Substrate for Reward Learning

It has been proposed that the cellular locus for the changes in firing observed at DA neurons during reward learning *in vivo* is in the striatum or in the glutamatergic input structures to DA neurons (Hyman et al., 2006; Nicola et al., 2000; Schultz, 1998). In both the striatum and the PFC, DA is released at discrete perisynaptic sites on or near glutamatergic spines where it has been demonstrated to play a critical role in synaptic plasticity (Gurden et al., 1999; Huang et al., 2004; Nicola et al., 2000; Otani et al., 1998; Otani et al., 2003; Reynolds and Wickens, 2000, 2002; Thomas and Malenka, 2003; Thomas et al., 2000). DA release is thought to interact with ongoing sensory-, motor-, and memory-related neural activity to trigger postsynaptic intracellular signaling cascades, teaching the striatum or PFC to learn specific contexts and actions associated with rewarding stimuli. Long-term synaptic and cellular modifications in these structures then result in changes in the network activity of the reward and/or motivational systems that drive behavior.

However, it is also possible that changes in synaptic transmission at DA neurons themselves represent a locus for components of reward learning, particularly in light of the various forms of plasticity at DA neurons recently described (see below). According to this hypothesis, a neutral stimulus (a tone, for example) drives weak glutamatergic input to DA neurons that does not evoke bursting. This subthreshold input to DA neurons is persistent (for 1-5 s), via either continuous presentation of the tone (Schultz, 1998) or sustained neural activity as has been described in the PFC (Constantinidis and Wang, 2004; Durstewitz et al., 2000; Goldman-Rakic, 1995; Wang et al., 2006; Wang, 1999) and entorhinal cortex (Egorov et al., 2002; Fransen et al., 2006). Repetitive pairing of the subthreshold stimulus with a primary reward (which drives bursting via a strong NMDAR activation) correlates the weak input with postsynaptic bursting. Following Hebb's postulate for associativity, this form of classical conditioning should strengthen the weak input, paralleling the many examples of spike-timing dependent plasticity (STDP) described in other neurons (Dan and Poo, 2004; Froemke and Dan, 2002; Wang et al., 2005), though on a slower timescale. As the previously weak synapse is strengthened, the tone eventually drives bursting on its own. Multiple factors suggest that synaptic plasticity induction in DA neurons may operate on slower timescales than classical STDP, in which single excitatory postsynaptic potentials (EPSPs) which reliably precede single postsynaptic APs within ~10-20 ms are potentiated after repetitive pairing of EPSP and AP, while EPSPs that lag postsynaptic spikes within ~50 ms are depressed, as per Hebb's postulate ("cells that fire together, wire together"). First, as mentioned previously, DA neurons are temporally imprecise neurons: their intrinsic pacemaker limits their ability to be correlated with precisely timed input, they fire slowly (1-5 Hz tonic firing, 10-50 Hz bursting) and irregularly enough that individual spikes cannot be used for synchronization or prediction. Additionally, other forms of synaptic plasticity in tonically active neurons are either not highly spike-timing sensitive or spike-timing independent (Bagnall and du Lac, 2006; Coesmans et al., 2004; Nelson et al., 2005; Zhou and Poo, 2004). Finally, this form of plasticity is hypothesized to be expressed at NMDARs (see below), which have significantly slower kinetics than AMPARs and are

voltage-dependent due to pore block by Mg^{2+} at hyperpolarized voltages, requiring time at depolarized voltages to open.

As burst firing of DA neurons has been shown to be NMDAR-dependent and AMPAR-independent (Chergui et al., 1994; Chergui et al., 1993; Overton and Clark, 1992; Tong et al., 1996a; Zweifel et al., 2009), a critical component of this "burst timing-dependent plasticity" hypothesis is that NMDAR-mediated transmission must be plastic.

1.4.1 SYNAPTIC PLASTICITY AT DA NEURONS

1.4.1.1 Plasticity of AMPAR-mediated synaptic transmission

Over the past decade, numerous studies have characterized a variety of forms of classical and experience-dependent synaptic plasticity in midbrain DA neurons (Bellone and Luscher, 2006; Bonci and Malenka, 1999; Chen et al., 2008; Hyman et al., 2006; Kauer, 2004; Liu et al., 2005; Mameli et al., 2007; Pu et al., 2006; Saal et al., 2003; Stuber et al., 2008; Thomas and Malenka, 2003; Ungless et al., 2001). Both conventional LTP and LTD of AMPARs have been described as well as experience-dependent correlates of LTP and LTD after exposure to drugs of abuse, stress, and food conditioning.

1.4.1.2 Limited Significance of AMPAR Plasticity at DA Neurons

Two recent studies have serious implications for the significance of AMPAR plasticity at DA neurons (Tsai et al., 2009; Zweifel et al., 2009). As mentioned above, significant evidence from anesthetized animals has indicated that burst firing, the relevant output for DA neurons in signaling reward, is mediated by NMDARs and not by AMPARs (Chergui et al., 1994; Chergui et al., 1993; Christoffersen and Meltzer, 1995; Overton and Clark, 1992; Tong et al., 1996a). Zweifel and colleagues confirmed this result using a knockout of the obligatory NR1 subunit of the NMDAR expressed only in DA neurons via dopamine reuptake transporter (DAT) (Engblom et al., 2008; Zweifel et al., 2008). When they behaviorally characterized these animals lacking NMDA-mediated

burst firing in DA neurons, the animals exhibited impaired acquisition of conditioned behavioral responses as well as cue learning for predicting appetitive and aversive events. However, a variety of other measures of DA-dependent behaviors were normal.

Furthermore, an even more recent study (Tsai et al., 2009) has demonstrated that burst firing of DA neurons is sufficient for behavioral conditioning by circumventing NMDARs to artificially activate phasic firing with optogenetic techniques in behaving animals. Tsai et al. selectively targeted the light-activated gene channelrhodopsin-2 (ChR2) (Arenkiel et al., 2007; Boyden et al., 2005; Zhang et al., 2006; Zhang et al., 2007) to DA neurons via the tyrosine hydroxylase gene in Cre transgenic animals with local injection of adenoassociated virus. An optical probe was lowered into the midbrain and DA neurons were phasically activated by excitation of ChR2, which was sufficient to induce conditioned place preference in the absence of environmental reinforcers.

Together, these studies suggest that NMDARs at DA neurons are necessary for burst firing which is sufficient for subsequent reward learning. They also significantly diminish the significance of previous results on AMPAR plasticity at DA neurons, which become extremely challenging to interpret in light of the findings by Zweifel et. al. and Tsai et al.

1.4.1.3 Plasticity of $GABA_A$-Mediated Synaptic Transmission

Given the well-characterized role for $GABA_A$ and $GABA_B$ receptors in regulating the firing of DA neurons *in vivo* (Brazhnik et al., 2008; Celada et al., 1999; Erhardt et al., 2002; Tepper and Lee, 2007; Tepper et al., 1995; Tepper et al., 1998) and the hypothesized role of GABAergic feedback during reward learning (Brown et al., 1999; Contreras-Vidal and Schultz, 1999; Houk et al., 1995), the demonstration that GABAergic transmission at DA neurons is also plastic in an experience-dependent manner (Liu et al., 2005; Melis et al., 2002; Nugent et al., 2007) represents a compelling extension of the previous plasticity work at DA neurons. This is reinforced by exciting recent reports showing that lateral habenula, which responds to negative reward and aversive outcomes (reward omission or punishment), inhibits DA neurons, presumably

through GABAergic pathways (Hikosaka et al., 2008; Hong and Hikosaka, 2008; Matsumoto and Hikosaka, 2007, 2009).

1.4.1.4 Agonist-Induced Enhancement of DA Neuron NMDARs

Though the mechanisms driving the forms of plasticity discussed above are not well understood, they demonstrate that synaptic transmission at DA neurons is indeed plastic and that this plasticity is sensitive to environmental modulation (*i.e.* conditioning and/or learning, exposure to drugs of abuse and stressors).

It has also been shown that NMDARs at DA neurons can also exhibit some degree of plasticity, though in these cases it was induced by perfusion or incubation of brain slices with receptor agonists (Argilli et al., 2008; Borgland et al., 2006; Ungless et al., 2003).

1.4.2 PLASTICITY OF NMDARS IN OTHER NEURONS

Though not nearly so common as classical AMPAR plasticity, examples of synaptic plasticity of NMDARs exist and are becoming more prevalent (Carroll and Zukin, 2002)Bashir et al., 1991; Bellone and Nicoll, 2007; Harney et al., 2008; Kwon and Castillo, 2008; Morishita et al., 2005; O'Connor et al., 1994; Rebola et al., 2008; Selig et al., 1995; Sobczyk and Svoboda, 2007; Xie et al., 1992). NMDARs have been shown to be mobile in the postsynaptic membrane (Tovar and Westbrook, 2002) and to change during development in the visual cortex in an experience-dependent manner (Philpot et al., 2001; Quinlan et al., 1999; Snyder et al., 2001). In addition, NMDARs in the dentate gyrus of the hippocampus express mGluR-dependent synaptic plasticity (Harney et al., 2006; O'Connor et al., 1994), both LTP and LTD of NMDARs has been demonstrated in CA1 neurons (Bashir et al., 1991; Morishita et al., 2005; Selig et al., 1995) and CA3 pairs have been shown to express state-dependent LTD of NMDARs (Montgomery and Madison, 2002; Montgomery et al., 2001; Montgomery et al., 2005). More recent studies have explored the mechanistic basis of a postsynaptic form of NMDAR LTP in CA3 neurons, which were previously thought to only express presynaptically-mediated

plasticity (Kwon and Castillo, 2008; Rebola et al., 2008). The majority of these forms of NMDAR plasticity also critically depend on postsynaptic Ca^{2+} concentration.

1.4.3 METAPLASTICITY

The plasticity of NMDARs is of particular interest due to its dominant role in controlling the plasticity of AMPARs as well a variety of ion channels that have been shown to regulate intrinsic excitability (Campanac and Debanne, 2007; Daoudal and Debanne, 2003; Debanne et al., 2003; Johnston and Narayanan, 2008; Narayanan and Johnston, 2007, 2008). Thus, changes in NMDARs should influence the subsequent plasticity of AMPARs (as well as ion channels). A change in the capacity of a neuron to express plasticity is termed "metaplasticity" - the plasticity of plasticity (Abraham, 2008; Abraham and Bear, 1996). For example, in the visual cortex, changes in experience during development can dramatically alter the level and stoichiometry of NMDAR expression in pyramidal neurons (Chen and Bear, 2007; Philpot et al., 2007; Philpot et al., 2003; Philpot et al., 2001; Quinlan et al., 1999). This in turn influences the capacity of AMPARs to undergo and express NMDAR-dependent LTP and LTD. When NMDARs are functionally depressed, only very little AMPAR plasticity can be induced. However, when NMDARs are functionally enhanced, significant AMPAR plasticity can be observed. Other potential loci for metaplasticity in addition to the NMDAR have also been identified (Bellone et al., 2008; Chevaleyre and Castillo, 2004; Edwards et al., 2008; Jung et al., 2008; Pelkey et al., 2008; Thiagarajan et al., 2007; Thiagarajan et al., 2005).

1.5 Hypotheses and specific Aims

NMDARs at DA neurons are critical for burst firing, which drives goal-directed behavior and reward learning. Coincident activation of NMDARs by cue inputs and burst firing at DA neurons may occur during *in vivo* reward learning via two potential mechanisms: 1) continuous presentation of the cue during the task, and 2) persistent

activity of glutamatergic input structures to DA neurons. These processes are not mutually exclusive and may operate in concert. We have recently described a form of supralinear Ca^{2+} signaling in DA neurons: facilitation of spike-evoked Ca^{2+} signals via PI-coupled receptor enhancement of CICR, similar to what has been observed in hippocampus. This process can be recruited by pairing weak, persistent presynaptic stimulation with postsynaptic spikes, reminiscent to the neural activity that may occur *in vivo* during reward learning. As supralinear Ca^{2+} signaling has been shown to drive plasticity in cerebellum, an associative learning structure with historical parallels to DA neurons, we have applied a supralinear Ca^{2+} signaling protocol to drive plasticity of NMDARs in DA neurons. The overall hypothesis of this work is that NMDARs in DA neurons are plastic in an activity dependent manner that exhibits cellular features congruent with a potential cellular substrate for reward based reinforcement learning.

The first specific aim will examine the plasticity of NMDARs at midbrain DA neurons using a protocol designed to mimic cue-reward pairing in behaving animals. The activity of NMDARs will be monitored by recording excitatory postsynaptic currents (EPSCs) evoked by local synaptic stimulation using whole-cell patch-clamp electrophysiology at midbrain DA neurons in acute slices from young adult rats. An *in vitro* pairing protocol designed to simulate *in vivo* reward learning will be applied to individual neurons based on our previous study regarding supralinear Ca^{2+} signaling at DA neurons. The stimulus requirements and cellular mechanisms of plasticity will be explored using physiological and pharmacological techniques as well as Ca^{2+} imaging and flash photolysis of caged compounds.

The second specific aim will address the effects of repeated amphetamine experience on Ca^{2+} signaling and NMDAR plasticity. Two groups of rats will receive once per day intraperitoneal injections of either saline or amphetamine for 7 days. Acute slices will be prepared from treated animals 18-24 hours after final injections. Ca^{2+} signaling and NMDAR plasticity as described in Aim 1 will be compared between neurons from saline- vs. amphetamine-treated animals.

CHAPTER 2: MATERIALS AND METHODS

2.1 Animals and *In Vivo* Drug Treatment

All animal procedures were approved by the University of Texas Institutional Animal Care and Use Committee. Male Sprague-Dawley rats (4-8 weeks old, Harlan Life Sciences) were group housed (2-3 animals per cage) in standard conditions at the University of Texas Animal Resource Center. For Aim 2, 4-5 week old rats were individually removed from their home cage and habituated to handling and a novel cage for 15-20 min once per day for 2-3 days. For injections, animals were removed from their home cage, given single interperitoneal injections with amphetamine (5 mg/kg) or saline (0.9% w/v) once per day for 7 days, and then placed in the habituated environment for 15-20 min before being returned to their home cage. Slices were prepared 18 to 24 hours after the last injection.

2.2 Acute Brain Slice Preparation and Solutions

Animals were deeply anesthetized with halothane and rapidly decapitated. Horizontal midbrain slices (200 μm) were cut with a vibratome (Leica) in ice-cold cutting solution containing (in mM): 205 sucrose, 2.5 KCl, 1.25 NaH_2PO_4, 25 $NaHCO_3$, 0.5 $CaCl_2$, 7.5 $MgCl_2$, and 10 glucose, saturated with 95% O_2/5% CO_2 (~300 mOsm/kg). Slices were incubated at 35ºC for >1 hr in recovery solution containing (in mM): 126 NaCl, 2.5 KCl, 1.2 NaH_2PO_4, 2.4 $MgCl_2$, 2.4 $CaCl_2$, 11 glucose, 21.4 $NaHCO_3$, 1.3 ascorbate, 3 pyruvate, saturated with 95% O_2/5% CO_2 (pH 7.4, ~300 mOsm/kg). Recordings were made at 34-35ºC in a chamber perfused at ~2.5 ml/min with recording solution containing (in mM): 126 NaCl, 2.5 KCl, 1.2 NaH_2PO_4, 1.2 or 0.1 $MgCl_2$, 2.4 $CaCl_2$, 11 glucose, 21.4 $NaHCO_3$, saturated with 95% O_2/5% CO_2 (pH 7.4, ~295

mOsm/kg). The majority of NMDAR plasticity experiments were conducted with a pipette solution containing (in mM): 120 K-gluconate or K-methylsulfate, 20 KCl, 1.5 $MgCl_2$, 10 HEPES, 0.025 EGTA, 2 Mg-ATP, 0.2 Na_2-GTP, and 10 Na_2-phosphocreatine (pH 7.25, 285 mOsm/kg). For experiments in which the internal solution contained BAPTA or Fluo5F (see below), EGTA was omitted. For experiments examining LTP induction in physiological extracellular Mg^{2+} at depolarized voltages 120 mM Cs-methanesulfonate and 20 mM CsCl replaced K-gluconate/K-methylsulfate and KCl, respectively. For conductance analysis, NMDARs were activated by local microiontophoresis of 100 mM NMDA and 10 mM HEPES (pH 7.3) through a high resistance pipette while recording with an internal solution containing (in mM): 115 Cs-methanesulfonate, 20 CsCl, 1.5 $MgCl_2$, 10 HEPES, 5-10 EGTA, 2 Mg-ATP, 0.2 Na_2-GTP, 10 Na_2-phosphocreatine, and 1 QX-222 (pH 7.25, ~285 mOsm/kg). Perforated patch firing experiments were conducted by tip filling pipettes with 135 mM KCl and 10 mM HEPES (pH 7.3, 295 mOsm/kg) and then backfilling with this solution plus 50-250 ug/ml gramicidin D.

2.3 Electrophysiology

Neurons were visualized using an upright microscope with IR-DIC optics (Olympus). For plasticity experiments whole-cell voltage-clamp recordings were performed at a holding potential of -62 mV, corrected for a liquid junction potential of -7 mV, unless otherwise noted. Pipette resistance was 2.0-2.5 MΩ. Pipette capacitance was neutralized but series resistance was left uncompensated. Input resistance (typically 200 to 300 MΩ) and holding current (typically 0 to -150 pA) were monitored continuously; experiments were discarded if they changed by more than 25% or 60 pA, respectively, or if series resistance increased above 16 MΩ. A Multiclamp 700B amplifier (Molecular Devices) was used to record the data, which were filtered at 2-10 kHz, digitized at 4-20 kHz, and collected using AxoGraph X (AxoGraph Scientific).

For NMDAR conductance analysis, 1.5 to 2.0 MΩ pipettes were used. Series resistance (4-12 MΩ) was compensated by >70% using the compensation/prediction circuit of an Axopatch 200B amplifier (Molecular Devices) after pipette capacitance neutralization. Neurons were voltage-clamped in whole-cell mode at -67 mV (after junction potential correction) and stepped to various command voltages to measure NMDAR currents. Neurons were accepted for subsequent analysis only if uncompensated R_s remained below 12 MΩ.

For perforated patch experiments, spontaneous action potential amplitude and access resistance were monitored for 20-30 min after gigaseal formation to ensure adequate access before commencing experiments. Access resistance during recording was between 20 and 40 MΩ.

2.4 Identification and Anatomical Location of DA Neurons

Putative DA neurons were identified by spontaneous pacemaker firing at 1-4 Hz with broad (>1.2 ms duration) spike waveforms in cell-attached mode prior to break-in and the presence of large whole-cell I_h currents after break-in (>200 pA in response to a 1.5-s voltage step from -62 mV to -112 mV). All neurons presented in this study exhibited at least 20 pA $I_{K(Ca)}$ amplitude. Aim 1 of this study sampled predominately from neurons in the rostro-medial SNc (~85%) as well as the lateral VTA (~15%), within 100 μm from the medial border of the medial terminal nucleus of the accessory optic tract (MT) in horizontal slices. Aim 2 was restricted solely to neurons in the VTA. These neurons were always located between 50 and 150 μm medial to the medial border of MT. They were only slightly rostral or caudal (<50 μm) to the respective borders MT. The electrophysiological criteria for DA neuron identification described above are generally accepted for these areas (Ford et al., 2006; Riegel and Williams, 2008; Wanat et al., 2008).

Experiments conducted with Cs^+-based internal solutions (NMDAR conductance analysis and plasticity experiments in 1.2 mM extracellular Mg^{2+} at depolarized V_m), were performed exclusively in rostro-medial SNc to increase the likelihood of recording from DA neurons. For these experiments, I_h was >50 pA (measured immediately after break-in) and all neurons fired in regular pacemaker mode (albeit with significantly broadened action potentials) during cell-attached recording. Previous studies have shown that >50 pA I_h is an adequate marker for DA neurons while recording with Cs^+-based internal solutions via post-hoc tyrosine hydroxylase staining (Borgland et al., 2006; Cruz et al., 2004; Jones and Kauer, 1999). Due to the low permeability of Cs^+ through SK channels, it was impractical to record $I_{K(Ca)}$ for these experiments (Shin et al., 2005).

2.5 Synaptic Stimulation

Synaptic stimuli (50 μs) were generated via an Iso-Flex stimulus isolator (A.M.P.I.) in constant current mode and applied at 0.05 Hz using bipolar tungsten electrodes (100-150 μm tip separation) placed 50-150 μm rostral to the recorded cell. The identity of the glutamtergic inputs to DA neurons stimulated in this manner is unknown. To isolate NMDAR EPSCs, recordings were performed in the presence of DNQX (10 μM), picrotoxin (100 μM), eticlopride (100 nM), and CGP55845 or CGP54626 (50-200 nM) to block AMPA, $GABA_A$, DA D_2, and $GABA_B$ receptors, respectively. Most experiments were performed in low Mg^{2+} (0.1 mM) aCSF to remove blockade of NMDARs, unless otherwise mentioned. Some experiments were conducted without a $GABA_B$ antagonist – no differences were observed and the two groups of experiments were combined. Stimulation intensity was adjusted (20-60 μA) to elicit relatively small NMDAR EPSCs (30-90 pA) in 0.1 mM Mg^{2+} (see Table S1). EPSCs thus evoked were completely blocked by the NMDAR antagonist DL-AP5 (50-100 μM, n = 12). Experiments conducted in 1.2 mM Mg^{2+} with K^+-based internal used stimulation intensities up to 120 μA to evoke resolvable EPSCs. Stimulation artifacts were removed

from EPSC traces in the figures for clarity. AMPAR EPSCs were recorded at -62 or -77 mV in the absence of DNQX and in physiological Mg^{2+} (1.2 mM) solution with similar stimulation intensity to that used for NMDAR EPSCs in 0.1 mM Mg^{2+}. EPSCs thus recorded were blocked by an AMPA/kainate receptor antagonist DNQX (10 μM) (95% ± 1% inhibition, n = 3).

2.6 Facilitation of $I_{K(Ca)}$

To examine the effect of sustained synaptic stimulation on spike-evoked Ca^{2+} signals, $I_{K(Ca)}$ was measured after triggering a single unclamped AP via a 2-ms depolarizing pulse from -62 mV to -7 mV. The integral of the outward tail current, *i.e.*, $I_{K(Ca)}$, was calculated between 20 ms and 400-600 ms after the depolarizing pulse. We have shown previously that $I_{K(Ca)}$ thus measured is action potential-dependent (it is completely eliminated by TTX), is mediated by Ca^{2+}-sensitive SK channels (it is blocked by apamin), and hence can be used as a readout of AP-induced Ca^{2+} transients (Cui et al., 2007). The magnitude of $I_{K(Ca)}$ facilitation by synaptic stimulation was calculated by comparing $I_{k(Ca)}$ evoked in isolation with $I_{k(Ca)}$ evoked 60 or 100 ms after a 0.25 to 1.5 s train of 50-Hz synaptic stimulation, after subtracting the trace of synaptic stimulation alone. For plasticity experiments, facilitation of $I_{K(Ca)}$ by 1 s of synaptic stimulation was measured immediately before induction, using a single AP, instead of a burst of APs, in order to avoid potential contaminating influence on LTP induction. For experiments addressing the role of PKA and PKC in Ca^{2+} signaling and plasticity, facilitation of $I_{K(Ca)}$ was compared between control internal solution and internal solution containing either PKI or chelerythrin via bath perfusion of the $mGluR_{1/5}$ agonist DHPG (1 to 10 μM) in order to normalize PI-coupled receptor activation intensity across solutions and remove any potentially contaminating influence of discrepancies in synaptic activation of these receptors. In these cases, average $I_{K(Ca)}$ was measured for 5-10 min before perfusion and compared with the peak enhancement of $I_{K(Ca)}$ by DHPG.

2.7 Plasticity Induction

The routine plasticity induction protocol consisted of sustained synaptic stimulation (70 stimuli at 50 Hz) paired with a postsynaptic burst of 5 unclamped APs at 20 Hz, where the burst was delayed by 1 s from the onset of the synaptic stimulation. In this case synaptic stimulation extended 200 ms beyond the end of the burst, *i.e.*, until burst-evoked $I_{k(Ca)}$ mostly decayed, to ensure that synapses were activated while cytosolic Ca^{2+} concentration was elevated. Synaptic stimulation-burst pairing was repeated 10 times every 20 s. The same stimulation intensity used for monitoring NMDAR EPSCs was used for synaptic stimulation during induction. The magnitude of LTP was calculated by comparing averaged EPSC amplitudes from 10-min windows (30 traces) immediately before and 30-40 min after LTP induction. These windows were also used to assess PPR and $1/CV^2$. It should be noted that all neurons were held in a quiescent state (*i.e.* not tonically firing) at -62 mV during both EPSC monitoring and plasticity induction unless otherwise mentioned.

For input specificity experiments, the two stimulating electrodes were placed the same rostral distance from the recorded cell, but separated by at least 100 μm laterally. Independence of inputs was tested with cross paired-pulse analysis: after determination of basal EPSC amplitude and paired-pulse ratio ($EPSC_2/EPSC_1$) for each input, the opposing input was substituted for the second pulse. A lack of paired-pulse depression or facilitation during substitution confirmed the absence of interaction between the two inputs.

In some neurons, sustained synaptic stimulation used for induction produced a slow outward current ($I_{syn\text{-}slow}$). This is caused by strong PI-coupled receptor activation generating sufficient cytosolic IP_3 levels to elicit SK channel opening via waves of intracellular Ca^{2+} release in the absence of VACC-mediated influx (Cui et al., 2007; Morikawa et al., 2003). As such, $I_{syn\text{-}slow}$ was never observed in slices treated with CPA

(10 μM) or with a cocktail of PI-coupled receptor antagonists. Neurons with large $I_{syn-slow}$ (>50 pA) were excluded from the initial analyses for two reasons: first, $I_{syn-slow}$ is associated with large, propagating Ca^{2+} waves that invade the dendrites in DA neurons, which we suspected might alter the processing of spike-evoked Ca^{2+} signals by plasticity machinery. In addition, neurons with large $I_{syn-slow}$ frequently exhibited rundown of both $I_{syn-slow}$ itself and burst-induced $I_{K(Ca)}$ during repeated synaptic stimulation-burst pairing. This rundown is most likely due to depletion of intracellular Ca^{2+} stores with repeated, large Ca^{2+} release (Cui et al., 2007), and may also impair LTP induction. On average, $I_{syn-slow}$ was 21 ± 3 pA for the 31 neurons tested for NMDAR LTP with repeated pairing in 0.1 mM Mg^{2+} (control dataset; Figure 3.1B). Large $I_{syn-slow}$ (>50 pA, 103 ± 14 pA, n = 9) was routinely observed when NMDAR EPSCs were recorded in physiological Mg^{2+} (1.2 mM) solution at -62 mV with K^+-based internal solution, because of the relatively strong stimulus intensity (60-120 μA) necessary to evoke sizable (>20 pA) NMDAR EPSCs.

2.8 Flash Photolysis

Caged IP_3 (100 μM) was loaded into the cytosol through the whole-cell pipette for at least 20 min before the start of the experiment. A 1-ms UV pulse was applied using a xenon arc lamp (Cairn Research) to rapidly release IP_3 and the resulting SK-mediated outward current (I_{IP3}) was measured. The amount of photolysis is known to be proportional to the UV pulse intensity, which is proportional to the capacitance of the capacitor feeding current to the flash lamp. This capacitance was varied (50-4050 μF) to adjust the UV pulse intensity. The UV pulse was focused through a 60x objective onto a ~350-μm diameter area centered on the recorded neuron. The concentration (capacitance)-response (I_{IP3} amplitude) curve was fit with a logistic equation to determine the EC_{50} value (in μF) and the maximal I_{IP3} amplitude. The peak of I_{IP3} trace was sharp and did not show any plateau even with a supra-maximal intensity UV pulse, suggesting

that Ca^{2+} levels produced by released IP_3 do not saturate SK channels. A previous study demonstrated a roughly linear relationship between I_{IP3} amplitude and bulk cytosolic Ca^{2+} levels in DA neurons (Morikawa et al., 2000).

2.9 Imaging

Fluorescence imaging of intracellular Ca^{2+} was performed using fluo-5F (50 μM) loaded into the cytosol via the whole-cell pipette for at least 20 min before commencing experiments. Full-frame images in a single focal plane were captured at 15 Hz with a spinning disk confocal imaging system (Olympus) synchronized to synaptic stimulation and electrophysiological recording. Ca^{2+} signals from selected ROIs were expressed as $\Delta F/F = (F - F_{baseline})/(F_{baseline} - F_{background})$. Typically, 4-5 ROIs were placed along the proximal dendrites (<50 μm from the soma) in each neuron, and the ROI exhibiting the largest facilitation of burst-induced fluorescence change (ΔF/F) by synaptic stimulation was chosen for analysis. The peak ΔF/F value was measured to assess burst-evoked Ca^{2+} signals.

Morphological reconstruction was conducted by filling the neuron with 80 μM Alexa594 for 10-15 min via the patch pipette during electrophysiological characterization and then slowly removing the pipette to form an outside-out patch and re-seal the neuronal membrane. The slice was transferred to the stage of a 2-photon laser scanning microscopy system (Leica TCS SP5) and the neuron was imaged in a series of 1 μm optical z-sections. Image stacks were optimally projected into 2D images that were manually x-y aligned for presentation.

2.10 Conductance Analysis

NMDARs were activated by local microiontophoresis of 100 mM NMDA at the soma of the recorded neuron (10-20 μm away from the recording pipette) using 20-100 nA of ejection current for 20-100 ms through the pipette resistance of ~100 MΩ. NMDAR currents were recorded from -87 to +37 mV by stepping the V_c away from a rest of -67 mV. In each neuron, NMDAR currents were recorded at the full range of voltages 2 to 10 times to ensure the stability of the recording and the NMDAR responses. Averaged peak NMDAR currents at each voltage were used to plot the current-voltage (I-V) relationship, from which the reversal potential (E_{rev}) for each neuron was calculated via extrapolation from a linear fit between 0 and +10 mV. These values were then used to calculate the conductance-voltage (G-V) curve for each neuron via

$$G_V = I/(V - E_{rev}) \qquad \textit{(Equation 1)}$$

where G_V is the conductance at a given voltage V, and I is peak NMDAR current.

G_v was converted to fractional conductance (G/G_{max}) by normalizing to the maximal conductance for each neuron and the average G-V relationship across all neurons was constructed by plotting averaged G/G_{max} versus V_c and then fitting with a Boltzmann curve of the form:

$$G_V = G_{min} + (G_{max}-G_{min})/(1+exp[-(V_m-V_{1/2})/s]) \qquad \textit{(Equation 2)}$$

2.11 Drugs and Reagents

DNQX, DL-AP5, CGP55845, CGP54626, CPCCOEt, CPA, PKI (6-22), chelerythrine, QX-222, Ro 25-6981, and ifenprodil were purchased from Tocris

Bioscience (Ellisville, MO, USA). Caged IP_3 and Fluo-5F were purchased from Invitrogen (San Diego, CA). Alexa594 was a kind gift from the laboratory of Dr. Daniel Johnston. All other chemicals were purchased from Sigma-RBI (St. Louis, MO, USA).

2.12 Data Analysis and Statistics

Data are expressed as means ± SEM. Statistical significance was determined by Student's t-test (paired or unpaired) or ANOVA followed by Dunnett's test. Differences were considered significant at $p < 0.05$.

CHAPTER 3: RESULTS

3.1 Aim 1: Burst Timing-Dependent Synaptic Plasticity of NMDARs at DA Neurons

3.1.1 PAIRING PRESYNAPTIC INPUTS WITH POSTSYNAPTIC BURST FIRING TO MIMIC *IN VIVO* NEURAL DYNAMICS DURING LEARNING

3.1.1.1 Burst Pairing Drives LTP of NMDARs

To address the plasticity of NMDARs in DA neurons, we applied patch-clamp electrophysiological techniques to acute horizontal midbrain slices containing the SNc and VTA from adolescent/young adult rats (4 to 8 weeks). We first recorded pharmacologically isolated NMDAR EPSCs in whole-cell voltage-clamp at -62 mV in low Mg^{2+} (0.1 mM) to remove voltage-dependent Mg^{2+} blockade (Nowak et al., 1984). A bipolar stimulating electrode was placed 50-150 μm rostral to the recorded neuron to deliver relatively weak (20-60 μA stimulation intensity; 30-90 pA EPSCs) synaptic stimuli at 0.05 Hz. After 10 min of baseline EPSC recording, we delivered an LTP induction protocol consisting of a train of presynaptic stimulation (70 stimuli at 50 Hz) paired with a burst of 5 postsynaptic unclamped APs at 20 Hz (diagramed in Figure 3.1A, see Materials and Methods, section 2.6 and 2.7), which mimics burst firing observed in behaving rats (Hyland et al., 2002). The onset of the burst was delayed by 1 s from that of the synaptic stimulation train to emulate the delay between the presentation of cues and rewards *in vivo*. We found that repetitive synaptic stimulation-burst pairing (10 times every 20 s, a duty cycle used for *in vivo* reward learning in rats (Pan et al., 2005)) resulted in LTP of NMDAR EPSCs in some but not all neurons tested (Figure 3.1A,B). The pattern of synaptic stimulation used in the induction protocol can enhance AP-induced Ca^{2+} signals via activation of PI-coupled receptors, mainly $mGluR_1$ (Cui et al., 2007). To determine if this process influences LTP induction, we measured small-

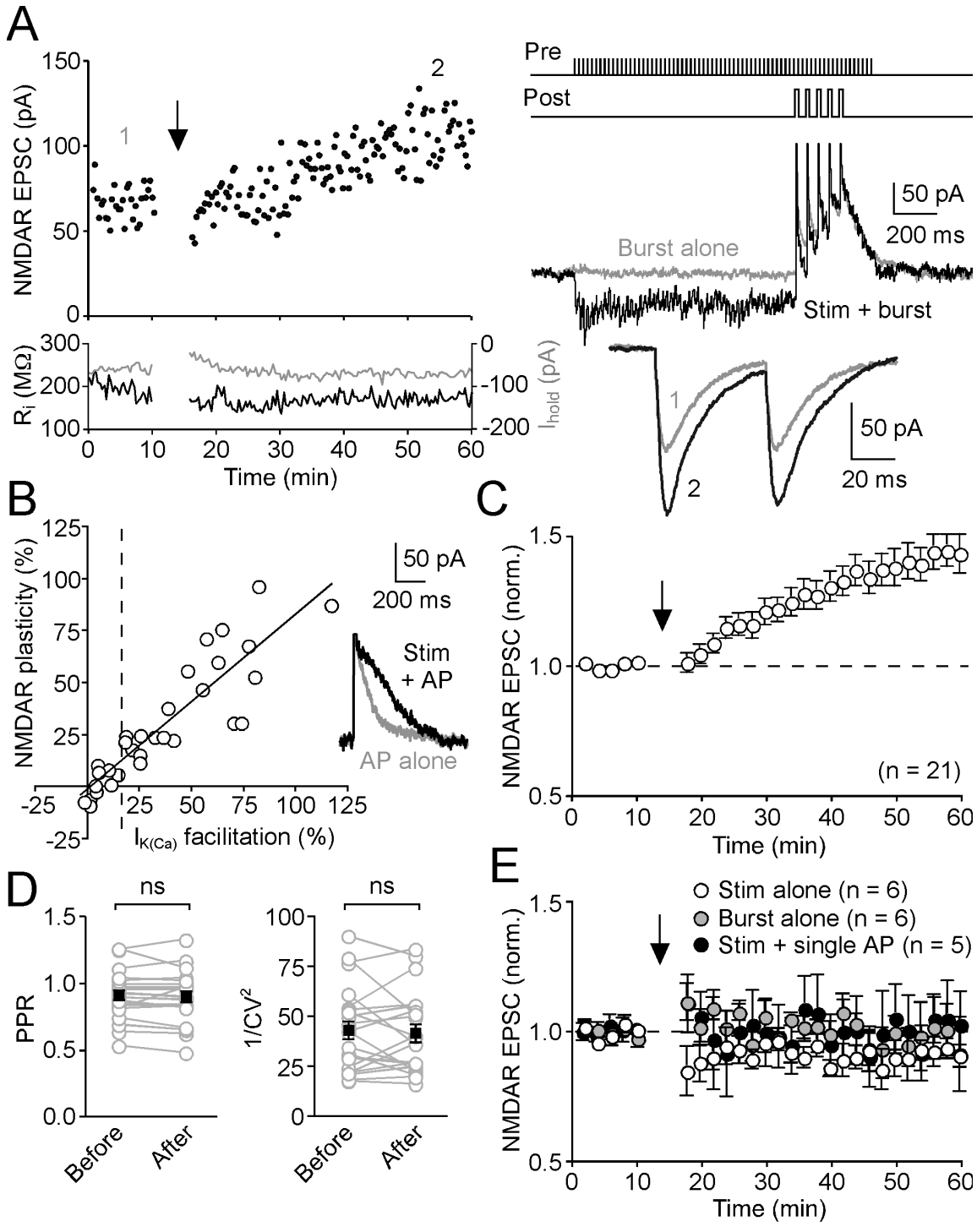
A
NMDAR EPSC (pA)
150
100
50
0
1
2
R_i (MΩ)
300
200
100
0
10
20
30
40
50
60
Time (min)
0
-100
-200
I_{hold} (pA)
Pre
Post
50 pA
200 ms
Burst alone
Stim + burst
1
2
50 pA
20 ms
B
NMDAR plasticity (%)
125
100
75
50
25
-25
25
50
75
100
125
-25
$I_{K(Ca)}$ facilitation (%)
50 pA
200 ms
Stim
+ AP
AP alone
C
NMDAR EPSC (norm.)
1.5
1.0
0.5
0
10
20
30
40
50
60
Time (min)
(n = 21)
D
PPR
1.5
1.0
0.5
0.0
ns
Before
After
$1/CV^2$
100
75
50
25
0
ns
Before
After
E
NMDAR EPSC (norm.)
1.5
1.0
0.5
0
10
20
30
40
50
60
Time (min)
Stim alone (n = 6)
Burst alone (n = 6)
Stim + single AP (n = 5)

Figure 3.1. Repeated Synaptic Stimulation-Burst Pairing Induces LTP of NMDAR EPSCs in DA Neurons.

(A) Representative experiment showing LTP of NMDAR EPSCs. Left: Time graph of NMDAR EPSC amplitude, input resistance (R_i, black), and holding current (I_{hold}, gray). The LTP induction protocol, which consisted of 10 synaptic stimulation-burst pairings (illustrated at top right), was delivered at the time indicated by the arrow. Middle right: Current traces evoked by burst alone (gray) and synaptic stimulation-burst pairing (black). Bottom right: Traces of EPSCs (averaged over 10 min) at times indicated by numbers in the EPSC time graph.

(B) Relationship between the magnitude of NMDAR LTP and facilitation of AP-evoked $I_{K(Ca)}$ by preceding synaptic stimulation for 31 neurons. Solid line is a linear fit to the data (r^2 = 0.8). Dashed vertical line indicates 15% $I_{K(Ca)}$ facilitation. Inset at right shows traces of $I_{K(Ca)}$ for a single AP alone (gray) and an AP following synaptic stimulation (black) from the same neuron as in (A).

(C) Summary time graph of NMDAR LTP for neurons that exhibited >15% $I_{K(Ca)}$ facilitation (n = 21). Each symbol represents mean normalized EPSC amplitude from a 2-min window.

(D) PPR (left) and $1/CV^2$ (right) were not significantly altered after LTP induction for the 21 neurons in (C). Black squares indicate mean.

(E) Summary time graph showing that synaptic stimulation alone (n = 6), burst alone (n = 6), and pairing synaptic stimulation with a single AP (n = 5) all failed to induce NMDAR LTP. Note that a small LTD was induced with synaptic stimulation alone.

conductance Ca^{2+}-sensitive K^+ (SK) currents ($I_{K(Ca)}$) activated by unclamped APs (see Materials and Methods, section 2.6). Immediately before induction, we tested each neuron for facilitation of $I_{K(Ca)}$ following synaptic stimulation by evoking a single AP at 60 ms after the offset of a 1-s stimulation train (example traces shown in inset of Figure 3.1B). The magnitude of NMDAR LTP, determined 30-40 min after induction, was positively correlated with that of $I_{K(Ca)}$ facilitation ($n = 31$, $r^2 = 0.80$; Figure 3.1B). On average, NMDAR EPSCs were potentiated by 43% ± 6% in 21 neurons that exhibited $I_{K(Ca)}$ facilitation >15%, whereas little to no LTP was observed when $I_{K(Ca)}$ facilitation was <15% (1% ± 2% change, $n = 10$; Figure 3.1C).

The paired-pulse ratio (PPR, 50-ms interstimulus interval, expressed as $EPSC_2/EPSC_1$) and the coefficient of variation (CV, expressed as $1/CV^2$) of EPSCs over the 10 min baseline period compared to 30-40 min after pairing were not significantly different in 21 neurons that exhibited LTP ($p > 0.05$ for both, paired t-test; Figure 3.1D), suggesting a postsynaptic locus of LTP expression via an increase in either receptor number or function (Malinow and Tsien, 1990; Zalutsky and Nicoll, 1990). Note that the PPR of NMDAR EPSCs in this study is similar to that previously reported for AMPARs at DA neurons (Bonci and Malenka, 1999; Gutlerner et al., 2002).

Due to the correlation between $I_{K(Ca)}$ facilitation and LTP in our initial findings (Figure 3.1B), all subsequent experiments were conducted in neurons that exhibited >15% $I_{K(Ca)}$ facilitation unless otherwise stated (Table 3.1). Table 3.1 also compares the size of $I_{K(Ca)}$ itself for single APs and bursts, and basal NMDAR EPSC size across all experimental groups. There were no significant differences in these parameters throughout the experiments presented unless specifically mentioned.

We next investigated the stimulus requirements for plasticity by systematically altering the induction protocol (Figure 3.1E). Repeated delivery of postsynaptic burst firing alone failed to induce LTP of NMDAR EPSCs (0% ± 3% change, $n = 6$). The converse paradigm, synaptic stimulation alone, produced a small but significant LTD (-8% ± 4% change, $n = 6$). Furthermore, no plasticity was observed when pairing was conducted with a single AP instead of a burst (-1% ± 10% change, $n = 5$). These results

Table 3.1. Summary of Parameters in Different Experimental Groups for Aim 1

Type of experiment	Plasticity (%)	Facilitation of $I_{K(Ca)}$ (%)	$I_{K(Ca)}$ (pA·s)	$I_{K(Ca)\text{-burst}}$ (pA·s)	Baseline EPSC (pA)	n
Control: >15% $I_{K(Ca)}$ facilitation	43 ± 6	51 ± 6	9 ± 1	34 ± 4	56 ± 4	21
Control: <15% $I_{K(Ca)}$ facilitation	1 ± 2***	5 ± 2***	7 ± 2	35 ± 11	58 ± 4	10
1.2 mM Mg^{2+}, $KMeSO_4$ ICS	-3 ± 3***	75 ± 10	7 ± 2	31 ± 5	30 ± 2**	10
0.1 mM Mg^{2+}, >50 pA $I_{syn\text{-}slow}$	-12 ± 6***	56 ± 14	11 ± 2	35 ± 4	61 ± 8	8
1.2 mM Mg^{2+}, $CsMeSO_3$ ICS	16 ± 6*	NA	NA	NA	23 ± 3**	8
Synaptic stimulation alone	-8 ± 4***	45 ± 6	7 ± 2	29 ± 5	69 ± 3	6
Burst alone	0 ± 3***	41 ± 6	9 ± 2	32 ± 8	51 ± 9	6
Single-AP pairing	-1 ± 10***	56 ± 8	7 ± 2	38 ± 6	48 ± 8	5
CPA	2 ± 4***	0 ± 2***	2 ± 0**	14 ± 2*	43 ± 2	6
PI-coupled receptor blockade	-6 ± 4***	2 ± 3***	9 ± 3	31 ± 7	57 ± 5	6
BAPTA	-1 ± 5***	4 ± 1***	2 ± 0**	7 ± 1**	43 ± 4	6
PKI	-3 ± 6***	9 ± 3***	9 ± 1	38 ± 4	47 ± 3	7
Chelerythrine	28 ± 7	37 ± 7	7 ± 2	27 ± 5	40 ± 2	4
SCH 23390	38 ± 9	44 ± 10	5 ± 2	21 ± 6	49 ± 4	5
AP5	-1 ± 2***	56 ± 13	5 ± 1	25 ± 5	44 ± 11	4
Burst timing:						
500 ms before onset	-10 ± 4***	43 ± 10	8 ± 2	33 ± 6	55 ± 7	5
250 ms before onset	-22 ± 7***	42 ± 14	10 ± 4	31 ± 10	57 ± 9	4
Onset	-3 ± 10***	64 ± 9	7 ± 2	26 ± 5	56 ± 5	4
200 ms after onset	3 ± 5**	46 ± 10	5 ± 3	19 ± 10	47 ± 9	3
500 ms after onset	20 ± 6	44 ± 8	6 ± 1	24 ± 5	47 ± 10	5
60 ms after offset	13 ± 14*	52 ± 13	6 ± 2	25 ± 2	48 ± 4	4
120 ms after offset	6 ± 5***	46 ± 10	5 ± 1	25 ± 6	50 ± 5	5
Input specificity:						
Paired	65 ± 16	63 ± 11	6 ± 2	31 ± 6	51 ± 10	4
Unpaired	2 ± 2***	35 ± 8			56 ± 8	
NR2 subunit composition:						
Ro 25-6981	29 ± 6	54 ± 18	7 ± 1	26 ± 4	42 ± 4	4
Ifenprodil	38 ± 7	56 ± 7	7 ± 1	28 ± 5	43 ± 7	3
Zn^{2+}	42 ± 9	50 ± 6	7 ± 1	27 ± 5	43 ± 7	4
Depotentiation:						
Synaptic stimulation alone	30 ± 6	32 ± 9	5 ± 1	28 ± 9	59 ± 9	4
Single-AP pairing	35 ± 7	47 ± 16	8 ± 2	26 ± 5	53 ± 3	4
Failed LTP expression	5 ± 3**	6 ± 2**	10 ± 3	40 ± 5	48 ± 10	3
AMPAR LTD:						
Burst pairing	-29 ± 3***	76 ± 14	9 ± 2	40 ± 8	139 ± 21	5
Synaptic stimulation alone	-26 ± 3***	60 ± 15	11 ± 2	32 ± 7	157 ± 37	3

The magnitude of synaptic stimulation-induced facilitation of $I_{K(Ca)}$ shown in this table was always obtained with a single AP evoked 60 ms after the offset of 1-s synaptic stimulation (see Materials and Methods). All data are mean ± SEM. *$p < 0.05$, **$p < 0.01$, ***$p < 0.001$ vs. the control: >15% $I_{K(Ca)}$ facilitation group (ANOVA followed by Dunnett's test). Statistical comparison with this group was not made for the baseline EPSC data in the two groups tested for AMPAR LTD. NA indicates experiments where it was not possible to measure $I_{K(Ca)}$ or facilitation (see text).

show that LTP of NMDARs is associative and requires presynaptic input coordinated with postsynaptic bursting.

Intrinsic cellular differences in Ca^{2+} signaling or biases in the strength of synaptic activation may exert contaminating influences on plasticity. We therefore confirmed that NMDAR LTP was not correlated with either the size of $I_{K(Ca)}$ itself for single APs (r^2 = 0.01) and bursts (r^2 = 0.0005; Figure 3.2A) or initial EPSC amplitude (r^2 = 0.006; Figure 3.2B) for the 31 neurons in Figure 3.1B.

Thus, NMDARs in DA neurons express LTP that is induced in an associative manner that requires postsynaptic bursting and is correlated with synaptic facilitation of spike-evoked Ca^{2+} signals during pairing.

3.1.1.2 LTP of NMDARs in 1.2 mM Extracellular Mg^{2+}

The initial set of experiments described above in Figures 3.1 and 3.2 were conducted in 0.1 mM extracellular Mg^{2+} in order to record NMDAR EPSCs evoked with relatively weak stimulation intensities at a physiologically relevant holding voltage (-62 mV). Numerous studies have used this approach to analyze NMDARs and synaptic plasticity (Harvey and Svoboda, 2007; Harvey et al., 2008; Selig et al., 1995; Sobczyk et al., 2005; Sobczyk and Svoboda, 2007; Xie et al., 1992); some have even directly confirmed that plasticity of NMDARs observed in low Mg^{2+} also occurs in physiological Mg^{2+} (Morishita et al., 2005; Rebola et al., 2008). This is in contrast to studies that have monitored NMDAR function by chronically depolarizing neurons filled with Cs^{+}-based internal solutions to +40 mV in voltage-clamp (Bellone and Nicoll, 2007; Borgland et al., 2006; Kwon and Castillo, 2008; Quinlan et al., 1999; Rebola et al., 2008; Saal et al., 2003; Schilstrom et al., 2006; Ungless et al., 2003). While both types of experiments represent non-physiological approaches to solving the technical problems of recording from ligand-gated channels with limited conductance at resting voltages, performing the experiments at near-physiological voltage with K^{+}-based internal solution in low Mg^{2+} allows us to take advantage of the properties of DA neurons to examine synaptic plasticity in a more controlled and detailed manner. We can more reliably identify DA

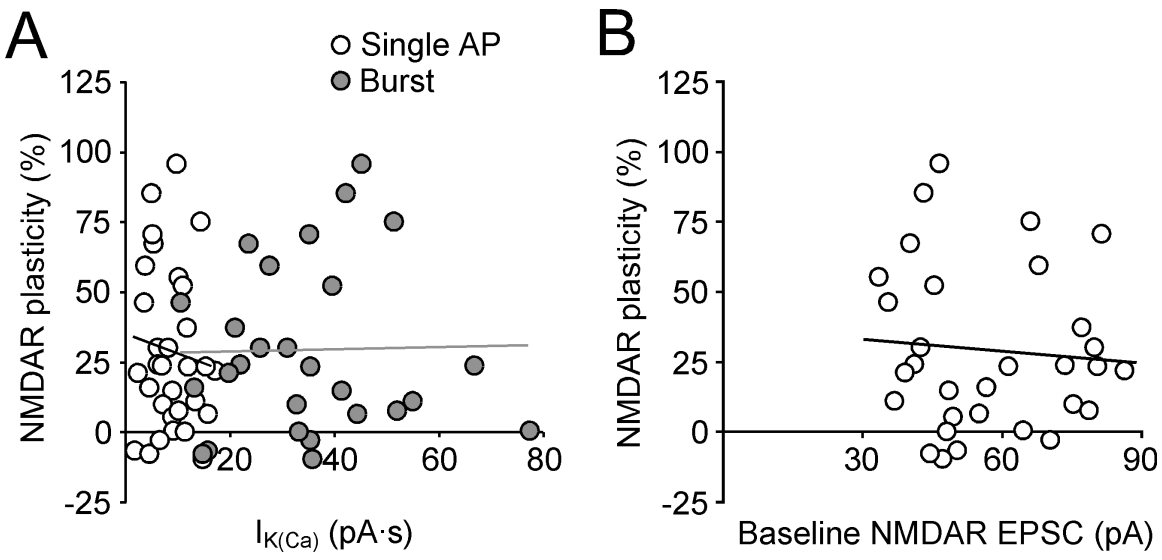

Figure 3.2. NMDAR LTP is Not Correlated with the Size of $I_{K(Ca)}$ or Baseline EPSC Amplitude.

(A) Relationship between the magnitude of NMDAR LTP and the size of $I_{K(Ca)}$ evoked by a single AP (white circles) or a burst of APs (gray circles) for the same 31 neurons shown in Figure 1B. Black line is a linear fit to single AP-evoked $I_{K(Ca)}$ data (r^2 = 0.01), while gray line is a linear fit to burst-induced $I_{K(Ca)}$ data (r^2 = 0.0005).

(B) Relationship between the magnitude of NMDAR LTP and baseline NMDAR EPSC amplitude for the same 31 neurons. The EPSC amplitude was averaged over the 10-min period (30 traces) preceding plasticity induction in each neuron. Black line represents linear fit to the data (r^2 = 0.006).

neurons based on physiological characteristics (Figures 1.2 and 1.3, see also Materials and Methods, section 2.4), in particular firing rate, action potential width, and I_h, all of which are distorted by Cs^+. We can also initiate appropriately timed single action potentials during the induction protocol, which is not possible with Cs^+ in the pipette due to its blockade of many K^+ channels causing poorly controlled burst firing of long duration plateau potentials in response to depolarization. Additionally, we can monitor spike-evoked Ca^{2+} signals via $I_{K(Ca)}$ (which is also significantly attenuated in Cs^+-based internal solutions due to the relatively low permeability of SK channels to Cs^+ (Shin et al., 2005)). Finally, we are not depolarizing the cell to +40 mV and dramatically altering intracellular Ca^{2+} signaling. In spite of all these caveats, it is important to demonstrate that the burst-pairing protocol can drive plasticity of NMDARs in physiological Mg^{2+}, regardless of the specific limitations of the experimental paradigm.

To that end, we first performed the identical experiment to that presented in Figure 3.1 in 1.2 mM extracellular Mg^{2+} (Figure 3.3). Stimulation intensity had to be significantly increased (47 ± 3 μA in 0.1 mM Mg^{2+}, n = 31 vs. 77 ± 5 μA in 1.2 mM Mg^{2+}, n = 10, $p < 0.0001$, unpaired t-test) in order to resolve NMDAR EPSCs during Mg^{2+} blockade at -62 mV (57 ± 4 pA in 0.1 mM Mg^{2+}, n = 31 vs. 30 ± 2 pA in 1.2 mM Mg^{2+}, n = 10, $p < 0.0001$, unpaired t-test). Under these conditions, little to no LTP occurred (Figure 3.3A-D) and there was no correlation between plasticity and facilitation of $I_{K(Ca)}$ (Figure 3.3B). However, we observed large, slow, outward currents during the pairing protocol in all experiments conducted in this manner (103 ± 14 pA, n = 9; Figure 3.3A and 3.3C). These slow outward currents ($I_{syn\text{-}slow}$) were caused by strong, phasic PI-coupled receptor activation generating sufficient cytosolic IP_3 levels to elicit SK channel opening via intracellular Ca^{2+} release (Cui et al., 2007; Fiorillo and Williams, 1998; Morikawa et al., 2000; Morikawa et al., 2003) (see Materials and Methods, section 2.7). $I_{syn\text{-}slow}$ results from a propagating Ca^{2+} wave that spreads through the soma and proximal dendrites, which may disrupt the normal Ca^{2+} signaling pathway(s) required for NMDAR LTP. Indeed, some experiments conducted in 0.1 mM Mg^{2+} displayed large (>50 pA)

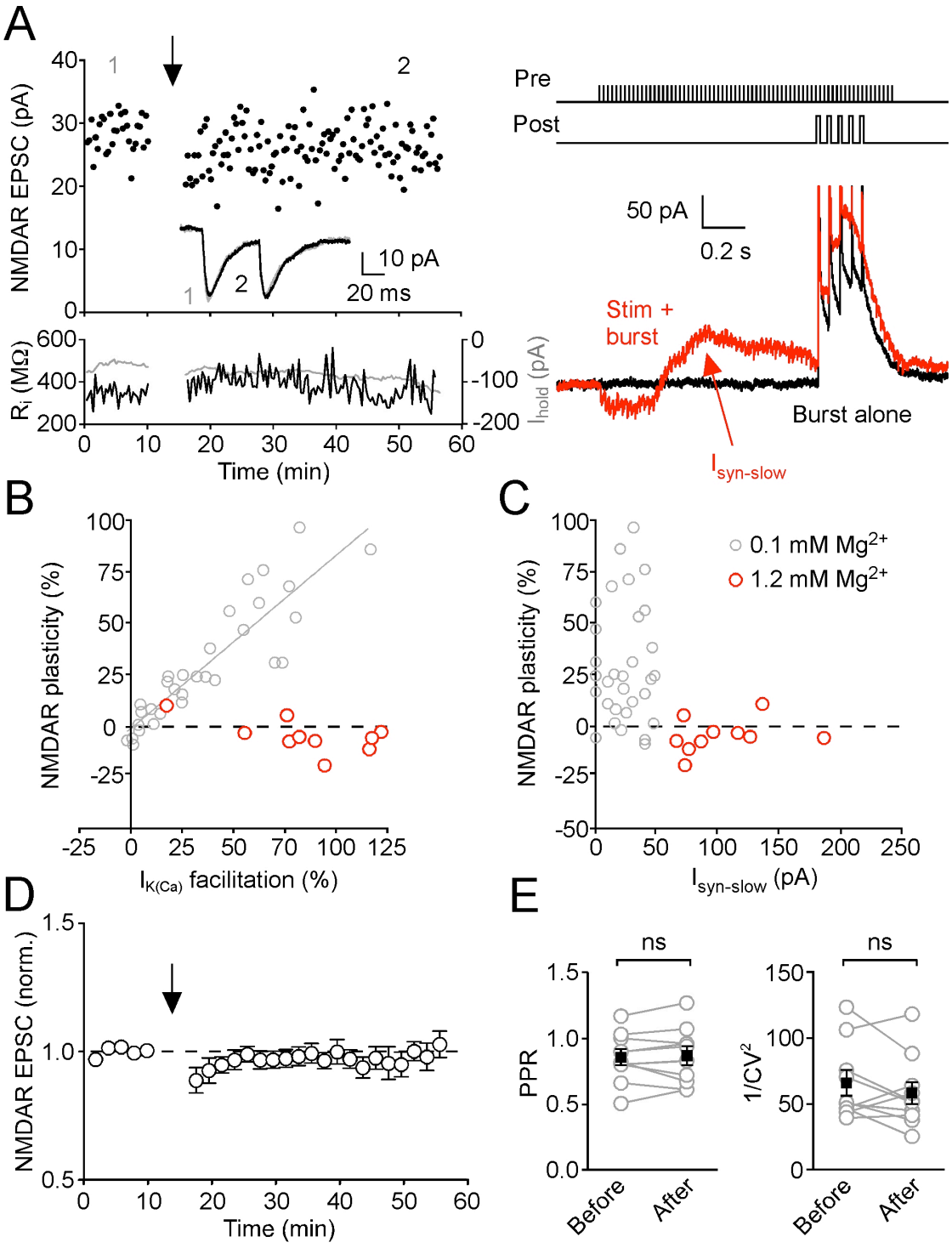
A
NMDAR EPSC (pA)
1
2
10 pA
20 ms
R_i (MΩ)
I_{hold} (pA)
Time (min)
Pre
Post
50 pA
0.2 s
Stim + burst
Burst alone
$I_{syn-slow}$
B
NMDAR plasticity (%)
$I_{K(Ca)}$ facilitation (%)
C
0.1 mM Mg^{2+}
1.2 mM Mg^{2+}
$I_{syn-slow}$ (pA)
D
NMDAR EPSC (norm.)
Time (min)
E
ns
PPR
$1/CV^2$
Before
After

Figure 3.3. Strong Stimulation During Pairing in 1.2 mM Mg^{2+} Prevents NMDAR LTP Induction by Recruiting Ca^{2+} Waves.

(A) Example experiment illustrating lack of NMDAR LTP in 1.2 mM extracellular Mg^{2+} is associated with large $I_{syn\text{-}slow}$ during burst pairing. Averaged NMDAR EPSCs (inset at left) are taken at the points indicated in the EPSC time graph. The pairing protocol is diagramed at top right; below are example traces in response to burst alone in black and pairing in red. Note the large, slow, outward current ($I_{syn\text{-}slow}$) during the train of NMDAR EPSCs.

(B) Experiments conducted in 1.2 mM Mg^{2+} failed to exhibit LTP despite significant facilitation of $I_{K(Ca)}$. Red open circles are 10 neurons recorded in 1.2 mM Mg^{2+} shown in contrast to the 31 control experiments conducted in 0.1 mM Mg^{2+} from Figure 3.1B (gray open circles).

(C) All experiments conducted in 1.2 mM Mg^{2+} exhibited large (>50 pA) $I_{syn\text{-}slow}$ (red open circles), the magnitude of which was not correlated with plasticity. The 31 control neurons from Figure 3.1B, which expressed significant correlation between facilitation of $I_{K(Ca)}$ and plasticity, showed little to no $I_{syn\text{-}slow}$ during pairing (gray open circles).

(D) Summary time graph of NMDAR EPSCs in response to burst pairing for experiments conducted in 1.2 mM Mg^{2+} (same neurons as in B and C). Pairing was delivered at the arrow.

(E) PPR and CV for the 10 neurons from B-D before and after burst pairing. Note that while initial PPR in 1.2 mM Mg^{2+} is similar to that in 0.1 mM, initial $1/CV^2$ is substantially increased in 1.2 mM Mg^{2+} (compare with Figure 3.1D).

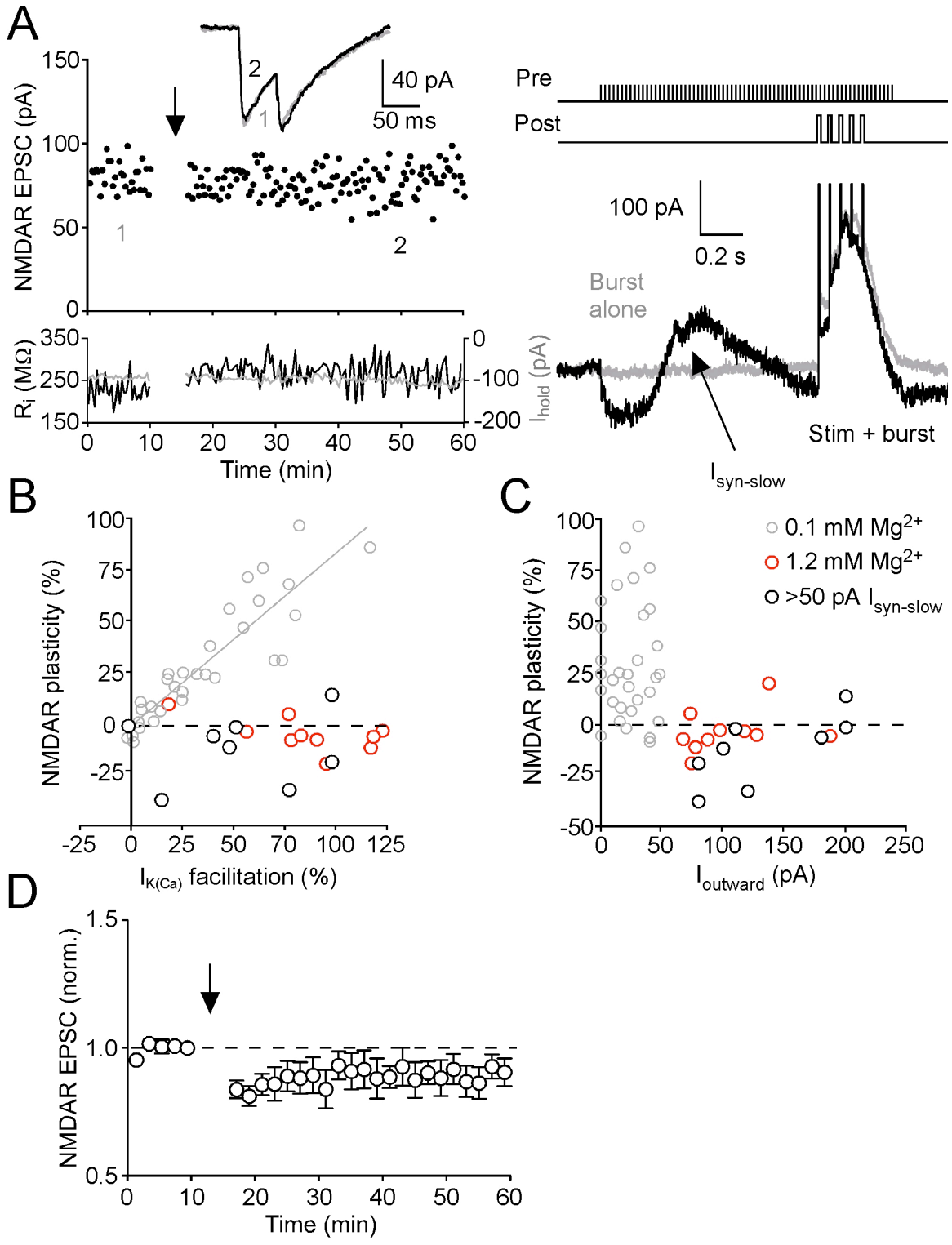
A
NMDAR EPSC (pA)
150
100
50
0
40 pA
50 ms
1
2
R_i (MΩ)
350
250
150
0
-100
-200
0 10 20 30 40 50 60
Time (min)
Pre
Post
100 pA
0.2 s
Burst alone
I_{hold} (pA)
Stim + burst
$I_{syn-slow}$
B
NMDAR plasticity (%)
100
75
50
25
0
-25
-25 0 25 50 70 100 125
$I_{K(Ca)}$ facilitation (%)
C
NMDAR plasticity (%)
0.1 mM Mg^{2+}
1.2 mM Mg^{2+}
>50 pA $I_{syn-slow}$
-50
0 50 100 150 200 250
$I_{outward}$ (pA)
D
NMDAR EPSC (norm.)
1.5
1.0
0.5
0 10 20 30 40 50 60
Time (min)

Figure 3.4. Ca^{2+} Waves During Pairing Inhibit NMDAR LTP in 0.1 mM Mg^{2+}.
(A) Example experiment conducted in 0.1 mM Mg^{2+} exhibiting significant $I_{syn\text{-}slow}$ during synaptic stimulation-burst pairing, as shown in the black pairing trace at right compared with burst alone in gray (pairing protocol is diagrammed above). Average NMDAR EPSCs are shown inset, taken from the times indicated.
(B) Lack of correlation between facilitation of $I_{K(Ca)}$ and NMDAR plasticity for experiments performed in 0.1 mM Mg^{2+} with >50 pA $I_{syn\text{-}slow}$ (black open circles, n =8). Gray open circles represent the 31 control LTP neurons from Figure 3.1B while red open circles are from the 10 neurons presented in Figure 3.3C recorded in 1.2 mM Mg^{2+}, all of which exhibited >50 pA $I_{syn\text{-}slow}$.
(C) Relationship between magnitude of $I_{syn\text{-}slow}$ and plasticity of NMDAR EPSCs for the neurons in (B).
(D) Summary time graph of NMDAR plasticity experiments from neurons with >50 pA $I_{syn\text{-}slow}$ in 0.1 mM Mg^{2+} (n = 8).

$I_{syn\text{-}slow}$, which obviated LTP (Figure 3.4). These experiments had previously been rejected from the initial data set of 31 neurons presented in Figure 3.1 due to concerns about strongly activating mGluRs and subsequent Ca^{2+} waves (see Materials and Methods, section 2.7). It should be noted that PPR was similar between experiments performed in 0.1 and 1.2 mM Mg^{2+} (compare Figures 3.1D and 3.3E), suggesting that presynaptic release was not altered by changes in extracellular Mg^{2+}, though $1/CV^2$ was significantly increased in 1.2 mM Mg^{2+}, consistent with stronger synaptic stimulation recruiting more presynaptic release sites. In addition, four measures of intrinsic cellular properties were not significantly different between experiments conducted in 0.1 vs. 1.2 mM Mg^{2+} (Table 3.2), reinforcing the idea that low Mg^{2+} has limited effects on the basic physiology of DA neurons.

Table 3.2. Comparison of Intrinsic Cellular Parameters between 0.1 and 1.2 mM Mg^{2+}

Condition	Frequency of Firing (Hz)	AP width (ms)	I_h (nA)	$I_{K(Ca)}$ (pA·s)	$I_{K(Ca)\text{-burst}}$ (pA·s)	n
0.1 mM Mg^{2+}	2.7 ± 0.1	1.4 ± 0.1	0.8 ± 0.1	8 ± 2	35 ± 7	31
1.2 mM Mg^{2+}	2.4 ± 0.2	1.5 ± 0.1	0.8 ± 0.1	7 ± 2	31 ± 5	10

Datasets are those presented in Figures 1.1D and 3.1B for 0.1 mM Mg^{2+} and Figure 3.3B and C for 1.2 mM Mg^{2+}. Firing frequency and AP width were measured in tight-seal cell-attached voltage-clamp prior to break-in (from >50 APs over >2 min). AP width was determined from the start of the inward component to the peak of the outward component of the cell-attached waveform as described (Ford et al., 2006). I_h was always measured ~2 min after break-in. There were no significant differences between groups for all parameters ($p > 0.05$, unpaired t-tests).

To abrogate the need for strong synaptic stimulation, an alternative approach was implemented. Neurons were filled with Cs^+-based internal solution and slightly depolarized (-47 to -62 mV). The Cs^+-based ICS reduced the current noise normally present at these voltages by blocking subthreshold K^+ channels, allowing us to resolve smaller NMDAR EPSCs (23 ± 3 pA, n = 8) at weaker stimulation intensities (20-60 μA) in 1.2 mM extracellular Mg^{2+}. Pairing presynaptic stimulation with postsynaptic bursting while holding at -60 to -70 mV produced >10% LTP in 6 out of 8 neurons tested under these conditions (23% ± 4% change, n = 6; Figure 3.5). Because measurable $I_{K(Ca)}$ was

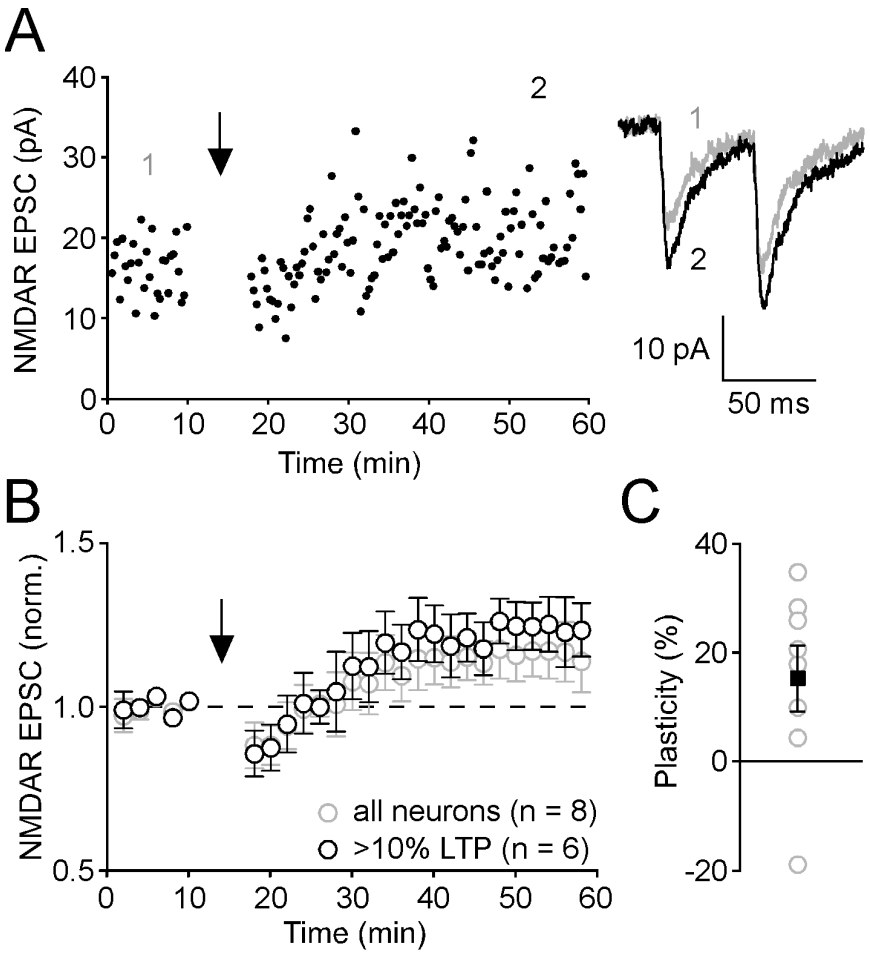

Figure 3.5. NMDAR LTP Can Be Induced in Physiological Mg^{2+}.
(A) Representative time graph showing LTP of NMDAR EPSCs recorded at -52 mV in 1.2 mM Mg^{2+} with Cs^{+}-based internal solution. Recording was switched to current clamp during synaptic stimulation-burst pairing (arrow). A 250-ms depolarizing current injection, which produced 4-6 postsynaptic spikes, was made at 1 s after the onset of 1.4-s synaptic stimulation during pairing. Pairing was repeated 10 times every 20 s. The membrane potential was maintained at ~-65 mV with constant current injection between pairings. Traces of NMDAR EPSCs (averaged over 10 min) at the times indicated are shown at right.
(B) Summary time graph of NMDAR plasticity experiments conducted in 1.2 mM Mg^{2+} with Cs^{+}-based internal solution. Pairing was performed in current clamp (n = 7) or in voltage clamp (n = 1). 6 out of 8 neurons exhibited >10% LTP, indicated by black open circles. Gray open circles represent data from all neurons.
(C) Amount of NMDAR plasticity expressed in all 8 individual experiments (gray open circles). Black square represents mean ± SEM.

not observed in these experiments, most likely due to the low permeability of SK channels to Cs^+ (Shin et al., 2005), it is not surprising that plasticity was not as robust as that shown in Figure 3.1, given the dependence of LTP on facilitation of $I_{K(Ca)}$, which may not have occurred in some of these experiments.

These results demonstrate that NMDAR LTP can be induced in physiological extracellular Mg^{2+}. They also suggest that intracellular Ca^{2+} waves recruited by strong, phasic activation of PI-coupled receptors by synaptic stimulation can interact with and possibly control the induction of plasticity by changing the dynamics of postsynaptic Ca^{2+} signaling.

3.1.1.3 Burst Pairing Drives LTD of AMPARs

We next examined the effect of the burst pairing protocol on AMPAR-mediated transmission (Figure 3.6). Here, AMPAR EPSCs were recorded at -62 or -77 mV in 1.2 mM Mg^{2+} with NMDARs intact, while synaptic stimulation-burst pairing was delivered at -62 mV. This resulted in LTD of EPSCs (-29% ± 3% change, n = 5; Figure 3.6B). The magnitude of LTD showed no correlation with $I_{K(Ca)}$ facilitation by synaptic stimulation (r^2 = 0.0003; Figure 3.6C). Furthermore, there was no difference ($p > 0.5$, unpaired t-test) in the amount of LTD expressed when postsynaptic burst firing was omitted and neurons received the synaptic stimulation train alone (-26% ± 3% change, n = 3; Figures 3.6B and C). This form of plasticity thus presumably corresponds to the mGluR-dependent but postsynaptic spike-independent LTD of AMPARs previously described in DA neurons (Bellone and Luscher, 2005, 2006; Mameli et al., 2007) mediated by rapid synthesis and synaptic exchange of lower conductance AMPARs. This postsynaptic expression mechanism is consistent with our observation that LTD produced by either protocol was not associated with significant changes in PPR (0.89 ± 0.12 vs. 0.85 ± 0.10 for pairing and 1.09 ± 0.35 vs 1.27 ± 0.39 for synaptic stimulation alone, $p > 0.1$ for both, paired-tests) or $1/CV^2$ (18.1 ± 1.9 vs. 18.7 ± 2.6 for pairing and 27.7 ± 11.8 vs. 25.4 ± 18.7 for synaptic stimulation alone, $p > 0.1$ for both, paired-tests). Note that initial PPR for these AMPAR experiments was similar both to NMDAR EPSCs

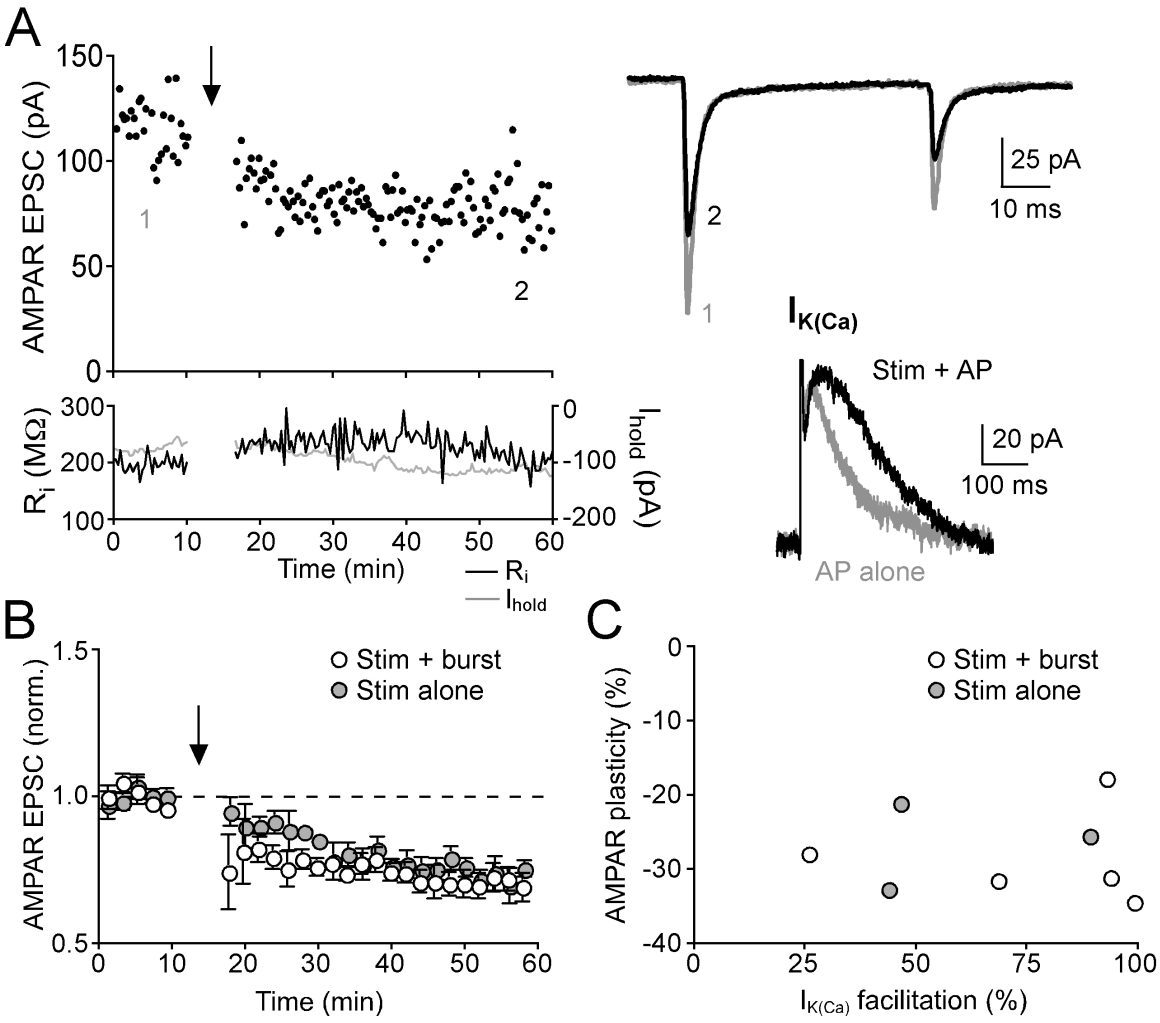

Figure 3.6. Repeated Synaptic Stimulation Induces LTD of AMPAR EPSCs Independent of Postsynaptic Burst Firing.

(A) Representative time graph depicting LTD of AMPAR EPSCs. Synaptic stimulation-burst pairing was delivered at arrow. Input resistance (R_i, black) and holding current (I_{hold}, gray) at -77 mV are shown below. Traces of AMPAR EPSCs (averaged over 10 min) at the times indicated are shown at top right. Facilitation of AP-evoked $I_{K(Ca)}$ in this neuron is shown at bottom right (gray: AP alone, black: AP preceded by synaptic stimulation).

(B) Summary time graph of AMPAR LTD for burst pairing experiments (n = 5) and experiments inducing LTD with synaptic stimulation alone (n = 3). Error bars indicate SEM.

(C) Relationship between the magnitude of AMPAR LTD and facilitation of $I_{K(Ca)}$ for experiments performed with burst pairing (white circles) and those with synaptic stimulation alone (gray circles).

recorded in 0.1 mM Mg^{2+} (Figure 3.1D) and also to that reported for AMPAR EPSCs in DA neurons by other groups (Bonci and Malenka, 1999; Gutlerner et al., 2002).

3.1.2 MECHANISMS OF INDUCTION OF NMDAR LTP

3.1.2.1 Induction of NMDAR LTP Requires Facilitation of Postsynaptic Spike-Evoked Ca^{2+} Signals Through PI-Coupled Receptor Activation and Release of Ca^{2+} from Internal Stores

We have previously shown that activation of PI-coupled receptors facilitates AP-evoked Ca^{2+} signals in DA neurons via an increase in IP_3 levels, which enhances IP_3R-dependent CICR from intracellular stores (Cui et al., 2007). This process may occur in a manner similar to what we hypothesize occurs at DA neurons *in vivo* during reward learning as weak persistent glutamatergic inputs representing cues precede strong postsynaptic burst firing driven by primary rewards or previously learned reward predicting cues. Furthering this idea, the data presented in Figure 3.1 suggest that coincident pre- and postsynaptic activity can drive plasticity of NMDARs when spike-evoked Ca^{2+} signals are facilitated by synaptic stimulation. We thus probed the mechanistic basis of this Ca^{2+} signaling cascade in NMDAR LTP. Treatment of slices with cyclopiazonic acid (CPA, 10 μM), which depletes intracellular Ca^{2+} stores (Seidler et al., 1989), eliminated the facilitation of $I_{K(Ca)}$ by synaptic stimulation (0% ± 2%, n = 6) as well as the induction of NMDAR LTP (2% ± 4% change, n = 6; Figures 3.7A-C). Consistent with its effects on intracellular Ca^{2+} stores and our previous study (Cui et al., 2007), CPA also decreased the size of $I_{K(Ca)}$ itself for single APs (2 ± 0 vs. 9 ± 1 pA·s for the 21 control LTP neurons from Figure 3.1, $p < 0.01$, ANOVA) and bursts (14 ± 2 vs. 34 ± 4 pA·s for the 21 control LTP neurons from Figure 3.1, $p < 0.05$, ANOVA). To circumvent the potential contaminating influence of decreasing this component of spike-evoked Ca^{2+} signals, we intervened further upstream in the Ca^{2+} signaling pathway by blocking the activation of PI-coupled receptors. We applied a cocktail of antagonists

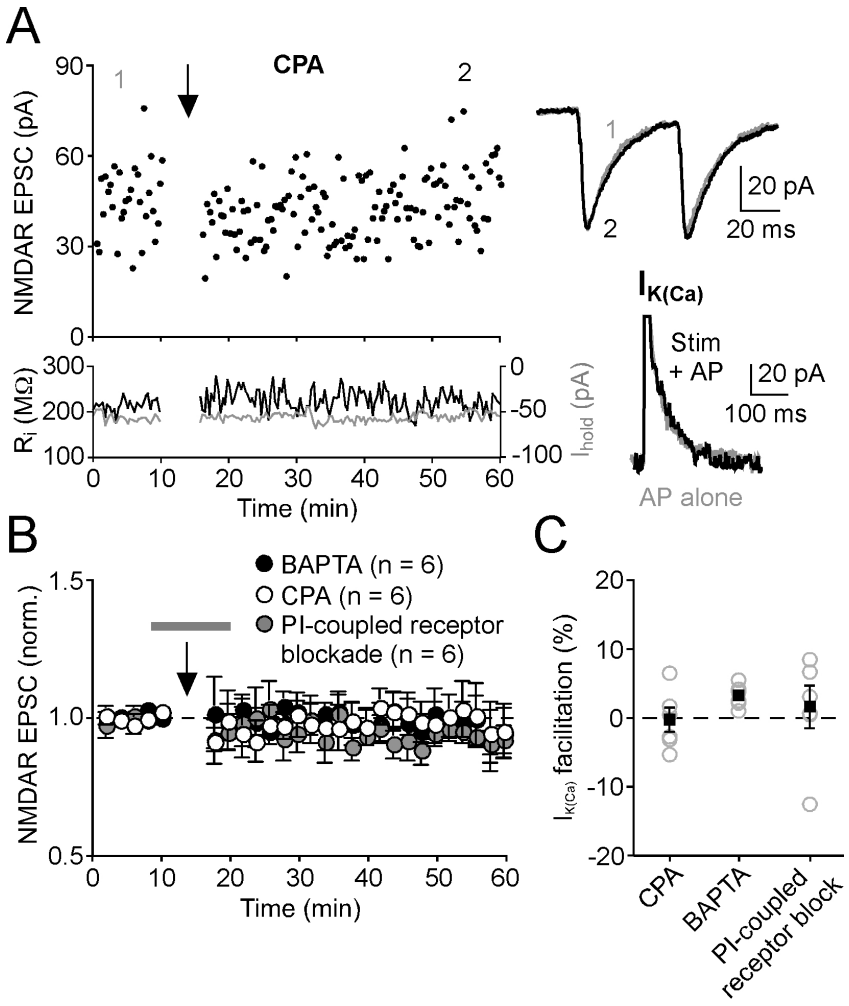

Figure 3.7. PI-Coupled Receptor Activation and Release of Ca^{2+} from Internal Stores Is Necessary for NMDAR LTP Induction.

(A) Time graph of a representative experiment conducted in the presence of CPA (10 μM). Sample traces to the right show average NMDAR EPSCs before (1) and after (2) synaptic stimulation-burst pairing (top traces) and $I_{K(Ca)}$ with (black) and without (gray) synaptic stimulation (bottom traces). Note the lack of facilitation of $I_{K(Ca)}$ by synaptic stimulation.

(B) Summary time graph of experiments conducted with 100 μM BAPTA in the patch pipette (black filled circles, n = 6), in the presence of CPA (open black circles, n = 6), and when PI-coupled receptors were blocked during the induction, as indicated by the gray bar, with a cocktail containing the $mGluR_1$ antagonist CPCCOEt (50-75 μM), the muscarinic acetylcholine receptor antagonist scopolamine (100 nM), and the α_1-adrenergic receptor antagonist prazosin (1 μM; gray filled circles, n = 6).

(C) Summary graph depicting lack of significant facilitation of $I_{K(Ca)}$ by synaptic stimulation in BAPTA, CPA, or during PI-coupled receptor blockade. Gray open circles indicate individual experiments; black squares represent mean.

including 75 μM CPCCOEt, 1 μM scopolamine and 100 nM prazosin to block $mGluR_1$, muscarinic acetylcholine and α_1-adrenergic receptors, respectively, all of which are PI-coupled and expressed in DA neurons (Fiorillo and Williams, 2000; Paladini and Williams, 2004). When applied immediately before and during pairing, the PI-coupled receptor antagonist cocktail abolished $I_{K(Ca)}$ facilitation (2% ± 3%, n = 6) and NMDAR LTP (-6% ± 4% change, n = 6; Figures 3.7B and 3.7C) without influencing $I_{K(Ca)}$ itself (single APs: 9 ± 3 pA·s, $p > 0.05$; bursts: 31 ± 7 pA·s, $p > 0.05$, both compared to the 21 control LTP neurons from Figure 3.1).

Finally, to rule out contributions from presynaptic or distributed network sources on Ca^{2+} signaling due to bath perfusion of CPA and the PI-coupled receptor antagonist cocktail, we confirmed that specifically loading the postsynaptic neuron with 100 μM BAPTA via the patch pipette blocked $I_{K(Ca)}$ facilitation (4% ± 1%, n = 6) and NMDAR LTP (-1% ± 5% change, n = 6; Figures 3.7B and 3.7C). Loading neurons with BAPTA was associated with a dramatic decrease in $I_{K(Ca)}$ itself (single APs: 2 ± 0 pA·s, $p < 0.01$; bursts: 7 ± 1 pA·s, $p < 0.01$, both compared to the 21 control LTP neurons from Figure 3.1) as would be expected from rapid and robust intracellular Ca^{2+} chelation of release from stores and/or voltage-gated Ca^{2+} influx through VACCs.

When considered in light of the data presented in Figures 3.1B and 3.1E, this series of experiments demonstrates that Ca^{2+} store-dependent enhancement of burst-induced Ca^{2+} signals by synaptic activation of PI-coupled metabotropic receptors is critical for LTP induction.

3.1.2.2 Protein Kinase A, but not Protein Kinase C, Regulates PI-coupled Receptor-Mediated Facilitation of Spike-Evoked Ca^{2+} Signals and the Induction of NMDAR LTP

The sensitivity of IP_3Rs to IP_3 can be increased by PKA-mediated phosphorylation (Tang et al., 2003; Wagner et al., 2008) while both PKA and PKC can regulate NMDARs in DA and other neurons (Borgland et al., 2006; Jia et al., 1998; Kwon and Castillo, 2008; Liao et al., 2001; Skeberdis et al., 2006; Ungless et al., 2003).

We therefore investigated the roles of PKA and PKC in facilitation of spike-evoked Ca^{2+} signaling and NMDAR LTP by loading recorded neurons with either the PKA inhibitor PKI (100-200 μM) or the PKC inhibitor Chelerythrine (10 μM) through the whole-cell pipette. We first tested the effect of PKI on the sensitivity of IP_3Rs to IP_3. By performing UV flash photolysis of caged IP_3 at different UV pulse intensities (expressed in μF; see Materials and Methods, section 2.8 and (Cui et al., 2007; Morikawa et al., 2000)) to vary the concentration of photoreleased IP_3, we could measure resulting SK-mediated outward currents (I_{IP3}) as a metric for IP_3R activation (Figure 3.8A). Intracellular PKI significantly increased the UV pulse intensity producing half maximal I_{IP3} amplitude (138 ± 12 μF in control, n = 5 vs. 220 ± 37 μF in PKI, n = 7, $p < 0.05$, unpaired t-test; Figure 3.8B), suggesting that IP_3 sensitivity is enhanced by tonic PKA activity. Although PKA is not known to modulate SK channel function, recent evidence indicates that PKA phosphorylation can regulate surface expression of SK2 channels (Lin et al., 2008; Ren et al., 2006). However, PKI failed to alter the maximal I_{IP3} amplitude in our experiments (data not shown). This may be due to the predominant expression of SK3 channels in DA neurons (Wolfart et al., 2001).

Intracellular PKI also significantly reduced the magnitude of $I_{K(Ca)}$ facilitation caused by bath perfusion of the mGluR agonist DHPG (1 μM) (92% ± 21% in control, n = 13 vs. 27% ± 10% in PKI, n = 10, $p < 0.01$, unpaired t-test; Figures 3.8C and 3.8D). In 5 PKI-loaded neurons that exhibited <20% $I_{K(Ca)}$ facilitation (9% ± 3%) in response to 1 μM DHPG, higher concentrations of DHPG (5-10 μM), which should further elevate cytosolic IP_3 levels, produced significantly larger $I_{K(Ca)}$ facilitation (221% ± 51%, $p < 0.05$, paired t-test; Figure 3.8E), consistent with the idea that PKI reduced the IP_3 sensitivity of IP_3Rs.

We next tested the effect of PKI on NMDAR LTP. Intracellular PKI suppressed facilitation of $I_{K(Ca)}$ by synaptic stimulation (9% ± 3%, n = 7) as well as the induction of LTP (-3% ± 6% change, n = 7; Figures 3.8F and 3.8G). In contrast, intracellular dialysis with the PKC inhibitor chelerythrine (10 μM), which has been shown to block LTP of NMDARs in the hippocampus (Kwon and Castillo, 2008), had no significant effect on

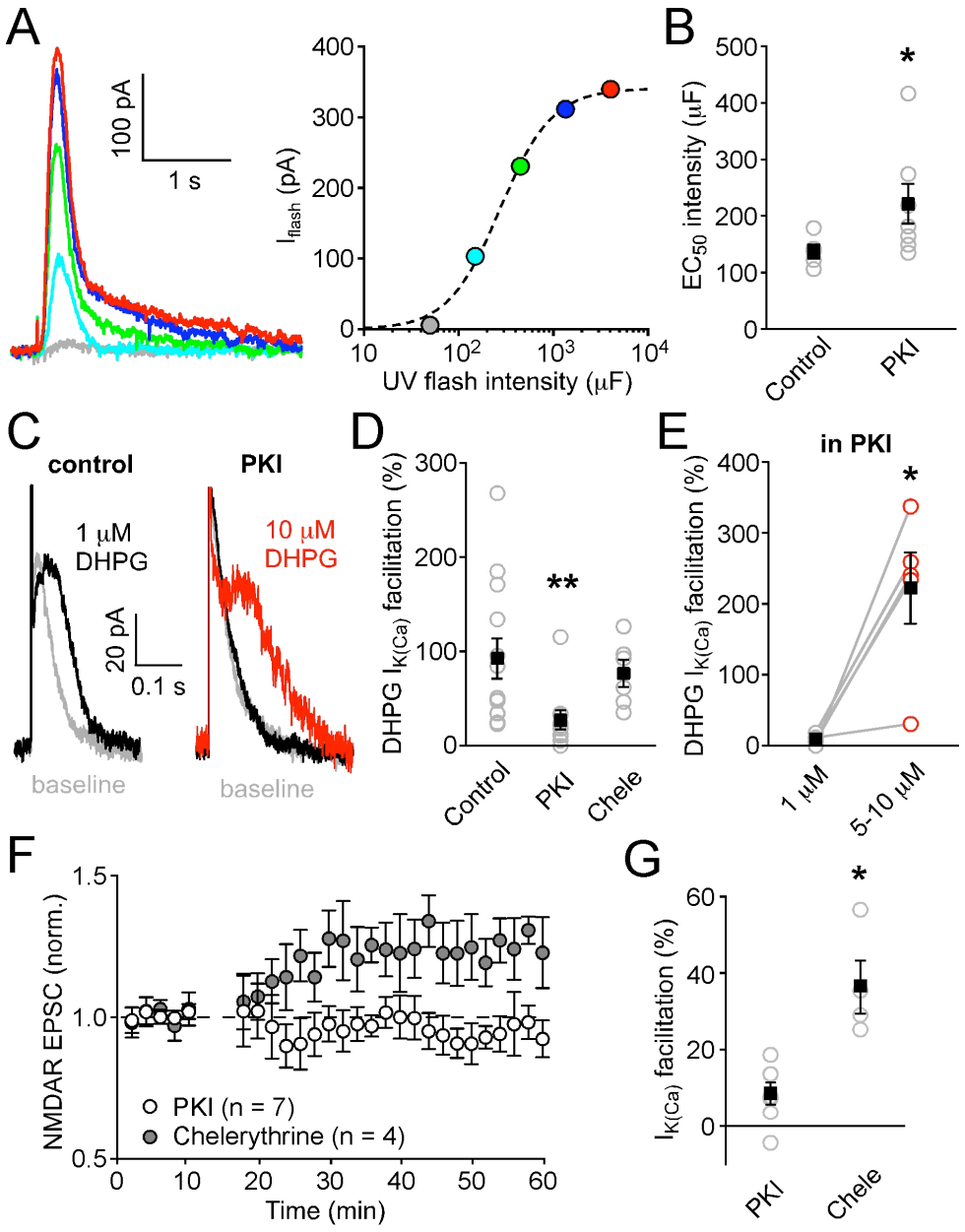

Figure 3.8. PKA Regulates IP_3 Sensitivity and Gates NMDAR LTP Induction.
(A) Left: Traces of I_{IP3} evoked with different UV pulse intensities in a PKI-loaded neuron. Colors indicate UV pulse intensity as shown in the plot at right, expressed in terms of the capacitance (μF) of the flash photolysis system. Dotted line represents fit to a logistic equation. EC_{50} intensity was 275 μF in this neuron.
(B) PKI (n = 7) significantly increased the EC_{50} intensity of I_{IP3} compared to control internal solution (n = 5, $p < 0.05$).

(C) Representative traces illustrating the effects of DHPG on single AP-evoked $I_{K(Ca)}$ recorded with control internal solution (left) or PKI (right). Facilitation of $I_{K(Ca)}$ could be reconstituted in PKI with a higher concentration of DHPG (red trace at right).
(D) PKI (n = 10), but not chelerythrine (n = 6), significantly reduced the effect of 1 μM DHPG on $I_{K(Ca)}$ ($p < 0.01$ vs. control internal solution, n = 13).
(E) The effects of DHPG at 1 μM vs. 5-10 μM are plotted for 5 PKI-loaded neurons ($p < 0.05$).
(F) Summary time graph showing that PKI (black open circles, n = 7), but not chelerythrine (gray filled circles, n = 4), blocked NMDAR LTP.
(G) Summary of $I_{K(Ca)}$ facilitation by synaptic stimulation in PKI and chelerythrine for experiments shown in (F; $p < 0.01$). Gray open circles indicate individual experiments; black squares represent mean.

facilitation of $I_{K(Ca)}$ by either DHPG perfusion (Figure 3.8D) or synaptic stimulation (Figure 3.8G), or on LTP of NMDARs (Figure 3.8F).

PKA activity thus regulates the induction of NMDAR LTP by augmenting PI-coupled receptor-mediated facilitation of Ca^{2+} signals. However, PKC does not appear to influence spike-evoked Ca^{2+} signals or plasticity of NMDARs in DA neurons.

3.1.2.3 NMDAR LTP is DA-Independent

Burst firing of DA neurons may provide a synaptic plasticity "teaching signal" in projection areas via synchronized, phasic DA release, thus driving reward-based learning (Reynolds et al., 2001; Schultz, 1998). DA neuron bursts may also trigger local Ca^{2+}-dependent release of DA in the SNc and/or VTA (Beckstead et al., 2004; Chen and Rice, 2001; Vandecasteele et al., 2008). Furthermore, activation of DA $D_{1/5}$ receptors by bath perfusion of agonists can produce enhancement of NMDAR EPSCs (Schilstrom et al., 2006), raising the possibility that local DA may play a role in LTP induction. However, significant NMDAR LTP was observed (38% ± 9% change, n = 5) when the DA $D_{1/5}$ receptor antagonist SCH 23390 (1 μM) was present during pairing (Figure 3.9). The DA D_2 receptor antagonist eticlopride (100-200 nM) was always present in the extracellular solution of all experiments presented in this study to block D_2 receptor-mediated IPSCs (Beckstead et al., 2004). Thus, DA release is not involved in the induction of NMDAR LTP by burst-pairing in DA neurons.

3.1.2.4 NMDAR Activation is Necessary for the Induction of NMDAR LTP

Recent studies on the plasticity of NMDARs at hippocampal mossy fiber synapses indicate that activation of NMDARs, in addition to activation of mGluRs, is required during LTP induction (Kwon and Castillo, 2008; Rebola et al., 2008). In order to test this possibility in DA neurons, we acutely blocked NMDARs with the NMDAR antagonist DL-AP5 (50-100 μM) immediately before and during induction (Figure 3.10). Perfusion of DL-AP5 after 10 min of baseline recording rapidly and completely blocked NMDAR EPSCs (from 44 ± 11 pA to 2 ± 1 pA, n = 4); the burst pairing protocol was

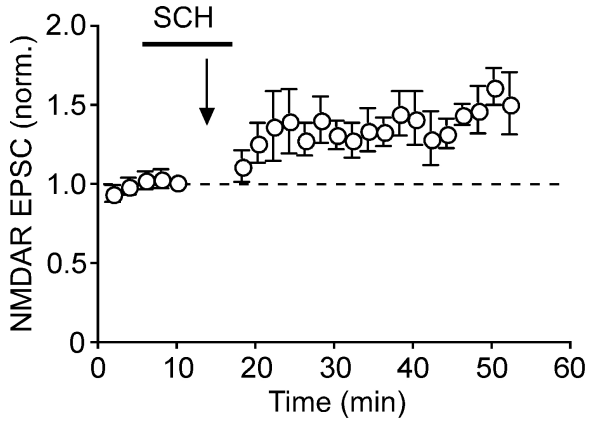

Figure 3.9. NMDAR LTP Does Not Require DA Receptor Activation.
Summary time graph of plasticity experiments where SCH 23390 (1 μM) was perfused during the induction protocol (as indicated by the black back; n = 5). All experiments were conducted with 100 nM Eticlopride in the aCSF. Each symbol represents mean ± SEM.

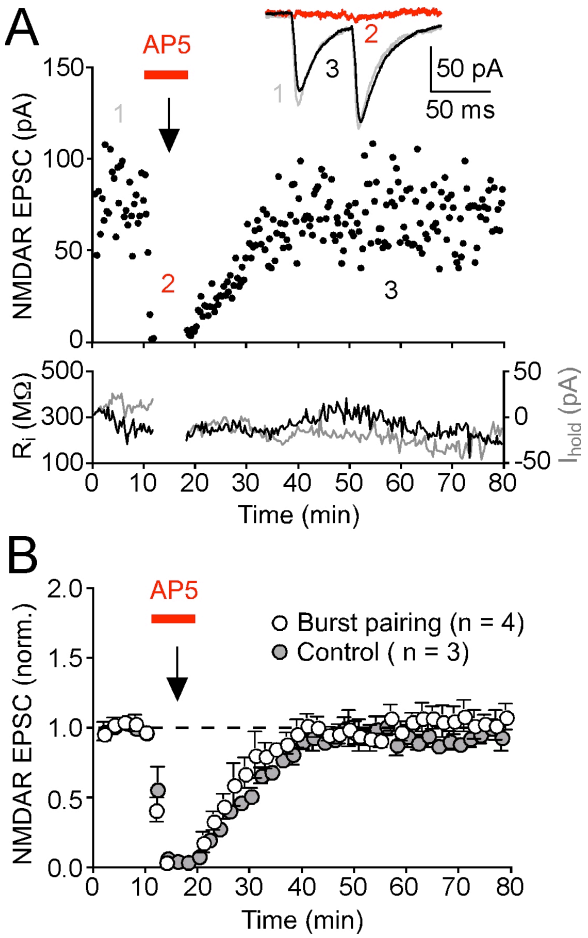

Figure 3.10. NMDAR LTP Requires NMDAR Activation During Synaptic Stimulation-Burst Pairing.

(A) Transiently blocking NMDARs with DL-AP5 (100 μM) during delivery of the induction protocol, as indicated by the red bar, prevented the development of LTP in this example experiment. Average NMDAR EPSCs taken at the times indicated are shown in inset for control (1), in AP5 (2), and after LTP induction and AP5 washout (3).

(B) Summary time graph of experiments where LTP was blocked by DL-AP5 (50-100 μM) perfused during the induction (n = 4). Summary of control experiments is also shown, where DL-AP5 (100 μM) was perfused and washed out without delivery of the induction protocol (n = 3).

delivered thereafter. DL-AP5 was washed out immediately after induction. Despite robust facilitation in all neurons tested (56% ± 13%, n = 4), none exhibited LTP of NMDAR EPSCs (-1% ± 2% change; Figure 3.10B). We further confirmed that the washout of DL-AP5 (100 μM) was complete in ~30 min when no burst pairing protocol was delivered (n = 3; Figure 3.10B). These results indicate that, similar to reports of NMDAR plasticity in other systems, the induction of NMDAR LTP in DA neurons by burst-pairing requires the activation of NMDARs themselves.

3.1.3 BURST-TIMING DEPENDENCE OF SYNAPTIC FACILITATION OF SPIKE-EVOKED CA^{2+} SIGNALS AND NMDAR PLASTICITY

Reward-based reinforcement learning, like most forms of learning, exhibits distinct temporal characteristics in behaving animals (Contreras-Vidal and Schultz, 1999; Delamater and Oakeshott, 2007; Hyman et al., 2006a; Ljungberg et al., 1992; Niv et al., 2005; Pan et al., 2005; Redish, 2004; Schultz, 1998, 2002, 2006; Waelti et al., 2001). In the standard and most effective training paradigm, termed delay conditioning, there is a delay of hundreds of milliseconds to several seconds between the onset of the cue and that of the reward, with the two stimuli overlapping in time (Fiorillo et al., 2003; Schwartz et al., 2002). In this case, the cue reliably predicts the reward at a set interval, making the computational process to link the two stimuli relatively simple. However, when the converse situation occurs, *i.e.* the reward is presented prior to the cue (backward conditioning), little to no learning occurs (Schwartz et al., 2002) because reward delivery is not contingent; there are no reward predictors, only post-reward stimuli. Due to these well-characterized features of reward learning, we examined the burst timing-dependence of NMDAR LTP at DA neurons to see if this cellular process could be congruent with what occurs in behaving animals by systematically varying the time at which the postsynaptic burst of APs was evoked relative to the presynaptic stimulation train (diagrammed in the boxed inset in Figure 3.11B). An important procedural note about these experiments is that all neurons were first tested for

facilitation of $I_{K(Ca)}$ at the routine 1 s timing interval with a single AP, as per the previous experiments described above and in Materials and Methods, section 2.6. These values are shown in Table 3.1. Facilitation of $I_{K(Ca)}$ at the timing interval at which pairing was conducted was also measured for each neuron and the relative facilitation, normalized to that observed at the routine 1 s delay, was reported below and in Figure 3.11. Thus, all neurons included for analysis expressed >15% faciltation of $I_{K(Ca)}$ at the conventional timing interval (1 s), and should express LTP if properly induced, as per Figure 3.1B.

3.1.3.1 Decreasing the Latency Between the Onset of Synaptic Stimulation and Postsynaptic Burst Firing

In the routine burst-pairing induction protocol, there is a 1-s delay between the onset of the 1.4-s synaptic stimulation train and that of the burst (see schematic and example traces in Figure 3.1A). Our first step in analyzing the timing-dependence of plasticity was to omit this delay; *i.e.* shift the onset of the burst forward in time to coincide with the onset of synaptic stimulation. Under this contingency, no LTP was induced (-3% ± 10% change, n = 4; Figure 3.11C). Similarly, no significant LTP was observed when the burst was elicited with a delay of 200 ms after the onset of synaptic stimulation (3% ± 5% change, n = 3). However, some LTP was induced when the burst occurred with a 500-ms delay during the pairing protocol (20% ± 6% change, n = 5), although reduced in magnitude compared to the LTP induced with a 1-s burst delay. In line with these observations, we found that the magnitude of $I_{K(Ca)}$ facilitation increased at longer delays between the onset of synaptic stimulation and burst firing in these neurons tested for the burst-timing dependence of LTP induction (Figure 3.11D), most likely reflecting gradual increases in cytosolic IP_3 levels associated with metabotropic receptor activation and the subsequent PI-hydrolysis cascade.

In a separate series of experiments, we directly examined the Ca^{2+} dynamics associated with this timing-dependence by fluorescence imaging of burst-induced Ca^{2+} signals after filling neurons with the Ca^{2+} indicator fluo-5F (50 μM) through the patch pipette. The magnitude of facilitation of burst-evoked fluorescence change also increased

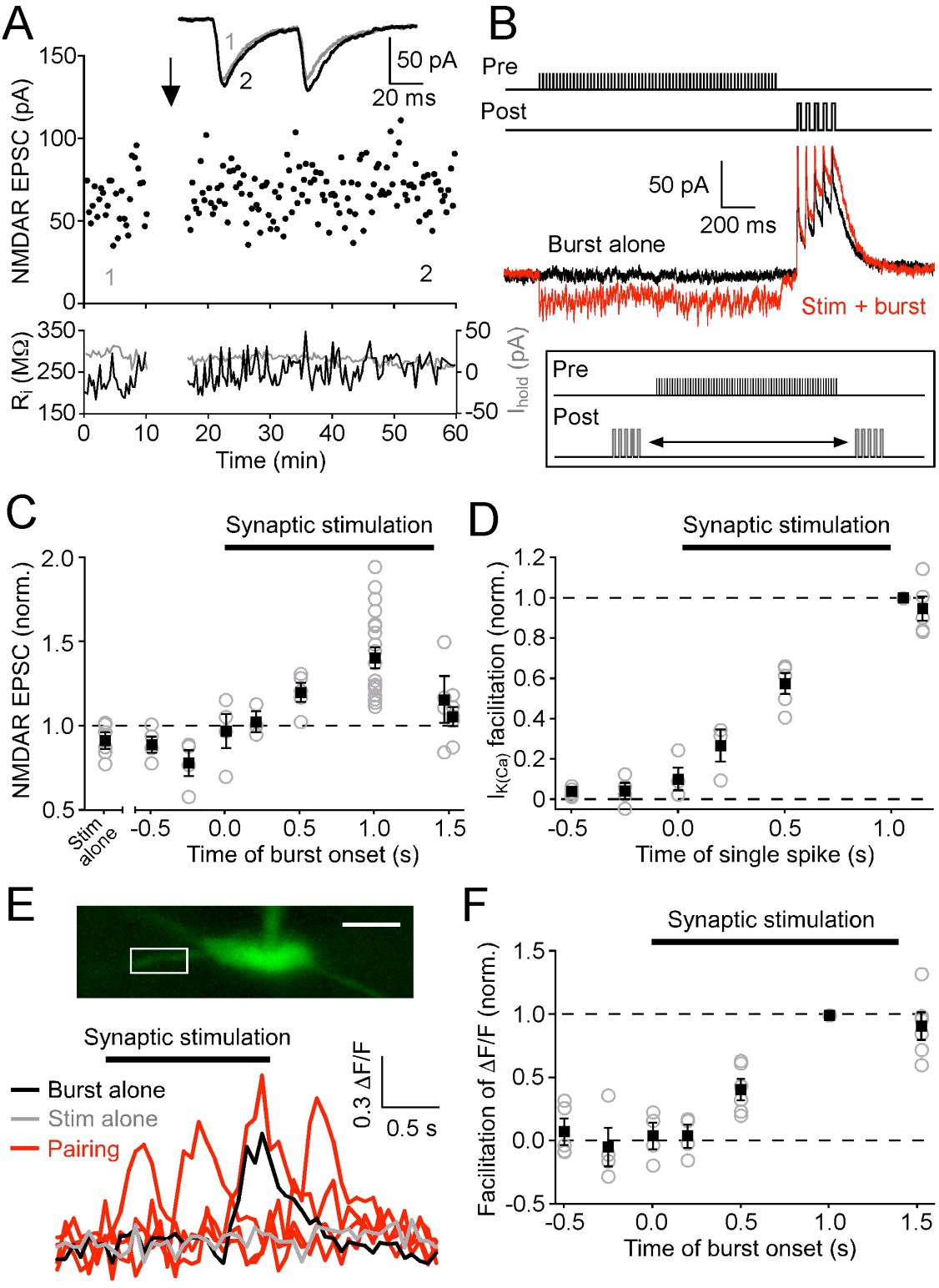
A
NMDAR EPSC (pA)
150
100
50
0
50 pA
20 ms
1
2
R_i (MΩ)
350
250
150
50
0
-50
I_{hold} (pA)
0
10
20
30
40
50
60
Time (min)
B
Pre
Post
50 pA
200 ms
Burst alone
Stim + burst
Pre
Post
C
Synaptic stimulation
NMDAR EPSC (norm.)
2.0
1.5
1.0
0.5
Stim alone
-0.5
0.0
0.5
1.0
1.5
Time of burst onset (s)
D
Synaptic stimulation
$I_{K(Ca)}$ facilitation (norm.)
1.2
1.0
0.8
0.6
0.4
0.2
0
-0.5
0.0
0.5
1.0
Time of single spike (s)
E
Synaptic stimulation
Burst alone
Stim alone
Pairing
0.3 ΔF/F
0.5 s
F
Synaptic stimulation
Facilitation of ΔF/F (norm.)
1.5
1.0
0.5
0.0
-0.5
-0.5
0.0
0.5
1.0
1.5
Time of burst onset (s)

Figure 3.11. Burst Timing-Dependence of NMDAR Plasticity and Associated Ca^{2+} Signals.

(A) Example experiment in which the burst was delayed by 120 ms after the offset of synaptic stimulation train during pairing, as illustrated at top right in (B).

(B) Middle: Sample traces show the response to postsynaptic burst alone (black) and synaptic stimulation-burst pairing with a 120-ms delay (red). Average EPSCs before (1) and after (2) 120-ms delay pairing taken at the times indicated are shown inset, top left. Box at bottom shows schematic representation of the experimental paradigm used to investigate the timing dependence of facilitation of spike-evoked Ca^{2+} signals and plasticity.

(C) Summary graph depicting the burst-timing dependence of NMDAR plasticity. The magnitude of LTP/LTD is plotted versus time of burst onset relative to the onset of 1.4-s synaptic stimulation (black bar) during the induction protocol. Individual experiments are shown as gray open circles; black squares represent mean. Data for the 1-s delay (n = 21) are from control LTP experiments with $I_{K(Ca)}$ facilitation >15% shown in Figure 1B, while the data for synaptic stimulation alone are from Figure 1E.

(D) Summary graph illustrating the timing dependence of $I_{K(Ca)}$ facilitation assessed using 1-s synaptic stimulation. Data are from neurons shown in (C); 21 neurons in the control LTP experiments with 1-s delay are not included. In order to measure $I_{K(Ca)}$ facilitation, a single AP was evoked at the indicated time relative to 1-s synaptic stimulation. The amount of $I_{K(Ca)}$ facilitation thus obtained was normalized to that measured at 60 ms after the offset of synaptic stimulation in each neuron. Therefore, data in the “60 ms after offset” group are all normalized to unity. Gray open circles represent data from individual experiments; black squares indicate mean.

(E) Example experiment imaging burst-evoked Ca^{2+} signals at various synaptic stimulation-burst timing intervals. Fluorescence changes were measured at the ROI indicated in the confocal fluorescence image of a DA neuron filled with fluo-5F (scale bar: 20 μm). Black and gray traces represent burst alone and synaptic stimulation alone, respectively, while red traces represent synaptic stimulation-burst pairing, in which the burst was evoked at onset, 500 ms after onset, 1 s after onset, and 120 ms after offset of 1.4-s synaptic stimulation (black bar).

(F) Summary graph showing the timing dependence of synaptic facilitation of burst-evoked Ca^{2+} signals. Facilitation is plotted versus time of burst onset relative to the onset of 1.4-s synaptic stimulation (black bar). The magnitude of facilitation was normalized to that produced when burst was elicited 1 s after onset of synaptic stimulation in each neuron. Gray open circles represent data from individual experiments, while black squares indicate mean.

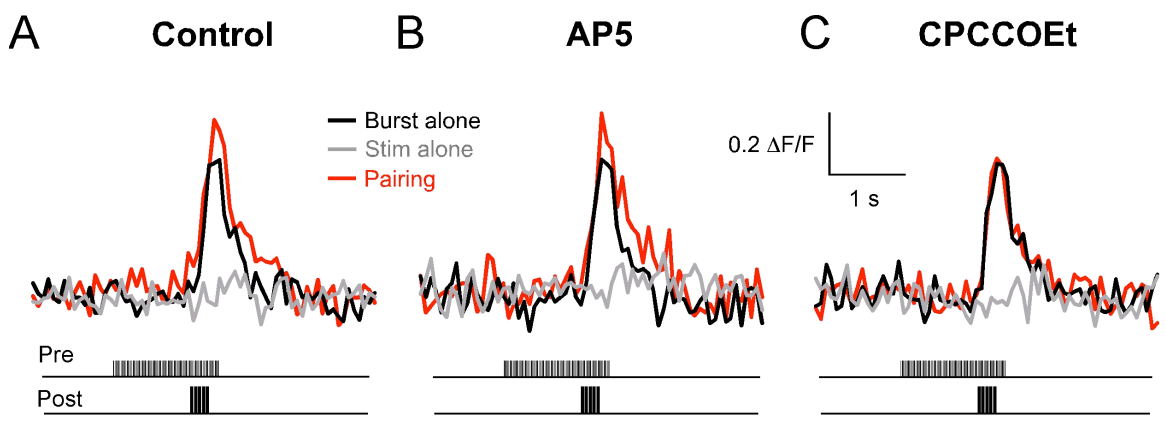

Figure 3.12. Example Pharmacology of Synaptic Facilitation of Burst-Evoked Ca^{2+} Signals during Imaging.
(A) Ca^{2+} fluorescence signal produced by a burst of 5 APs at 20 Hz (black trace) was facilitated (red trace) by 1.4-s synaptic stimulation, which evoked no detectable change in fluorescence by itself (gray trace). Experimental protocol is diagrammed below.
(B) Perfusion of DL-AP5 (100 μM) had no effect on fluorescence signals associated with burst alone (black trace), synaptic stimulation alone (gray trace), or synaptic stimulation-burst pairing (red trace).
(C) Perfusion of CPCCOEt (75 μM) in addition to DL-AP5 blocked synaptic facilitation of burst-evoked fluorescence change.

as the delay between the onset of synaptic stimulation and that of the burst was prolonged up to 1 s in 6 neurons tested (Figures 3.11E and 3.11F). Synaptic stimulation increased burst-evoked fluorescence change by 35% ± 5% (n = 6) at the routine 1-s delay. This increase was abolished by CPCCOEt (75 μM, n = 2; Figure 3.12), consistent with the role of $mGluR_1$ in synaptic facilitation (Cui et al., 2007), but was unaffected by DL-AP5 (50-100 μM, n = 4; Figure 3.12). No AP5-sensitive fluorescence change was observed with synaptic stimulation alone (Figure 3.12), indicating that NMDAR-mediated Ca^{2+} influx during synaptic stimulation did not contribute to the fluorescence signals detected with our imaging system.

3.1.3.2 Delaying the Postsynaptic Burst after the Offset of Synaptic Stimulation

Next, we delayed the burst until after the offset of the synaptic stimulation train. This resulted in a significant decrease in LTP with an interval of 60 ms (13% ± 14% change, n = 4) and near complete lack of LTP with a 120-ms interval (6% ± 5% change, n = 5; Figures 3.11A and 3.11C). In the 5 neurons in which pairing was conducted with a 120-ms interval, facilitation of $I_{K(Ca)}$ at 120 ms after the offset of synaptic stimulation was indistinguishable from that at 60 ms, the interval routinely used to assess $I_{K(Ca)}$ facilitation (Figure 3.11D).

Furthermore, Ca^{2+} imaging experiments confirmed that facilitation of burst-evoked fluorescence change was not significantly reduced when the burst was elicited at 120 ms after the offset of the 1.4-s synaptic stimulation train (Figures 3.11E and 3.11F), indicating that the decrease in LTP is not due to a reduction in synaptic facilitation of Ca^{2+} signaling. Indeed, IP_3-mediated enhancement of Ca^{2+} signals has been shown to last for hundreds of milliseconds because of prolonged lifetime of IP_3 binding to IP_3Rs (Sarkisov and Wang, 2008). In contrast, NMDAR EPSCs evoked by synaptic stimulation decayed by 80% ± 4% at 60 ms after the offset of stimulation in the 4 neurons tested at 60-ms interval for LTP induction, while the decay of NMDAR EPSCs was almost complete (96% ± 1%) at 120 ms in the 5 neurons tested for 120-ms interval. This implies that the burst may need to occur while NMDARs are activated during induction.

Therefore, the burst-timing dependence of LTP induction described here is shaped by the requirements for both PI-coupled receptor-mediated facilitation of burst-induced Ca^{2+} signals (Figures 3.1 and 3.7) and activation of NMDARs (Figure 3.10).

3.1.3.3 Negative Timing Intervals

Finally, we evoked burst firing before the onset of synaptic stimulation during induction to mimic backward conditioning. Sizable LTD of NMDARs was observed when the onset of the burst was placed 250 ms before that of the synaptic stimulation train (-22% ± 7% change, n = 4; Figure 3.11C). There was no significant change in either PPR or $1/CV^2$ after expression of LTD (0.84 ± 0.07 vs. 0.86 ± 0.06 and 41 ± 12 vs. 39 ± 10, respectively; $p > 0.5$ for both parameters, paired t-tests), suggesting a postsynaptic locus of LTD expression as for LTP (Figure 3.1D). When the interval between burst onset and synaptic stimulation was increased to 500 ms, where the burst-induced Ca^{2+} signal had minimal overlap, if any, with synaptic stimulation, the magnitude of LTD was reduced to a level comparable to that induced by presynaptic stimulation alone (500 ms before onset: -10% ± 4% change, n = 4 vs. stim alone: -8% ± 4% change, n = 6, $p > 0.5$, unpaired t-test). Stim alone data are from Figure 3.1E.

These results demonstrate that the relative timing between presynaptic stimulation and postsynaptic burst firing determines the direction and the magnitude of NMDAR plasticity in a manner congruent with what has been described for reward-based reinforcement learning in behaving animals.

3.1.4 INPUT SPECIFICITY AND SPIKE-CONDITIONAL REVERSIBILITY OF NMDAR PLASTICITY

3.1.4.1 NMDAR LTP Is Input Specific

The involvement of NMDAR activation in the induction of NMDAR LTP raises the possibility that NMDARs may be potentiated specifically at those synapses

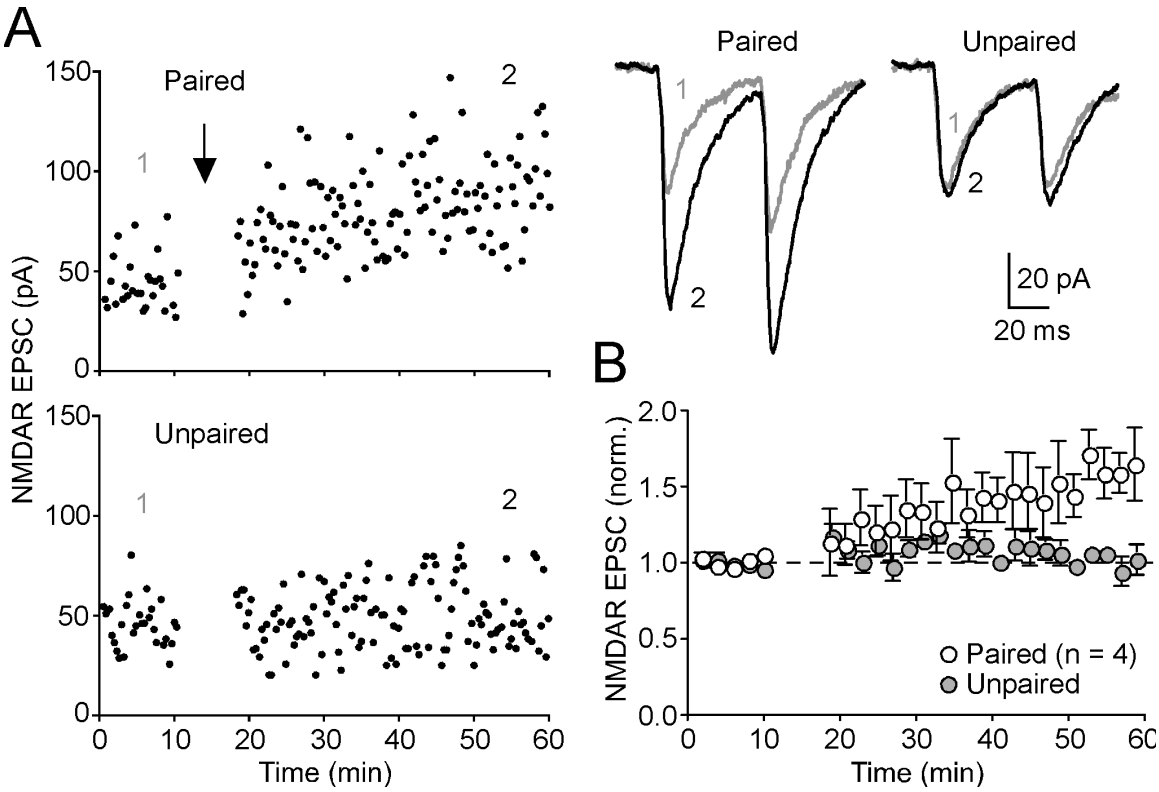

Figure 3.13. Input Specificity of NMDAR LTP.
(A) Time graphs of a representative experiment where two independent pathways were alternately stimulated via two extracellular electrodes while recording from a single neuron. During the induction, only one pathway was stimulated in conjunction with postsynaptic bursting (top, "paired"), while the other pathway was held silent (bottom, "unpaired"). Sample traces at top right show average NMDAR EPSCs taken at the times indicated for the paired (left) and unpaired (right) pathways.
(B) Summary time graph of NMDAR LTP in paired versus unpaired pathways in 4 neurons.

stimulated during induction. To test this possibility, we placed two stimulating electrodes rostal to the recorded neuron but separated from each other by >100 μm along the medio-lateral axis. After confirming the independence of the two pathways (see Materials and Methods, section 2.7), we monitored NMDAR EPSCs in each pathway for 10 min. Once a stable baseline was established, one pathway received sustained synaptic stimulation paired with burst firing while the other pathway was held silent (Figure 3.13). This produced significant LTP in the paired pathway with little change in the unpaired pathway (paired pathway: 65% ± 16% change vs. unpaired pathway: 2% ± 2% change, n = 4, $p < 0.05$, paired t-test), demonstrating that NMDAR LTP can be input specific.

3.1.4.2 Spike-Conditional Reversal of NMDAR LTP

It has been demonstrated that synapses that have undergone LTP can be "depotentiated" (Fujii et al., 1991; Kim et al., 2007; O'Dell and Kandel, 1994), usually by low frequency and/or intensity stimulation. Indeed, synaptic plasticity induced by correlated presynaptic and postsynaptic activity can be reversed by presynaptic stimulation in the absence of postsynaptic activation (Bellone and Nicoll, 2007; Fujii et al., 1991; Kim et al., 2007; Massey and Bashir, 2007; O'Dell and Kandel, 1994). To examine if NMDAR LTP could be reversed in DA neurons, we repeatedly delivered synaptic stimulation (10 times every 20 s) in the absence of postsynaptic activity ("pre alone", diagrammed in red inset at bottom of Figure 3.14B) 30 min after inducing LTP of NMDAR EPSCs (30% ± 6% change, n = 4; Figures 3.14A and 3.14B). This depotentiation protocol rapidly depressed previously potentiated NMDAR EPSCs back towards baseline in all 4 neurons tested (baseline: 59 ± 9 pA, LTP: 75 ± 10 pA, post-depotentiation: 57 ± 9 pA). Depotentiation was not associated with a change in either PPR or $1/CV^2$ (0.99 ± 0.10 vs. 1.00 ± 0.10 and 19 ± 4 vs. 17 ± 4, respectively; $p > 0.5$ for both parameters, paired t-test; Figures 3.14H and 3.14I). It should be noted that the same procedure, *i.e.* delivery of synaptic stimulation alone, also induced a small but rapid LTD of control EPSCs that had not undergone LTP induction (-8% ± 4% change, n = 6) (Figure 3.1E).

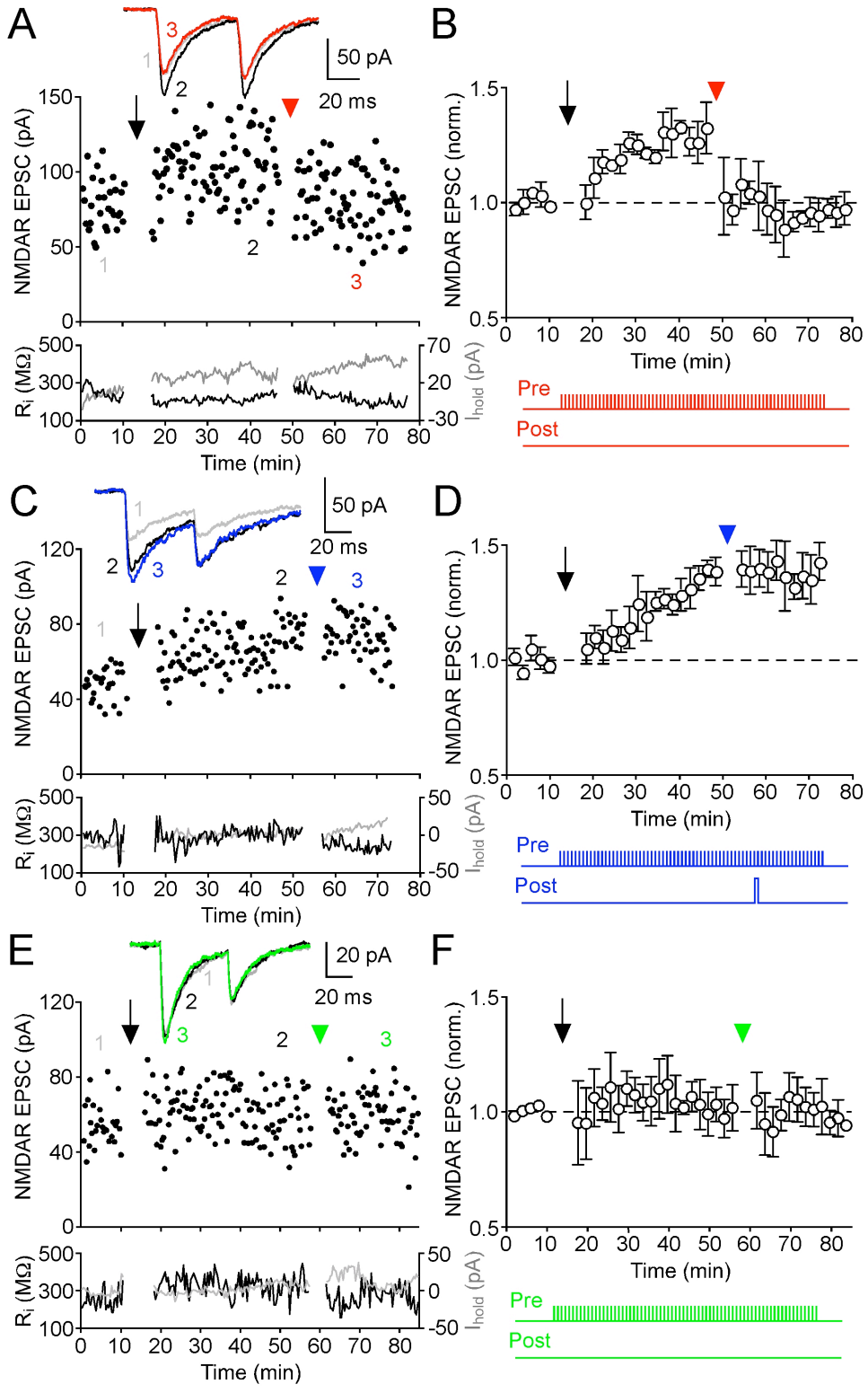
A
B
C
D
E
F
50 pA
20 ms
20 pA
NMDAR EPSC (pA)
NMDAR EPSC (norm.)
Ri (MΩ)
Ihold (pA)
Time (min)
Pre
Post

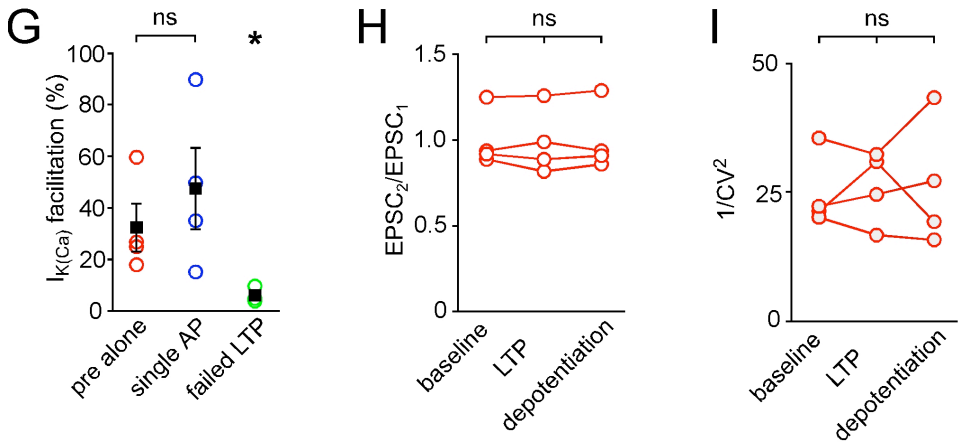

Figure 3.14. Spike-conditional reversal of NMDAR LTP.
(A) Representative experiment showing that repeated synaptic stimulation can depotentiate previously potentiated NMDAR EPSCs. The black arrow indicates LTP induction by synaptic stimulation-burst pairing, while the red arrowhead indicates the delivery of the depotentiation protocol consisting of synaptic stimulation alone. Average NMDAR EPSCs taken at the times indicated are shown in inset for control (1), after LTP (2), and after depotentiation (3).
(B) Summary time graph of depotentiation experiments (n = 4). Burst pairing protocol was delivered at the black arrow to induce LTP, while the depotentiation protocol (shown below in red) was applied at the red arrowhead.
(C) Time course of a representative experiment in which pairing synaptic stimulation with single postsynaptic APs during the depotentiation protocol prevented reversal of previously induced NMDAR LTP. LTP was induced at the black arrow, while the synaptic stimulation-single AP pairing protocol was applied at the blue arrowhead. Average NMDAR EPSCs are shown in inset for control (1), after LTP (2), and after single-AP pairing (3).
(D) Summary time graph of depotentiation experiments conducted by pairing synaptic stimulation with single postsynaptic spikes (shown below in blue; n = 4).
(E) Example experiment in which lack of facilitation of $I_{K(Ca)}$ during pairing resulted in no LTP and subsequently no depotentiation after presynaptic stimulation alone. Pairing was conducted at the black arrow while the depotentiation protocol was delivered at the green arrowhead. Average traces are shown inset at indicated times.
(F) Summary time graph of experiments showing that failure of LTP resulted in the ineffectiveness of the depotentiation protocol in depressing NMDAR EPSCs. Pairing was applied at the black arrow while the depotentiation protocol (shown below in green) was applied at the green arrowhead (n = 3).
(G) Summary of synaptic facilitation of $I_{K(Ca)}$ for the three different depotentiation experimental groups. LTP failure was presumably due to insufficient facilitation of spike-evoked Ca^{2+} signaling ($p < 0.05$), as per Figure 1B.

(H & I) Depotentiation was not accompanied by a change in either the paired pulse ratio (H) or in the coefficient of variation (I) of NMDAR EPSCs. Data are from the 4 neurons in (B).

We next inserted a single AP into the depotentiation protocol at 1 s after the onset of synaptic stimulation (the same interval as the burst in the pairing protocol, diagrammed in the blue inset at bottom of Figure 3.14D). Surprisingly, paring synaptic stimulation with single APs completely prevented depotentiation in 4 out of 4 neurons (baseline: 53 ± 3 pA, LTP: 71 ± 3 pA, post-single AP pairing: 71 ± 3 pA; Figures 3.14C and 3.14D). The same protocol also produced no change in control NMDAR EPSCs that had not undergone LTP induction (1% ± 8% change, n = 5; Figure 3.1E). Thus, synaptic stimulation paired with single spikes had no effect on NMDAR EPSCs regardless of whether they had been previously potentiated.

Finally, we investigated the effects of the depotentiation protocol in neurons that exhibited a lack of facilitation of $I_{K(Ca)}$ during the delivery of the burst-pairing protocol and thus failed to express LTP. In 3 neurons which expressed only 6% ± 2% $I_{K(Ca)}$ facilitation (Figure 3.14G), presynaptic stimulation alone had no effect on EPSCs that had not undergone LTP (baseline: 68 ± 7 pA, LTP: 71 ± 8 pA, post-depotentiation: 67 ± 7 pA; Figures 3.14E and 3.14F).

These results show that NMDAR LTP can be reversed in a spike conditional manner, which may depend on either the amount of PI-coupled receptor activation during depotentiation or previous expression of LTP.

3.1.5 NMDAR LTP IS UNLIKELY TO BE ASSOCIATED WITH A CHANGE IN SUBUNIT COMPOSITION

It has been shown that bath application of orexin A or DA $D_{1/5}$ receptor agonists produces long-lasting increases in NMDAR EPSCs via changes in the composition of NR2 subunits of NMDARs in DA neurons (Borgland et al., 2006; Schilstrom et al., 2006). An activity-dependent switch in NR2 subunit composition has also been reported at neonatal hippocampal synapses (Bellone and Nicoll, 2007). We therefore tested if burst-dependent LTP of NMDARs in DA neurons is also associated with a change in the subunit composition by comparing the effects of NMDAR subunit specific antagonists on

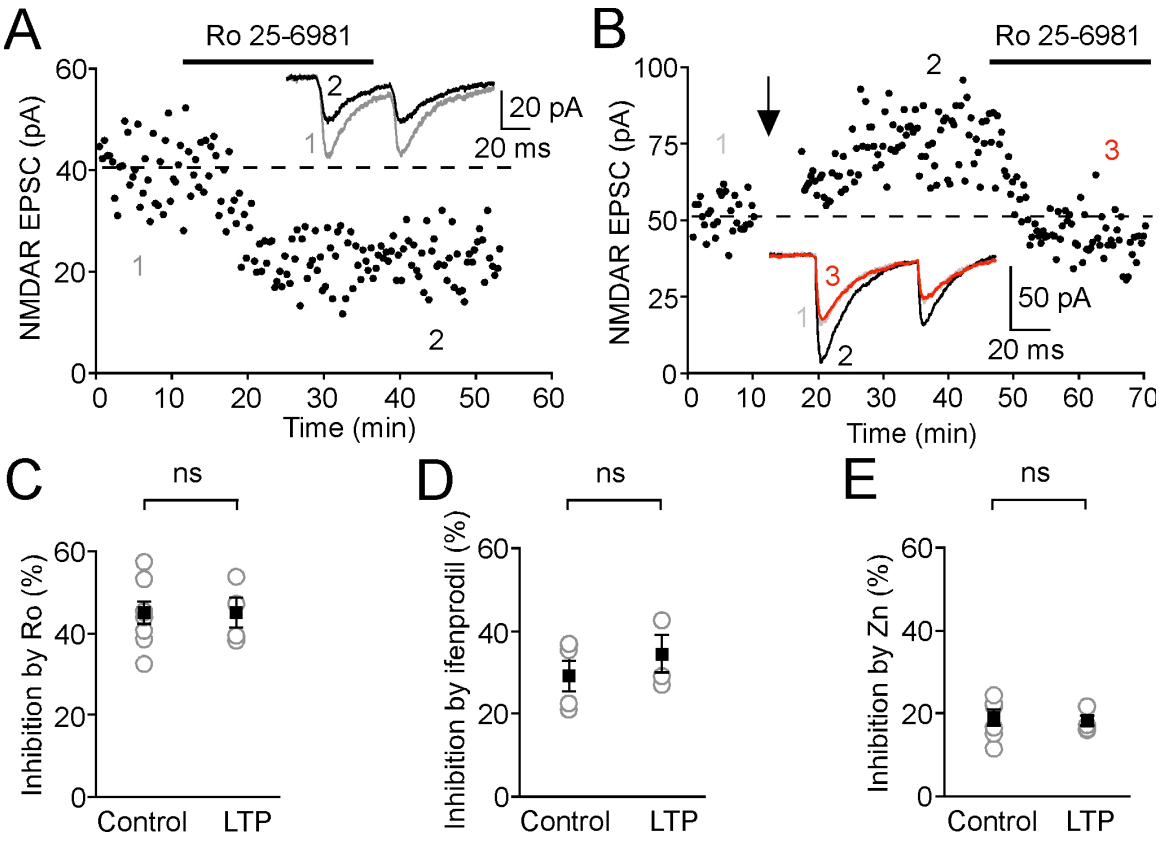

Figure 3.15. NMDAR LTP Is Unlikely to Be Expressed via a Change in NR2 Subunit Composition.

(A) Representative time graph showing the effect of Ro 25-6981 (1 μM) on control NMDAR EPSCs. Ro 25-6981 was perfused during the time indicated by the black bar. Average EPSCs before (1) and after Ro 25-6981 application (2) are shown in inset.

(B) Representative time graph depicting the effect of Ro 25-6981 (1 μM) on NMDAR EPSCs after successful induction of LTP. Burst pairing protocol was delivered at the arrow, while Ro 25-6981 was perfused during the time indicated by the black bar. Inset shows average EPSCs before (1) and after (2) LTP induction, together with the average EPSC after Ro 25-6981 application (3).

(C-E) Summary of the effects of Ro 25-6981 (1 μM; C), ifenprodil (3 μM; D), and Zn^{2+} (100 nM; E) on control NMDAR EPSCs (n = 6, n = 4, and n = 6, respectively) and potentiated EPSCs after LTP induction (n = 4, n = 3, and n = 4, respectively). Gray circles indicate data from individual neurons; black squares indicate mean ± SEM.

control NMDAR EPSCs versus potentiated EPSCs after successful LTP induction. We used three different NR2 subtype-specific antagonists: Ro 25-6981 (1 μM) and ifenprofil (3 μM), both NR2B-containing receptor antagonists, and Zn^{2+} (100 nM), an NR2A-containing receptor antagonist (Borgland et al., 2006; Fischer et al., 1997; Paoletti et al., 1997; Williams, 1993). None of these antagonists showed differential effects on control versus potentiated NMDAR EPSCs (Figure 3.15A-E), suggesting that the burst pairing protocol induces NMDAR LTP without a change in the relative NR2A or NR2B subunit-containing composition of NMDARs.

3.1.6 CONDUCTANCE ANALYSIS OF DA NEURON NMDAR RECEPTORS

NMDARs exhibit a range of molecular characteristics depending on subunit stoichiometry (Paoletti and Neyton, 2007; Yamakura and Shimoji, 1999), phosphorylation by various kinases (Chen and Roche, 2007; Lan et al., 2001; Liao et al., 2001; Skeberdis et al., 2006; Sobczyk and Svoboda, 2007), interaction with postsynaptic density proteins and subcellular distribution (Lin et al., 2006; Lin et al., 2004; Logan et al., 2007; Losi et al., 2003; Prybylowski et al., 2005; Vicini and Rumbaugh, 2000). Indeed, distinct NMDAR properties can be expressed in a pathway specific manner in the same neuron (Arrigoni and Greene, 2004; Kumar and Huguenard, 2003). In light of the critical role that NMDARs play in controlling burst firing of DA neurons *in vivo* (Chergui et al., 1994a; Chergui et al., 1993; Christoffersen and Meltzer, 1995; Kuznetsov et al., 2006; Overton and Clark, 1992; Tong et al., 1996a) and the novel cellular plasticity we have described above, we examined the basic voltage-dependence of activation of NMDARs in DA neurons to see if it differed significantly from canonical NMDARs reported in other systems. To this end, we recorded NMDAR currents evoked by fast, local microiontophoresis of 100 mM NMDA in 1.2 mM extracellular Mg^{2+} at a range of command voltages after filling the cell with a Cs^{+}-based internal solution containing 1 mM QX-222 (to block Na^{+} channels) and 5-10 mM EGTA (to limit activation of Ca^{2+}-gated channels; Figure 3.16A and 3.16B). In order to limit space-clamp errors while

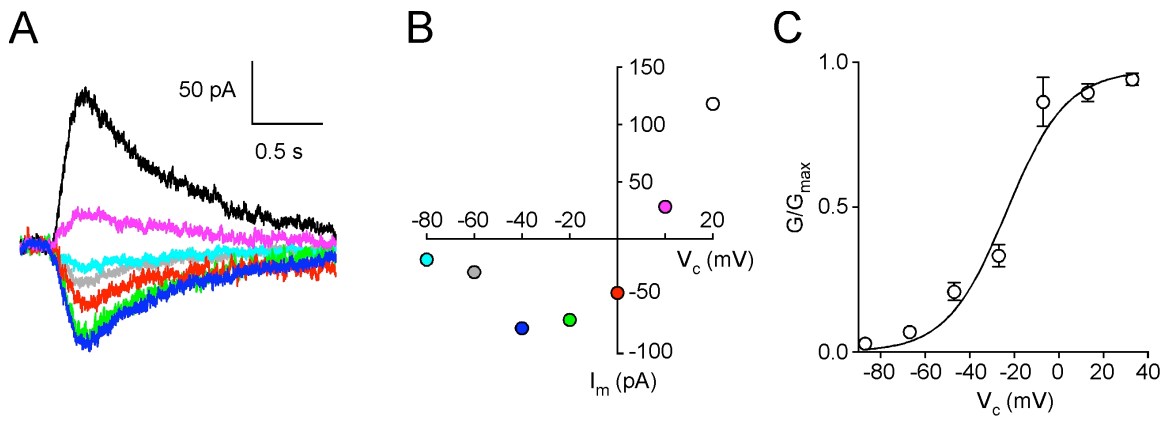

Figure 3.16. Ionic Conductance Analysis of DA Neuron NMDARs.
(A) Example traces of NMDAR currents activated at different command voltages by local microiontophoresis of 100 mM NMDA at the soma recorded under whole-cell voltage-clamp with Cs^+-based internal solution containing QX-222 and high EGTA. R_s was 9 to 12 MΩ before 70% compensation/prediction.
(B) Peak current-voltage relationship for traces shown in (A).
(C) NMDAR conductance-voltage relationship constructed from 10 experiments performed as described in (A) and (B). Averaged peak NMDAR currents at a range of command voltages were converted to fractional conductance in each neuron and combined. The resulting average G/G_{max} vs. V_c plot was fit with a Boltzmann curve (slope = 13.4 mV^{-1}, $V_{1/2}$ = -23.5 mV) after subtraction of liquid junction potential. Symbols represent mean ± SEM.

recording from neurons with elaborate dendritic trees in brain slices, NMDA was applied locally at the soma <20 μm from the recording pipette. Only neurons with stable series resistances (R_s) below 12 MΩ before at least 70% R_s compensation/prediction were accepted for analysis. Data from 10 such experiments were combined and the conductance-voltage relationship was constructed (Figure 3.16C; see Materials and Methods, section 2.10). A Boltzmann fit to the data yielded a $V_{1/2}$ of -23.5 mV and a slope of 13.4 mV^{-1}. These values are not significantly different from those described for NMDARs at conventional synapses in other neurons (Arrigoni and Greene, 2004; Kumar and Huguenard, 2003; Nowak et al., 1984) and are thus consistent with the observed subunit stoichiometry reported above for synaptic NMDARs in DA neurons (Figure 3.15).

3.2 Aim 2: Effects of Repeated Amphetamine Experience on Synaptic Facilitation of Spike-Evoked Ca^{2+} Signals and Plasticity of NMDARs at VTA DA neurons.

The results presented in Aim 1 implicate PI-coupled receptor activation and subsequent release of Ca^{2+} from internal stores in the plasticity of NMDARs in a manner regulated by the activity of protein kinase A, presumably through phosphorylation of the IP_3R (Tang et al., 2003; Wagner et al., 2008; Wagner et al., 2004; Wojcikiewicz and Luo, 1998). Substantial evidence links exposure to drugs of abuse with an upregulation of the adenylate cyclase/cAMP/PKA pathway (Nestler and Aghajanian, 1997; Peterson et al., 2006; Tolliver et al., 1999; White et al., 1995), even in humans (Hope et al., 2007). The addicted brain state resulting from chronic drug abuse is associated with pathological over-learning of cues associated with the drug experience as well as a devaluation of "natural" rewards (Berke and Hyman, 2000; Hyman, 2005; Hyman et al., 2006a; Kalivas et al., 2005; Kalivas and Volkow, 2005; Redish, 2004; Volkow et al., 2009; Volkow et al., 2005; Wojcikiewicz and Luo, 1998). We thus investigated the effects of repeated amphetamine (AMPH) experience on synaptic facilitation of spike-evoked Ca^{2+} signals and LTP of NMDARs.

For this set of experiments, we restricted our analysis to DA neurons located in the VTA as this area is thought to be more actively involved in processing environmental cue information related to drugs of abuse and is particularly important in the early stages of addiction (Cheer et al., 2007b; Di Chiara and Imperato, 1988; Everitt and Robbins, 2005). In addition, in order to be able to compare across treated and non-treated animals, we wanted to record from and stimulate a consistent and limited anatomical area, due to the variability in NMDAR EPSC amplitude, facilitation of $I_{K(Ca)}$, and plasticity that we observed in the previous Aim, where we stimulated and recorded from a large anatomical population of DA neurons across SNc and VTA.

3.2.1 REPEATED AMPHETAMINE EXPERIENCE BROADENS THE TIMING WINDOW FOR SYNAPTIC FACILIATION OF SPIKE-EVOKED CA^{2+} SIGNALS

We first compared synaptic facilitation of $I_{K(Ca)}$ between rats that had been treated once per day for 7 days with either saline or 5 mg/kg AMPH via intraperitoneal injection. We examined synaptic facilitation of $I_{K(Ca)}$ for both single APs and bursts at timing intervals of 0.25, 0.5, 1.0, and 1.5 s (schematic and examples shown in Figure 3.17A-D). In order to compare across animals, we attempted to normalize synaptic activation by NMDAR EPSC amplitude, setting stimulation intensity to evoke EPSCs in the range of ~30 to 40 pA (Figure 3.17G and Table 3.3). Previous studies have demonstrated no prolonged change in DA neuron NMDARs in response to drug experience, despite significant changes in AMPARs as discussed in the section 1.4.1.1-3 (Argilli et al., 2008; Saal et al., 2003; Schilstrom et al., 2006; Ungless et al., 2001). Experiments conducted in this manner showed a remarkable difference in the facilitation of $I_{K(Ca)}$ between neurons from AMPH- and saline-treated animals (Figures 3.17A-F). At all timing intervals tested, neurons from AMPH-treated animals exhibited significantly greater facilitation than those from saline-treated animals for both single APs ($n = 6$ for AMPH vs. $n = 7$ for saline, $p < 0.01$, unpaired t-tests) and bursts ($n = 4$ for AMPH vs. $n = 7$ for saline, $p < 0.05$, unpaired t-tests). There were no significant differences in basal $I_{K(Ca)}$ for single spikes or bursts between saline- and AMPH-treated animals (Table 3.3). Thus, repeated AMPH experience robustly alters intracellular Ca^{2+} signaling in DA neurons in a manner that may be critically important for the induction of synaptic plasticity.

3.2.2 REPEATED AMPHETAMINE EXPERIENCE INCREASES SUSCEPTIBILITY OF NMDARS TO LTP INDUCTION

Due to the strong correlation between facilitation of spike-evoked Ca^{2+} signals and plasticity of NMDARs reported in Aim 1, we proceeded to examine how repeated AMPH experience altered LTP. Experiments were again normalized via the NMDAR EPSC in order to compare across neurons from different treatment groups (Figure

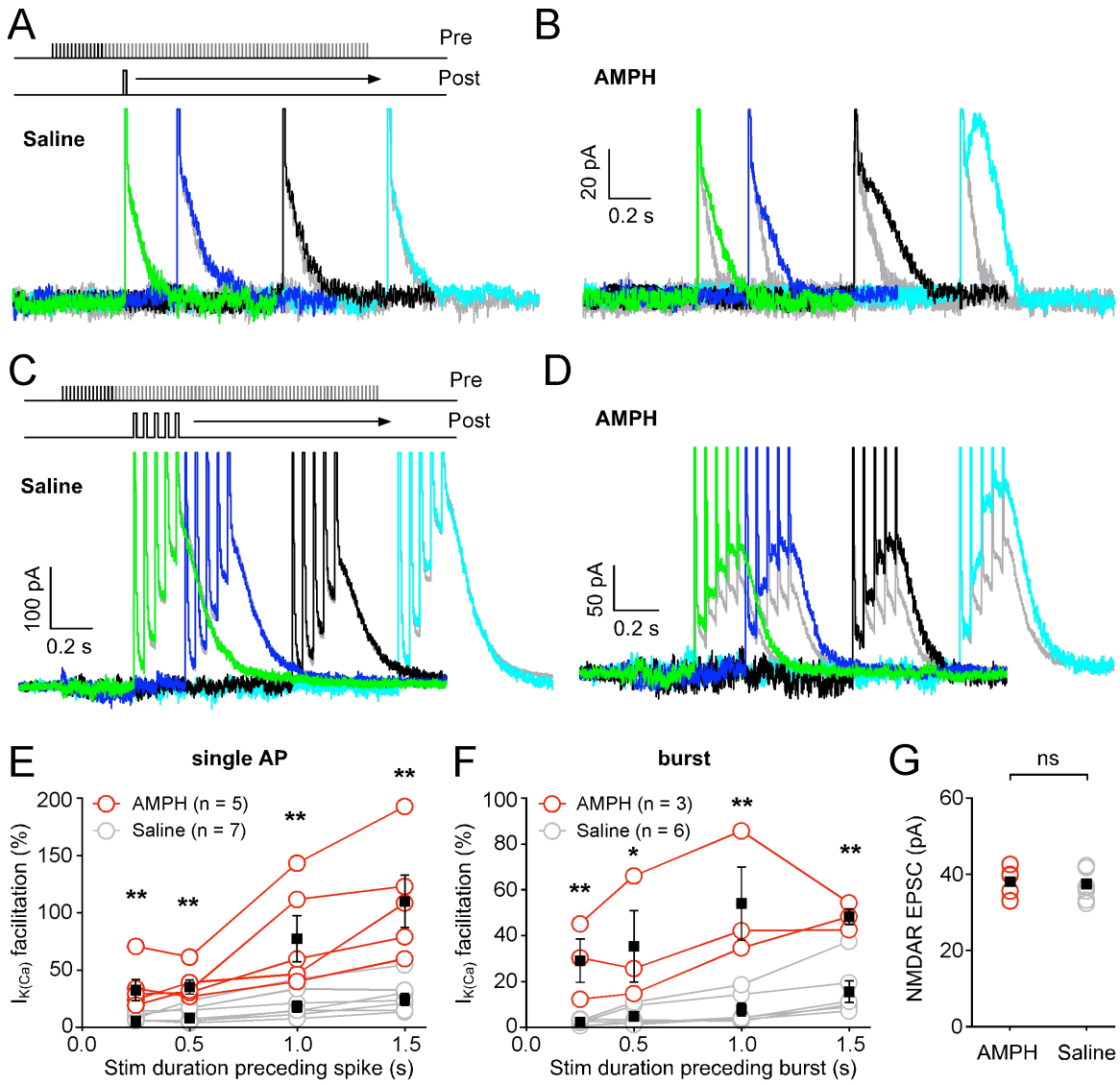

Figure 3.17. Repeated Amphetamine Experience Enhances Synaptic Facilitation of Spike-Evoked Ca^{2+} Signals in VTA DA Neurons.
(A-D) Representative traces illustrating the difference in synaptic facilitation of $I_{K(Ca)}$ between saline- (A, C) and AMPH-treated (B, D) rats using synaptic stimulation trains of 0.25 (green), 0.5 (blue), 1.0 (black), and 1.5 s (turquoise). A single AP (A, B) or a burst of 5 APs at 20 Hz (C, D) was evoked 100 ms after the offset of each synaptic stimulation train. Traces of $I_{K(Ca)}$ following synaptic stimulation are shown after subtraction of synaptic stimulation alone. Stimulation protocols are shown inset in A and C. Postsynaptic firing in the absence of synaptic stimulation is shown in gray for each timing interval.

(E-F) Summary graphs of synaptic facilitation of $I_{K(Ca)}$ at a range of timing intervals for both single APs (E) and bursts (F) in AMPH-treated (red) vs. saline-treated (gray) rats.
(G) NMDAR EPSC amplitudes used to evaluate timing-dependence of synaptic facilitation of $I_{K(Ca)}$ were comparable between neurons from saline- (gray) and AMPH-treated (red) rats.
Open circles indicate individual experiments; black squares represent means ± SEM.

3.18E and Table 3.2). In VTA neurons from saline-treated animals, synaptic stimulation at this intensity produced limited facilitation of $I_{K(Ca)}$ (7% ± 5% change, n = 6; Figure 3.18D) and no systematic change in synaptic efficacy in response to the conventional burst-pairing protocol (-1% ± 4% change, n = 6; Figure 3.18A,C,D). However, in VTA neurons from AMPH-treated animals, synaptic stimulation evoked substantial facilitation $I_{K(Ca)}$ (37% ± 6% change, n = 5, $p < 0.01$ compared to saline, unpaired t-test; Figure 3.18D) and subsequent burst pairing drove significant LTP of NMDAR EPSCs (24% ± 5% change, n = 5, $p < 0.01$ compared to saline, unpaired t-test; Figure 3.18B-D). This LTP was again not associated with a change in PPR or CV (Figures 3.18F and 3.18G, respectively), suggesting a postsynaptic locus for the changes in EPSC amplitude, similar to what was observed in Aim 1 (Figure 3.1D). The combined data set (neurons from both saline- and AMPH-treated animals) was well fit by a linear regression of $I_{K(Ca)}$ facilitation vs. NMDAR plasticity (slope = 0.75 ± 0.11, $r^2 = 0.84$; Figure 3.18D), similar to that seen in Aim 1 for both SNc and VTA neurons from naïve animals (slope = 0.84 ± 0.08, $r^2 = 0.79$; Figure 3.1B). This suggests that AMPH enhances LTP through changes in spike-evoked Ca^{2+} signaling and not through changing the sensitivity of downstream plasticity machinery.

These results, when combined with those presented in section 3.2.1, demonstrate that repeated amphetamine exposure can potently regulate Ca^{2+} signaling in DA neurons, which may have a number of significant effects, including but not limited to, increasing the plasticity of NMDARs and potentially altering the processes by which environmental cues are associated with motivational valence and goal-directed behaviors become reinforced.

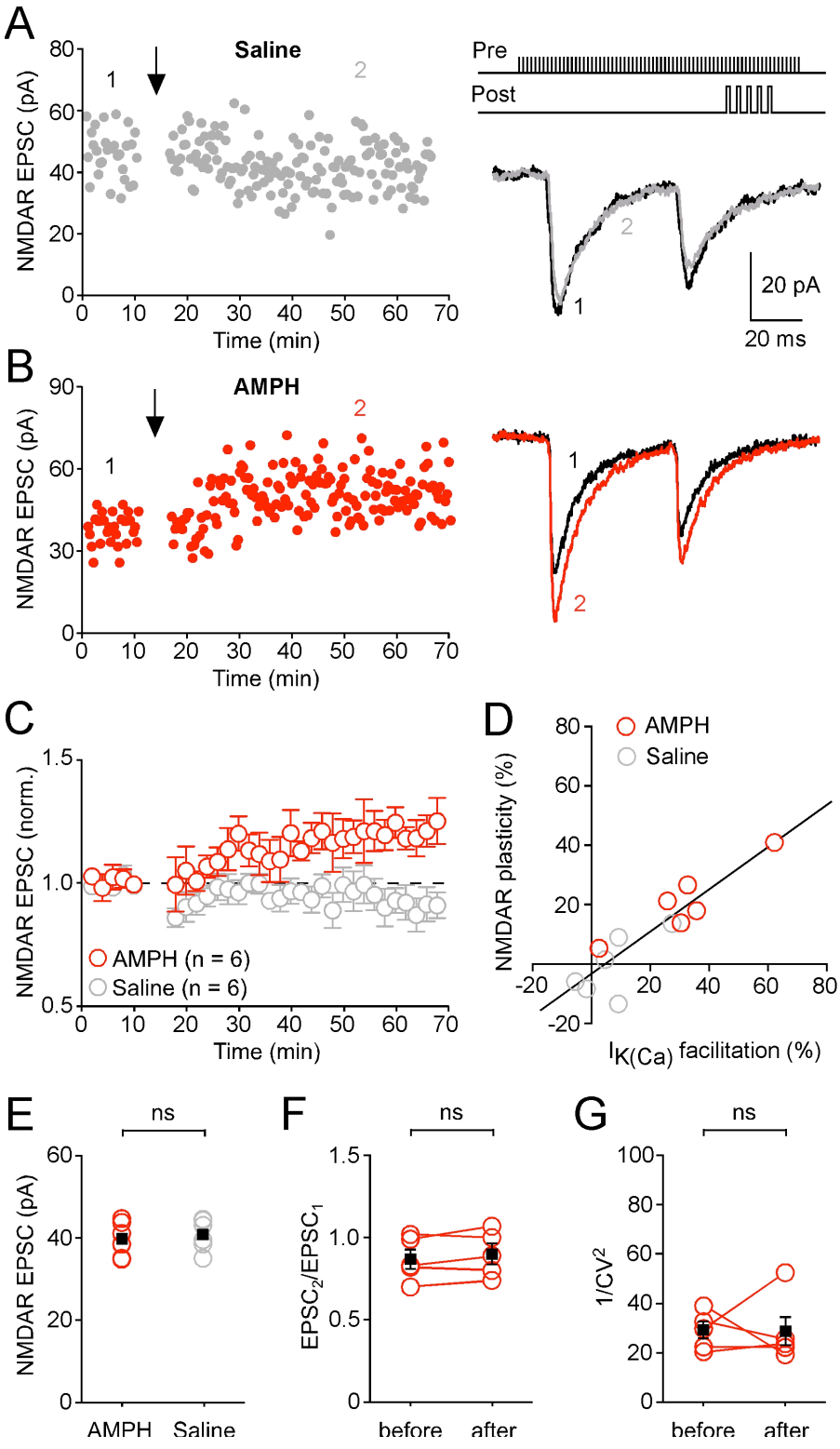
A
Saline
NMDAR EPSC (pA)
Time (min)
Pre
Post
20 pA
20 ms
B
AMPH
C
NMDAR EPSC (norm.)
AMPH (n = 6)
Saline (n = 6)
D
AMPH
Saline
NMDAR plasticity (%)
IK(Ca) facilitation (%)
E
ns
NMDAR EPSC (pA)
AMPH
Saline
F
ns
EPSC2/EPSC1
before
after
G
ns
1/CV2
before
after

Figure 3.18. Repeated Amphetamine Experience is Associated with Increased LTP of NMDARs in VTA DA Neurons.
(A-B) Representative experiments applying burst-pairing to induce NMDAR LTP in saline- (A; gray) and AMPH-treated (B; red) rats. Time graphs of NMDAR EPSC amplitude are shown on the left. The LTP induction protocol, which consisted of 10 synaptic stimulation-burst pairings every 20 s (illustrated at top right), was delivered at the time indicated by the arrow. Averaged NMDAR EPSCs taken at times indicated from the time graphs are shown at right.
(C) Summary time graph of NMDAR LTP experiments. Symbols represent means ± SEM
(D) The magnitude of NMDAR LTP is plotted versus the magnitude of synaptic facilitation of $I_{K(Ca)}$ in neurons examined for NMDAR LTP. Solid line is a linear fit to all neurons from both saline- and AMPH-treated rats ($r^2 = 0.84$).
(E) NMDAR EPSC amplitudes for plasticity experiments were comparable in neurons from saline- (gray) and AMPH-treated (red) rats.
(F-G) PPR and $1/CV^2$ were not significantly different after LTP induction for the 5 neurons from AMPH-treated rats that exhibited more than 15% facilitation of $I_{K(Ca)}$. Open circles indicate individual experiments; black squares represent means ± SEM. activate

Table 3.3. Summary of Parameters in Different Experimental Groups for Aim 2

Type of experiment	Plasticity (%)	Facilitation of $I_{K(Ca)}$ (%)	$I_{K(Ca)}$ (pA·s)	$I_{K(Ca)\text{-burst}}$ (pA·s)	Baseline EPSC (pA)	n
Timing of facilitation: saline	NA	18 ± 5	6 ± 2	31 ± 5	37 ± 1	7
Timing of facilitation: AMPH	NA	77 ± 20**	8 ± 2	28 ± 13	38 ± 2	5
Plasticity: saline	-1 ± 4	7 ± 5	7 ± 2	36 ± 6	40 ± 2	6
Plasticity: AMPH	24 ± 5**	37 ± 6**	5 ± 1	29 ± 7	41 ± 2	5

The magnitude of synaptic stimulation-induced facilitation of $I_{K(Ca)}$ shown in this table is for a single AP at 100 ms after the offset of 1-s synaptic stimulation (see Experimental Procedures). All data are mean ± SEM. *p < 0.05, **p < 0.01, ***p < 0.001 difference from respective saline group (unpaired t-test).

CHAPTER 4: DISCUSSION

This study represents the first demonstration of activity-dependent synaptic plasticity of NMDARs at midbrain DA neurons. This form of plasticity may be particularly important for *in vivo* reward learning in light of the critical role NMDARs play in burst firing of DA neurons. In support of this idea, plasticity of DA neuron NMDARs exhibited numerous features that were congruent with a putative cellular substrate for reward learning, as described below. Furthermore, repeated *in vivo* amphetamine experience dramatically altered spike-evoked Ca^{2+} signals in DA neurons and thus strongly influenced the induction of synaptic plasticity of NMDARs.

To summarize the major experimental results presented in this study, which will be considered in detail below: repetitive pairing of sustained presynaptic stimulation with postsynaptic firing can drive LTP of NMDAR EPSCs, in a manner that is associative and requires postsynaptic bursting. This form of LTP appears to be expressed via a change in postsynaptic receptor number and/or function. The induction of NMDAR LTP is dependent upon both synaptic facilitation of burst-evoked Ca^{2+} signals via PI-coupled receptors generating IP_3, which requires PKA but not PKC, and concomitant activation of NMDARs. The timing dependence of LTP is shaped by these two requirements in that the burst first needs to occur with a certain delay (~0.5-1 s) after the onset of synaptic stimulation, reflecting the time required for synaptic stimulation to cause a rise in IP_3 levels, and the burst must also take place prior to or immediately (within tens of milliseconds) after the termination of synaptic stimulation so that NMDARs are activated at the time of the burst. Intriguingly, LTD of NMDAR EPSCs is induced when the burst precedes synaptic stimulation during the induction protocol, although the data presented here provide limited mechanistic insight into this process (Harney et al., 2006). In addition, DA neuron NMDAR LTP is input specific, reversible in a spike-conditional manner, DA-independent, and does not appear to be expressed by a change in NR2A- or NRB-containing subunit stoichiometry. LTP is not observed when strong, phasic

activation of PI-coupled receptors during pairing recruits IP_3-mediated Ca^{2+} waves. Also, the burst-pairing protocol used to induce LTP of NMDARs produces LTD of AMPARs, presumably through a previously described mGluR-dependent process (Bellone and Luscher, 2005, 2006; Mameli et al., 2007). Finally, repeated *in vivo* amphetamine experience profoundly increased facilitation of spike-evoked Ca^{2+} signals in DA neurons, broadening the timing window, and resulting in enhanced NMDAR LTP compared to neurons from saline-treated animals.

The activity-dependent plasticity of NMDARs demonstrated in this study represents a novel mechanism for long-term regulation of DA neuron output. It may also exhibit metaplastic consequences, interacting with and/or controlling previously described forms of synaptic plasticity including spike-timing LTP of AMPAR-mediated transmission (Argilli et al., 2008; Chen et al., 2008; Liu et al., 2005; Luu and Malenka, 2008), as well as plasticity of $GABA_A$R-mediated transmission, both of which are NMDAR-dependent in DA neurons (Engblom et al., 2008; Nugent et al., 2007; Zweifel et al., 2008).

4.1 Mechanisms of NMDAR LTP in DA Neurons

4.1.1 INDUCTION

Ca^{2+} signals triggered by postsynaptic APs play a critical role in the induction of most forms of synaptic plasticity (Linden, 1999; Sjostrom and Nelson, 2002). Study of the role of spikes in plasticity has previously been mostly restricted to integrate and fire neurons, which generally rest at a hyperpolarized voltage and fire only in response to excitatory input, usually with millisecond level precision. DA neurons, however, are pacemakers: they have an internally generated oscillator that brings the neuronal voltage to threshold autonomously at 1-5 Hz. The precision of this form of firing is on the order of tens to hundreds of milliseconds in slices and significantly less *in vivo*, due to constant bombardment by synaptic input. Furthermore, it has been shown that single spikes in DA

neurons are initiated in the axon and can propagate and trigger Ca^{2+} influx through the dendritic arbor with high efficiency (Gentet and Williams, 2007; Hausser et al., 1995; Wilson and Callaway, 2000). Thus, single APs may represent background activity and may not be an accurate or effective signal for implementing synaptic plasticity rules. Consistent with this idea, the induction of NMDAR LTP in this study requires burst firing, as pairing synaptic stimulation with a single AP was ineffective at driving plasticity (Figure 3.1E). Spike-timing LTP of AMPARs in DA neurons also utilizes bursting, though at 10 Hz instead of 20 (Argilli et al., 2008; Chen et al., 2008; Liu et al., 2005; Luu and Malenka, 2008); however, it is not known how dependent this form of plasticity is on firing pattern as the parameter space remains completely unexplored. Bursts can be differentiated from single spikes on the basis of their Ca^{2+} signals and downstream channel activation in DA (Cui et al., 2007) and other neurons (Christie et al., 1996; Kampa et al., 2006, 2007; Kampa and Stuart, 2006; Letzkus et al., 2006; Markram et al., 1995; Nevian and Sakmann, 2004, 2006). Spike timing-dependent plasticity requires precision on the order of milliseconds (Dan and Poo, 2004; Markram et al., 1997; Sjostrom and Nelson, 2002), while burst timing occurs on the order of tens to hundreds of milliseconds. This epoch is more consistent with the physiology of DA neurons as well as the behavioral timescales on which this sort of learning occurs. As the burst appears to be the relevant *in vivo* response to rewards and reward-predicting cues, while ongoing single-spiking activity may represent basal activity, perhaps burst timing-dependent plasticity is simply an alternative implementation of the same sort of spike-timing plasticity architecture, but scaled up in time, firing, and Ca^{2+} requirements.

Clearly, this is an incomplete picture, as burst-induced Ca^{2+} signals need to be amplified by preceding activation of PI-coupled receptors, which recruits CICR via IP_3Rs on intracellular stores, to effectively induce LTP of NMDARs in DA neurons (Figures 3.1B, 3.7, 3.8, and 3.11). How is it that burst-associated Ca^{2+} transients are insufficient to drive plasticity by themselves? It may be a mechanism similar to that described for localized Ca^{2+} signaling and LTD of AMPAR EPSCs at parallel fiber synapses on cerebellar Purkinje neurons (Sarkisov and Wang, 2008; Wang et al., 2000). Here,

climbing fiber activation and subsequent dendritic Ca^{2+} spike generation do not evoke large enough Ca^{2+} transients in dendritic spines to reach the threshold for plasticity induction unless CICR is triggered by appropriately-timed parallel fiber inputs to activate mGluRs and producing local IP_3 increases. The main difference between NMDAR LTP in DA neurons and AMPAR LTD in Purkinje neurons is the involvement of NMDAR activation in the induction. At parallel fiber-Purkinje neuron synapses, which lack NMDARs, chemical compartmentalization offered by dendritic spines restricts IP_3 and Ca^{2+} signaling to individual spines, thereby mediating synapse specificity of plasticity (Nimchinsky et al., 2002; Wang et al., 2000). However, such compartmentalization of IP_3-dependent Ca^{2+} signaling may not occur at glutamatergic synapses on DA neurons, which are mostly formed on dendritic shafts (Carr and Sesack, 2000; Charara et al., 1996). Indeed, in DA neurons, synaptic activation of mGluRs augments burst-induced Ca^{2+} transients throughout individual dendrites (Cui et al., 2007). Therefore, the localized signal underlying the input specificity of NMDAR LTP is presumably provided by NMDARs causing Ca^{2+} influx only at activated synapses, which would be below the spatial resolution of the confocal imaging system used in our study. In support of this idea, synaptic activation of Ca^{2+}-permeable AMPARs has been shown to produce highly localized (~1 μm) Ca^{2+} transients in aspiny dendrites mediating input-specific Ca^{2+} signaling and plasticity (Goldberg et al., 2003; Soler-Llavina and Sabatini, 2006). The requirement for coactivation of NMDARs (Figure 3.10) and mGluRs, together with the dependence on intracellular Ca^{2+} stores, is in line with recent studies demonstrating input-specific LTP of NMDAR EPSCs at hippocampal mossy fiber synapses (Kwon and Castillo, 2008; Rebola et al., 2008). It should also be noted that Ca^{2+} transients resulting from NMDAR-induced Ca^{2+} influx can be amplified via an mGluR- and IP_3-dependent CICR mechanism at Schaffer collateral synapses on hippocampal CA1 pyramidal neurons (Dudman et al., 2007).

Abundant evidence implicates PKA in multiple aspects of synaptic plasticity (Micheau and Riedel, 1999; Nguyen and Woo, 2003; Wang et al., 2006a). In particular, PKA has been shown to gate the induction of AMPAR LTP by modulating CaMKII and

SK2 channels in the hippocampus and amygdala (Blitzer et al., 1998; Faber et al., 2008; Lin et al., 2008; Wang et al., 1991). Our data show that PKA gates the induction of NMDAR LTP in DA neurons through tonic enhancement of IP_3R function (Figure 3.8). LTP induction may also be affected by PKA regulation of NMDAR-mediated Ca^{2+} influx (Skeberdis et al., 2006). The present work does not directly rule out a contribution of PKA in the expression of NMDAR LTP. The data clearly support PKA's role in induction; however, it is possible that PKA activity is also involved in the expression of LTP (Schilstrom et al., 2006; Skeberdis et al., 2006). This could be addressed by performing experiments with PKI in the patch pipette while reconstituting facilitation of $I_{K(Ca)}$ and plasticity by stimulating strongly enough to overcome the inhibition of IP_3Rs. We showed that this is conceptually feasible by increasing mGluR agonist concentration (Figures 3.8C and 3.8E) and it should therefore be possible synaptically as well.

Finally, to more comprehensively define the cellular mechanisms responsible for triggering this form of plasticity, it would be particularly interesting to probe the local Ca^{2+} signals at activated synapses in DA neurons during induction in order to analyze the contributions from bursts, facilitation, NMDARs and other potential sources, such as L-type VACC. In addition, changes in the number of spikes within a burst and/or their frequency may also influence plasticity induction, presumably through changing these local Ca^{2+} signals. As noted in the introduction (section 1.2.2.2), burst firing in DA neurons is graded *in vivo*. In this study, we have restricted postsynaptic bursting to 5 spikes at 20 Hz; it would be interesting to investigate plasticity induction with alterations in this paradigm that reflect the range of burst firig observed *in vivo*. This would also be an excellent starting point to launch an investigation into how changes in postsynaptic Ca^{2+} are transduced into increases in NMDAR EPSCs. Are conventional cascades like CaMKII involved or are novel 2^{nd} messenger systems and effectors recruited?

4.1.2 EXPRESSION

Burst-dependent LTP of NMDARs appears to be expressed postsynaptically by a process distinct from that previously described for enhancement of NMDAR EPSCs via

perfusion of metabotropic agonists in DA neurons (Figures 3.1D, 3.8 and 3.15) (Borgland et al., 2006; Schilstrom et al., 2006; Ungless et al., 2003). Activation of orexin-1 receptors induces PKC-dependent translocation of NR2A-containing NMDARs to the synapse (Borgland et al., 2006). PKC-mediated recruitment of NMDARs has also been implicated in NMDAR LTP at hippocampal mossy fiber synapses (Kwon and Castillo, 2008). However, pharmacological inhibition of PKC failed to affect NMDAR LTP in our study (Figure 3.8F). Furthermore, the effects of NR2A- and NR2B subunit-containing antagonists on NMDAR EPSCs were not altered after LTP expression. Although we cannot rule out potential changes in NR2C/D subunits (Harney et al., 2008), these subunits make relatively small contributions to NMDAR EPSCs in DA neurons (Figure 3.15) (Borgland et al., 2006), at least in older animals (Brothwell et al., 2008; Jones and Gibb, 2005). Therefore, enhanced function of individual NMDAR channels and/or increased synaptic expression of existing NMDARs with no change in the subunit composition are most likely to mediate the expression of LTP (Chen and Roche, 2007).

We cannot exclude contributions from other, more unconventional sources. A recently described alternative mechanism may also play a role in this form of plasticity via increased stability of NMDARs in the postsynaptic density (Mao et al., 2009). NMDARs have classically been thought of as tightly anchored in the membrane and not subject to the same constitutive and activity-dependent internalization as AMPARs. However, recent evidence suggests that movement of NMDARs into, through, and out of the membrane is significantly more dynamic than had previously been appreciated (Carroll and Zukin, 2002; Lau and Zukin, 2007; Montgomery and Madison, 2002, 2004; Montgomery et al., 2001; Montgomery et al., 2005; Newpher and Ehlers, 2008; Nong et al., 2003; Nong et al., 2004; Perez-Otano and Ehlers, 2005; Perez-Otano et al., 2006; Roche et al., 2001; Tovar and Westbrook, 2002; Zhao et al., 2008). Therefore, perhaps NMDAR LTP in DA neurons is mediated by synaptic stabilization of pre-existing receptors from internalization. The accumulation of functional postsynaptic proteins via enhancing their stability presumably has a relatively slow time course, at least compared

to AMPAR insertion during LTP at conventional synapses, which is congruent with the leisurely (~10 min) development of NMDAR LTP at DA neurons.

The delayed time-course of NMDAR LTP is curious, particularly in light of the rapidity of depotentiation. What other processes may account for the delayed increase in NMDAR EPSCs after pairing? Plasticity may be protein synthesis-dependent, requiring new receptors to be synthesized, trafficked and inserted. Other components of the NMDAR signaling complex may need to be manufactured, like postsynaptic anchoring proteins, scaffolding substrates, etc. An alternative possibility, distinct from the physical dynamics of protein synthesis and trafficking, is that the slow development of LTP is the result of multiple, competing plasticity processes induced during the pairing protocol. Depending on the synapse and the induction protocol, LTP (and/or LTD) can be accompanied by a variety of short-term plasticities (Hennig et al., 2008; Zucker and Regehr, 2002) involving classical vesicle depletion and presynaptic Ca^{2+} accumulation (Neher and Sakaba, 2008) as well as enhancement of release machinery via phosphorylation (Evans and Morgan, 2003; Leenders and Sheng, 2005), cannabinoid-mediated processes (Chevaleyre et al., 2006), activity-dependent changes in ion channels (Catterall and Few, 2008; Wang, 2008), and even activation of presynaptic conductances by decreases in cleft Ca^{2+} accompanying sustained pre- and postsynaptic spiking (Phillips et al., 2008; Smith et al., 2004). Most of these processes decay rapidly, which limits their ability to suppress NMDAR LTP over the initial 5-10 minutes after pairing. Most are also expressed presynaptically and thus should be detected by changes in PPR immediately after pairing, which we did not observe, suggesting that these mechanisms are unlikely to mediate the slow development of NMDAR LTP. An important caveat is that PPR analysis of transmission in brain slices using synaptic stimulation of numerous presynaptic axons with limited postsynaptic voltage control is not the most robust detection method for changes in release probability. Furthermore, even AMPAR LTP in DA neurons exhibits a relatively slow development after spike-timing induction (Argilli et al., 2008; Chen et al., 2008; Liu et al., 2005; Luu and Malenka, 2008), possibly reflecting the very different timescales of computation performed by DA neurons

(hundreds of milliseconds to seconds) vs. conventional integrate and fire neurons of the neocortex and hippocampus (milliseconds to tens of milliseconds). This is consistent with the argument presented above (in section 4.1.1) regarding a slower, higher-order plasticity induction architecture in DA neurons dependent on bursts and not single spikes.

4.2 Comparison and Integration with Other Forms of Plasticity

4.2.1 NMDAR PLASTICITY IN DA NEURONS VS. OTHER NEURONS

While dwarfed by the preponderance of research on AMPAR plasticity, activity-dependent plasticity of NMDAR-mediated transmission has previously been observed in the brain using a variety of induction protocols, mostly in the hippocampus of young animals (Bashir et al., 1991; Bellone and Nicoll, 2007; Harney et al., 2008; Kwon and Castillo, 2008; Morishita et al., 2005; O'Connor et al., 1994; Rebola et al., 2008; Selig et al., 1995; Sobczyk and Svoboda, 2007; Xie et al., 1992). The NMDAR plasticity described in the present study differs significantly from these previous reports. First, none of these studies addressed the role of postsynaptic APs in LTP induction or their timing-dependence. Indeed, the plasticity in the present study required a delay between the onset of presynaptic stimulation and postsynaptic burst firing, which is not necessary for any of the previously described forms of plasticity. In addition, many of the previous reports did not require significant postsynaptic activity, limiting the associativity of the respective changes in synaptic efficacy, unlike the NMDAR plasticity in the present study. Second, many of the previous reports of NMDAR plasticity are from young animals (postnatal day 2-21), and some even report that plasticity is absent in older (P16-28) animals (Bellone and Nicoll, 2007; Sobczyk and Svoboda, 2007), while NMDAR LTP in DA neurons induced by burst pairing does not appear to depend on age and is present even at P50. Third, the plasticity presented in this study is dependent on PKA activity, presumably via constitutive phosphorylation of IP_3Rs, and independent of PKC, in contrast to other reports (Kwon and Castillo, 2008; Rebola et al., 2008; Sobczyk and

Svoboda, 2007). Distinguishing the present work even further, no previous study has reported activity-dependent, spike-conditional reversal of NMDAR LTP or showed that exogenous substances self-administered by humans (amphetamine) influences plasticity.

Despite these distinctions, it is important to note the general similarities between the present work and previous studies. NMDAR plasticity is broadly dependent on intracellular Ca^{2+}, activation of PI-coupled receptors (Harney et al., 2006; O'Connor et al., 1994; Rebola et al., 2008; Sobczyk and Svoboda, 2007) and release of Ca^{2+} from intracellular stores (Kwon and Castillo, 2008). It appears to be postsynaptically expressed (Harney et al., 2008; Harney et al., 2006; Kwon and Castillo, 2008; Rebola et al., 2008; Selig et al., 1995), though this has not been definitively confirmed outside of dentate gyrus (Harney et al., 2008). Other parallels include the requirement for NMDAR activation during pairing (Kwon and Castillo, 2008; Rebola et al., 2008; Sobczyk and Svoboda, 2007), input specificity (Bellone and Nicoll, 2007; Kwon and Castillo, 2008; Selig et al., 1995; Sobczyk and Svoboda, 2007), and dependence on postsynaptic protein kinases (Kwon and Castillo, 2008; Morishita et al., 2005; Rebola et al., 2008; Selig et al., 1995; Sobczyk and Svoboda, 2007), though there are discrepancies about which kinases are important.

4.2.2 NMDAR PLASTICITY AS A FORM OF METAPLASTICITY IN DA NEURONS

As mentioned above, this study represents the first demonstration of activity-dependent plasticity of NMDAR-mediated synaptic transmission in DA neurons. There are, however, reports of changes in NMDAR function in DA neurons after bath perfusion or incubation of slices with metabotropic receptor agonists (Argilli et al., 2008; Borgland et al., 2006; Schilstrom et al., 2006; Ungless et al., 2003). These experiments likely stem from the hypothesis that regulating NMDARs represents a potent mechanism for controlling the ability of other receptors (*i.e.* AMPA and $GABA_A$) to undergo further plasticity, and were presumably influenced by previous demonstrations of synaptic metaplasticity through NMDARs in visual cortex and hippocampus (Abraham, 2008;

Abraham and Bear, 1996; Abraham et al., 2001; Chen and Bear, 2007; Jung et al., 2008; Philpot et al., 2007; Philpot et al., 2003; Quinlan et al., 1999; Yashiro and Philpot, 2008). As mentioned above, there are forms of LTP of both AMPA- (Argilli et al., 2008; Chen et al., 2008; Liu et al., 2005; Luu and Malenka, 2008) and $GABA_A$-receptors (Nugent et al., 2007) that are dependent on NMDARs in DA neurons and may thus be targets for metaplasticity. These studies have focused on the plasticity of these receptors in response to drugs of abuse, which is particularly interesting in light of the significant *in vivo* behavioral data showing that inhibition of DA neuron NMDARs, via either local antagonist injection or cell-type specific genetic knockout, blocks measures of reward learning and drug seeking behavior (Borgland et al., 2006; Engblom et al., 2008; Harris and Aston-Jones, 2003; Harris et al., 2004; Kalivas and Alesdatter, 1993; Li and Wolf, 1999; Wolf and Jeziorski, 1993; Zweifel et al., 2008). We suggest that these *in vivo* intervention experiments should be cautiously interpreted, due to the critical roles of NMDARs in driving burst firing as well as in controlling the induction of various forms of synaptic plasticity. However, this avenue of research may well be a fruitful one to pursue, particularly in light of the success gleaned from investigating metaplasticity in the hippocampus and cortex.

One potential strategy for parsing out the relative contributions of AMPAR plasticity vs. NMDAR plasticity *in vivo* in response to drugs of abuse might be to locally co-inject amphetamine along with a DA $D_{1/5}$ antagonist into the VTA, where local amphetamine has been shown to be sufficient to induce behavioral sensitization (Cador et al., 1999; Kalivas and Weber, 1988; Perugini and Vezina, 1994; Vezina et al., 2002). Potentiation of AMPARs in DA neurons in response to drugs of abuse has been shown to depend on $D_{1/5}$ receptors (Argilli et al., 2008; Schilstrom et al., 2006), while the form of NMDAR plasticity that we have described in this study is DA independent (Figure 3.9). If AMPAR LTP is more important in mediating behavioral responses to drugs of abuse, then the cocktail of AMPH and DA antagonists should dramatically decrease measures of reinforcement (sensitization, self-administration, condition-place preference, etc.). Conversely, if the "learning" associated with drug experience is regulated more by

NMDAR plasticity, these paradigms should be unaffected by the DA antagonist cocktail. These pharmacological experiments could be strengthened by examining inducible, DA neuron-specific knockouts of DA receptors (Baik et al., 1995; Miner et al., 1995).

4.3 IP_3R as a Metaplastic Locus

As mentioned above, there have been numerous demonstrations of metaplasticity via NMDARs (Abraham, 2008; Abraham and Bear, 1996; Abraham et al., 2001; Chen and Bear, 2007; Jung et al., 2008; Philpot et al., 2007; Philpot et al., 2003; Quinlan et al., 1999; Yashiro and Philpot, 2008). Recently, an ever-increasing number of alternative substrates for metaplasticity are being reported, including various ion channels and intracellular signaling cascades (Pelkey et al., 2008; Thiagarajan et al., 2007; Thiagarajan et al., 2005), cannabinoid systems (Chevaleyre and Castillo, 2004; Edwards et al., 2008), and mGluRs (Bellone et al., 2008; Clem et al., 2008; Jin et al., 2007). In addition, given the critical role of spike-evoked Ca^{2+} signals in the induction of plasticity at most synapses in the brain, activity-dependent changes in local ion channels may represent a source of metaplasticity by controlling the waveform of local and/or backpropagating spikes (Frick et al., 2004; Gasparini et al., 2007; Hoffman et al., 1997; Losonczy et al., 2008; Magee and Johnston, 1997, 2005). Our results take this idea a step further by suggesting that changes in spike-evoked Ca^{2+} mediated by alterations in the sensitivity Ca^{2+} release from intracellular stores via IP_3Rs through PKA phosphorylation represent a novel locus for metaplasticity (Figure 3.8). We feel that this is particularly significant due to our demonstration that repeated *in vivo* amphetamine experience increases the spike-evoked Ca^{2+} signaling in VTA DA neurons (Figure 3.17), presumably through PKA-mediated phosphorylation of IP_3Rs (Hope et al., 2007; Nestler and Aghajanian, 1997; Peterson et al., 2006; Tang et al., 2003; Tolliver et al., 1999; Wagner et al., 2008; Wagner et al., 2004; White et al., 1995; Wojcikiewicz and Luo, 1998), resulting in increased plasticity (Figure 3.18).

It would be exciting to examine if changes in spike-evoked Ca^{2+} signals via alterations in IP_3Rs (or RyRs) can influence plasticity at other, "classical" synapses. Indeed, changes in the cAMP/AC/PKA pathway after drug experience have been reported across a range of brain regions (Crawford et al., 2004; Hope et al., 2007; Peterson et al., 2006; Self et al., 1995; Tolliver et al., 1999), thus providing a common pathophysiological causation for this putative form of metaplasticity. Considering the important roles of these brain regions, in particular the nucleus accumbens, striatum and prefrontal cortices, in addiction (Day and Carelli, 2007; Everitt and Robbins, 2005; Hyman, 2005; Hyman et al., 2006a; Jones and Bonci, 2005; Kalivas and Volkow, 2005; Kauer and Malenka, 2007; Melis et al., 2005; Nestler and Aghajanian, 1997; Redish, 2004; Volkow et al., 2009; Wolf et al., 2004), metaplasticity via the IP_3R may play an important part in controlling the rewiring of the neural circuitry responsible for addictive behavior.

4.4 Linking Cellular Plasticity to Behavior

Directly demonstrating that cellular forms of learning account for behavior has been a longstanding challenge throughout the field of neuroscience. Despite over 30 years of intensive study by thousands of neuroscientists, only recently has LTP in the hippocampus been conclusively linked to *in vivo* learning and memory (Bliss et al., 2006; Pastalkova et al., 2006; Whitlock et al., 2006). While this result is reassuring, the investment in time and energy it took to produce indicates the enormity of the task to definitively connect cellular processes observed *in vitro* with behavioral output *in vivo*. Despite these intimidating obstacles, it is nonetheless important to utilize what has been learned regarding the relevance of cellular plasticity to behavioral learning and discuss the possible implications and consequences for NMDAR LTP in DA neurons on behavior.

4.4.1 DA NEURON NMDAR PLASTICITY AND *IN VIVO* REWARD LEARNING

In behaving animals, DA neurons "learn" to respond to inherently neutral environmental cues with synchronized bursts of activity after repeated pairing of cue and reward (or reward-predicting stimuli) (Pan et al., 2005; Schultz, 1998). Several modeling studies have addressed the neurobiological substrates underlying the conditioning of DA neuron responses (Brown et al., 1999; Contreras-Vidal and Schultz, 1999; Houk et al., 1995). One of these models postulates that plasticity of synapses onto DA neurons is involved in this learning process (Contreras-Vidal and Schultz, 1999). In awake rats, it has also been shown that excitatory responses of PPTN neurons to auditory cues (which play an important role in driving DA neuron burst responses to those cues) remain constant during cue-reward learning (Pan and Hyland, 2005). Since the PPTN gives rise to direct glutamatergic (and cholinergic) inputs to DA neurons (Charara et al., 1996), this raises the possibility that plasticity of glutamatergic synapses onto DA neurons may play a role in the development of conditioned burst responses. Therefore, in light of the prominent role of NMDARs in the generation of DA neuron bursts (Chergui et al., 1994a; Morikawa et al., 2003; Overton and Clark, 1997; Tong et al., 1996a), the activity-dependent plasticity of NMDARs described in this study may contribute to the acquisition of cue responses. The synaptic stimulation-burst pairing protocol was designed to emulate what we hypothesized was occurring during the cue-reward pairing paradigm at DA neurons, taking advantage of our previous results regarding supralinear spike-evoked Ca^{2+} signals in DA neurons (Cui et al., 2007). Thus, sustained synaptic stimulation mimics the working memory-type persistent input activated by the presentation of the cue (Brown et al., 1999; Funahashi et al., 1989) and the postsynaptic burst corresponds to that triggered by the reward (or previously learned reward-predicting cue). In our model, potentiated NMDARs at those synapses activated during pairing mediate the transient burst response to the cue after conditioning.

It is important to note if LTP of NMDARs at DA neurons contributes to *in vivo* reward learning as we have described, it should be accompanied by mechanisms to dampen the effect of the prolonged duration of the cue input. The increases in DA

neuron firing in response to cues after learning are phasic (only a few hundred milliseconds), while we hypothesize that the glutamatergic signals relaying cue information to the DA neuron from PFC, SC, PPTN, and elsewhere are persistent. Therefore, this prolonged input must be actively shaped into the phasic response after learning. Possible termination mechanisms could consist of SK channel activation in DA neurons themselves, possibly via mGluR-mediated Ca^{2+} waves (Fiorillo and Williams, 1998; Morikawa et al., 2003), recruitment of appropriately timed GABAergic input via either striatal feedback (Brown et al., 1999; Houk et al., 1995) or local interneurons (Hikosaka et al., 2008; Hong and Hikosaka, 2008; Matsumoto and Hikosaka, 2007, 2009), or could perhaps involve distal changes in the input structures to DA neurons, converting their persistent glutamatergic output into a more transient form in response to learning.

A further caveat regarding NMDAR LTP at DA neurons is that we are not suggesting that this process mediates reward learning in its entirety. Downstream target structures including the striatum and prefrontal cortex are certainly involved in encoding and storing the associations formed during reward learning (Brown et al., 1999; Contreras-Vidal and Schultz, 1999; Costa, 2007; Day and Carelli, 2007; Everitt and Robbins, 2005; Kheirbek et al., 2008; Reynolds et al., 2001; Schultz, 1998, 2006; Surmeier et al., 2007), and afterward, during maintenance once associations become habitual (Everitt and Robbins, 2005; See et al., 2007; Vanderschuren et al., 2005; Wickens et al., 2007; Yin et al., 2009). Therefore, we suggest that this local process of plasticity at DA neurons contributes to developing these associations, particularly during the early stages, facilitating the transfer of burst firing from primary rewards to reward-predicting stimuli.

4.4.2 TIME SCALES OF NMDAR PLASTICITY AND BEHAVIORAL LEARNING

A particularly interesting feature of the plasticity observed in the present study is the burst timing-dependence of the induction, which appears quite similar to the timing

rule governing cue-reward learning in behaving animals (Pan et al., 2005). In one of the standard and most effective training paradigms, "delay conditioning," hundreds of milliseconds to several seconds seperates the onset of the cue from that of the reward, with the two stimuli overlapping in time (Fiorillo et al., 2003; Schwartz et al., 2002). For NMDAR LTP in DA neurons, the requirement of the delay (~0.5-1 s) and the overlap between synaptic stimulation and burst firing during induction reflects first, the activation of PI-coupled receptors and gradual accumulation of cytosolic IP_3, and second, NMDAR activity. Furthermore, induction of LTD when the burst precedes synaptic stimulation during the burst pairing protocol is congruent with the ineffectiveness of backward conditioning in which the reward is presented prior to the cue (Schwartz et al., 2002). As mentioned above, the timing rule described here is distinct from that for the spike timing-dependent plasticity reported in a variety of neurons (Dan and Poo, 2004; Sjostrom and Nelson, 2002), including DA neurons (Liu et al., 2005; Luu and Malenka, 2008), in which the plasticity is sensitive to the timing of presynaptic and postsynaptic spikes on a timescale of tens of milliseconds, which is both much shorter than the timescales encountered during behavioral conditioning (Drew and Abbott, 2006) and far beyond the temporal precision of DA neuron firing, even *in vitro*.

4.4.3 REVERSIBILITY OF NMDAR LTP AND EXTINCTION

The neural processes that underlie behavioral learning are thought to involve both reversible and irreversible components (Medina et al., 2002; Pan et al., 2008). Indeed, an unresolved issue in the field is how much of behavioral extinction is mediated by unlearning vs. new learning (Mauk and Ohyama, 2004; Quirk and Mueller, 2008). In the case of synaptic plasticity at DA neurons, our results show that NMDAR LTP can be reversed, or depotentiated, by repeated delivery of synaptic stimulation alone (Figure 3.14), which is reminiscent of the extinction of learned responses when the conditioning cue is repeatedly presented without the expected reward (Schultz, 1998; Tobler et al., 2003; Waelti et al., 2001). What is remarkable about this form of depotentiation is that it is completely conditional upon the presence of a single postsynaptic spike during the

presynaptic stimulation train, suggesting that single AP-evoked Ca^{2+} transients, facilitated by IP_3-dependent CICR, can serve to prevent depotentiation (presumably, this spike must be appropriately timed, as is the case for burst firing during induction (Figure 3.11), though we have not addressed this in the current study). Therefore, a pause in tonic single-spike activity of DA neurons, as observed at the time of the expected reward when the learned cue is presented alone, may be necessary for extinction of phasic burst responses to the cue (Pan et al., 2008; Tobler et al., 2003).

Computationally, the reversibility of plastic changes in synaptic strength has certain advantages over encoding changes in contingency by new learning, not least of which is efficiency given limited bandwidth and/or storage capacity in the respective circuitry. Indeed, a recent study combining *in vivo* DA neuron recording during reward learning coupled with modeling has suggested that extinction of reward associations is mediated by three distinct, but interacting, processes: passive forgetting, new inhibitory learning, and active unlearning (Pan et al., 2008). This last active unlearning process is congruent with what we have observed for NMDAR LTP at DA neurons (Figure 3.14).

Global AMPAR LTP at DA neurons induced by *in vivo* cocaine exposure can also be reversed relatively easily (Bellone and Luscher, 2006), suggesting that reversibility may be a common feature of DA neuron synaptic plasticity as a flexible mechanism for handling a variety of changing reward contingencies in the face of limited computational capacity (at least compared to pyramidal neurons (Frick and Johnston, 2005; Losonczy et al., 2008; Poirazi et al., 2003; Polsky et al., 2004; Wu and Mel, 2009)). In addition, there is a recent report that LTD of NMDAR EPSCs in hippocampal CA1 neurons can also be reversed ("dedepression") (Morishita and Malenka, 2008), furthering the hypothesis that NMDAR-mediated transmission can be highly dynamic under the appropriate circumstances.

4.5 Future Directions

4.5.1 FUTHER MECHANISTIC CHARACTERIZATION

There are numerous mechanistic questions raised by the present study. Addressing them may be important not only in terms of novel cellular plasticity but also for insight which could be translated into therapeutic approaches to treat disorders that involve aberrant reward learning and/or valuation (see *in vivo* discussion below). One of the most striking features of the plasticity reported here is the spike-conditional reversal of LTP by stimuli mimicking *in vivo* extinction protocols. We show that depotentiation does not occur unless LTP has previously occurred, but it is unclear if this is a function of induction (is there an mGluR activation threshold for depotentiation as well as potentiation?) vs. expression (can only those NMDARs that have been potentiated be depotentiated?). What features of the single postsynaptic spike paired with the presynaptic stimulation train prevent depotentiation? Does that spike need to be facilitated by PI-coupled receptor activation? Does it require intact Ca^{2+} stores? Is there a timing window during which the spike must occur? Additionally, are certain channels, kinases, or other intracellular signaling molecules preferentially involved in depotentiation vs. potentiation, as has been described for anther form of NMDAR plasticity (Morishita and Malenka, 2008)? These are all exciting questions which can be addressed in a relatively straightforward manner.

Another important issue left unresolved by our study concerns the mechanisms of expression of LTP, as discussed above (in section 4.1.2). Addressing this, along with the other mechanistic subjects mentioned throughout the discussion, in particular how induction is accomplished (section 4.1.1), may yield functional insights into how depotentiation works, as well as help to develop tools to influence reward learning *in vivo* (see below).

It would also be particularly interesting to investigate the process by which *in vivo* amphetamine experience increases spike-evoked Ca^{2+} signaling and plasticity. We presume that this occurs through an upregulation in the cAMP/AC/PKA axis, given its well-established increase after drug administration and reports that PKA increases IP_3R function through phosphorylation (Hope et al., 2007; Nestler and Aghajanian, 1997;

Peterson et al., 2006; Tang et al., 2003; Tolliver et al., 1999; Wagner et al., 2008; Wagner et al., 2004; White et al., 1995; Wojcikiewicz and Luo, 1998) as well as our results presented in Figure 3.8. However, we have not yet performed the experiments to conclude this. Further exploration and characterization of this process is necessary and may yield clues into the cellular processes that underlie how addiction hijacks learning and motivational circuitry (Berke and Hyman, 2000; Everitt and Robbins, 2005; Hyman, 2005; Hyman et al., 2006a; Jones and Bonci, 2005; Kalivas and Volkow, 2005; Nestler and Aghajanian, 1997; Redish, 2004).

4.5.2 DOES DA NEURON NMDAR LTP OCCUR *IN VIVO*?

The most important question to be addressed in the wake of the present study is whether this form of plasticity participates in reward learning *in vivo* in behaving animals. This presents a particularly challenging scenario, as even performing conventional single-unit extracellular recordings of DA neural activity during reward learning has only been reported by a limited number of researchers in rodents (Pan et al., 2005; Roesch et al., 2007). However, new approaches and technical advancements are allowing this experiment to be implemented more broadly (Guohong Cui, personal communication). Perhaps even more daunting is the fact that NMDAR LTP is synapse specific and would thus be very challenging if not impossible to observe *ex vivo*, as has been done for global AMPA plasticity at DA neurons. In addition, local NMDA EPSPs would be very hard to observe with field potential recording, particularly on the background of significant spontaneous activity from postsynaptic pacemaking and presynaptic bombardment. Thus, postsynaptic voltage-control and the ability to monitor subthreshold conductances necessitates either sharp microelectrode or whole-cell *in vivo* patch clamp approaches. There are currently no reports of *in vivo* patching of DA neurons, even in anesthetized animals (though it is apparently possible; Robert C. Froemke, personal communication), though there are previous reports of *in vivo* sharp microelectrode recordings from DA neurons in anesthetized animals (Grace and Bunney, 1980; Tepper et al., 1987). Due to these significant difficulties, an alternative plan of

attack may have to be devised, perhaps through somehow tagging activated synapses *in vivo* during learning for subsequent *ex vivo* examination. A stepwise, indirect approach may also yield results; first, develop a method to selectively block NMDAR LTP through local pharmacological or genetic intervention, possibly by altering IP_3R receptor phosphorylation, demonstrating its necessity for reward learning. Then, reconstitute plasticity by artificially potentiating NMDARs in response to a non-reward. These conceptual experiments all have significant challenges associated with them; as mentioned above, demonstrating participation of cellular plasticity in behavior is a particularly difficult goal, but one with far-reaching and exciting consequences.

4.5.3 CAN WE EXPLOIT NMDAR LTP *IN VITRO* TO INTERVENE IN REWARD LEARNING *IN VIVO*?

If it can be convincingly shown that NMDAR LTP is engaged in reward learning *in vivo*, it would be particularly appealing to attempt to recruit the depotentiation process to reverse previously made associations that are "inappropriate," such as those associated with addictive behaviors like drug experience, gambling, and obsessive compulsive disorder. This may represent a novel, therapeutic approach for numerous disorders that resist conventional treatment (Redish, 2004). In addition, artificial manipulation of reward learning via NMDAR plasticity could facilitate investigations into the contribution(s) of changes in DA signals during learning to decision making and valuation (Doya, 2008; Niv, 2007; Schultz, 2006).

CHAPTER 5: CONCLUSION

This dissertation reports a novel form of activity-dependent synaptic plasticity of NMDARs at midbrain DA neurons that may represent a cellular substrate of reward-based reinforcement learning. Plasticity of DA neuron NMDARs displayed a range of features that were consistent with a neuronal model of reward learning, including associativity, input specificity, requirement of postsynaptic burst firing, behaviorally appropriate timing-dependence, reversibility, and modulation by *in vivo* amphetamine experience. This form of plasticity also exhibited mechanistic properties that had not previously been described, at DA neurons or elsewhere, including requirements for postsynaptic bursting, facilitation of spike-evoked Ca^{2+} signals by PI-coupled receptor stimulation, IP_3R activation and release of Ca^{2+} from intacellular stores, and independence from local DA. In addition, the induction protocol used to drive NMDAR LTP resulted in LTD of AMPA-mediated transmission. When considered in light of the metaplastic influence of NMDAR plasticity on AMPAR and $GABA_AR$ plasticity, this result suggests that a highly complex interplay between the various forms of plasticity previously reported and the NMDAR plasticity reported in the present study sculpts synaptic efficacy at DA neurons to control DA release in target structures and mediate reward learning.

Changes in DA neuron firing rate encode reward contingency and drive learning. We have discovered a novel, local mechanism for specific control over the output of DA neurons that exhibits cellular learning rules congruent with behavioral reward learning. This mechanism is significantly altered by *in vivo* amphetamine experience in a manner consistent with the overlearning and enhanced motivational significance of cues associated with drug intake displayed by human addicts. We therefore conclude that synaptic plasticity of NMDAR-mediated transmission at DA neurons represents an important locus for the neural processes that optimally guide behavior and become corrupted in disease states.

REFERENCES

Abraham, W.C. (2008). Metaplasticity: tuning synapses and networks for plasticity. Nat Rev Neurosci *9*, 387.

Abraham, W.C., and Bear, M.F. (1996). Metaplasticity: the plasticity of synaptic plasticity. Trends Neurosci *19*, 126-130.

Adcock, R.A., Thangavel, A., Whitfield-Gabrieli, S., Knutson, B., and Gabrieli, J.D. (2006). Reward-motivated learning: mesolimbic activation precedes memory formation. Neuron *50*, 507-517.

Arenkiel, B.R., Peca, J., Davison, I.G., Feliciano, C., Deisseroth, K., Augustine, G.J., Ehlers, M.D., and Feng, G. (2007). In vivo light-induced activation of neural circuitry in transgenic mice expressing channelrhodopsin-2. Neuron *54*, 205-218.

Argilli, E., Sibley, D.R., Malenka, R.C., England, P.M., and Bonci, A. (2008). Mechanism and time course of cocaine-induced long-term potentiation in the ventral tegmental area. J Neurosci *28*, 9092-9100.

Bagnall, M.W., and du Lac, S. (2006). A new locus for synaptic plasticity in cerebellar circuits. Neuron *51*, 5-7.

Bao, S., Chan, V.T., and Merzenich, M.M. (2001). Cortical remodelling induced by activity of ventral tegmental dopamine neurons. Nature *412*, 79-83.

Bashir, Z.I., Alford, S., Davies, S.N., Randall, A.D., and Collingridge, G.L. (1991). Long-term potentiation of NMDA receptor-mediated synaptic transmission in the hippocampus. Nature *349*, 156-158.

Bellone, C., and Luscher, C. (2006). Cocaine triggered AMPA receptor redistribution is reversed in vivo by mGluR-dependent long-term depression. Nat Neurosci *9*, 636-641.

Bellone, C., Luscher, C., and Mameli, M. (2008). Mechanisms of synaptic depression triggered by metabotropic glutamate receptors. Cell Mol Life Sci *65*, 2913-2923.

Bellone, C., and Nicoll, R.A. (2007). Rapid bidirectional switching of synaptic NMDA receptors. Neuron *55*, 779-785.

Benes, F.M. (2001). Carlsson and the discovery of dopamine. Trends Pharmacol Sci *22*, 46-47.

Berger, B., Gaspar, P., and Verney, C. (1991). Dopaminergic innervation of the cerebral cortex: unexpected differences between rodents and primates. Trends Neurosci *14*, 21-27.

Berke, J.D., and Hyman, S.E. (2000). Addiction, dopamine, and the molecular mechanisms of memory. Neuron *25*, 515-532.

Berridge, K.C. (2006). The debate over dopamine's role in reward: the case for incentive salience. Psychopharmacology (Berl).

Berridge, K.C., Venier, I.L., and Robinson, T.E. (1989). Taste reactivity analysis of 6-hydroxydopamine-induced aphagia: implications for arousal and anhedonia hypotheses of dopamine function. Behav Neurosci *103*, 36-45.

Bissiere, S., Humeau, Y., and Luthi, A. (2003). Dopamine gates LTP induction in lateral amygdala by suppressing feedforward inhibition. Nat Neurosci *6*, 587-592.

Bonci, A., and Malenka, R.C. (1999). Properties and plasticity of excitatory synapses on dopaminergic and GABAergic cells in the ventral tegmental area. J Neurosci *19*, 3723-3730.

Borgland, S.L., Taha, S.A., Sarti, F., Fields, H.L., and Bonci, A. (2006). Orexin A in the VTA is critical for the induction of synaptic plasticity and behavioral sensitization to cocaine. Neuron *49*, 589-601.

Borst, A., and Theunissen, F.E. (1999). Information theory and neural coding. Nat Neurosci *2*, 947-957.

Boyden, E.S., Zhang, F., Bamberg, E., Nagel, G., and Deisseroth, K. (2005). Millisecond-timescale, genetically targeted optical control of neural activity. Nat Neurosci *8*, 1263-1268.

Brazhnik, E., Shah, F., and Tepper, J.M. (2008). GABAergic afferents activate both GABAA and GABAB receptors in mouse substantia nigra dopaminergic neurons in vivo. J Neurosci *28*, 10386-10398.

Brown, H., and Difrancesco, D. (1980). Voltage-clamp investigations of membrane currents underlying pace-maker activity in rabbit sino-atrial node. J Physiol *308*, 331-351.

Brown, J., Bullock, D., and Grossberg, S. (1999). How the basal ganglia use parallel excitatory and inhibitory learning pathways to selectively respond to unexpected rewarding cues. J Neurosci *19*, 10502-10511.

Campanac, E., and Debanne, D. (2007). Plasticity of neuronal excitability: Hebbian rules beyond the synapse. Arch Ital Biol *145*, 277-287.

Cannon, C.M., and Palmiter, R.D. (2003). Reward without dopamine. J Neurosci *23*, 10827-10831.

Carr, D.B., and Sesack, S.R. (2000). Projections from the rat prefrontal cortex to the ventral tegmental area: target specificity in the synaptic associations with mesoaccumbens and mesocortical neurons. J Neurosci *20*, 3864-3873.

Carroll, R.C., and Zukin, R.S. (2002). NMDA-receptor trafficking and targeting: implications for synaptic transmission and plasticity. Trends Neurosci *25*, 571-577.

Celada, P., Paladini, C.A., and Tepper, J.M. (1999). GABAergic control of rat substantia nigra dopaminergic neurons: role of globus pallidus and substantia nigra pars reticulata. Neuroscience *89*, 813-825.

Cheer, J.F., Aragona, B.J., Heien, M.L., Seipel, A.T., Carelli, R.M., and Wightman, R.M. (2007). Coordinated accumbal dopamine release and neural activity drive goal-directed behavior. Neuron *54*, 237-244.

Chen, B.S., and Roche, K.W. (2007). Regulation of NMDA receptors by phosphorylation. Neuropharmacology *53*, 362-368.

Chen, B.T., Bowers, M.S., Martin, M., Hopf, F.W., Guillory, A.M., Carelli, R.M., Chou, J.K., and Bonci, A. (2008). Cocaine but not natural reward self-administration nor passive cocaine infusion produces persistent LTP in the VTA. Neuron *59*, 288-297.

Chen, W.S., and Bear, M.F. (2007). Activity-dependent regulation of NR2B translation contributes to metaplasticity in mouse visual cortex. Neuropharmacology *52*, 200-214.

Chergui, K., Akaoka, H., Charlety, P.J., Saunier, C.F., Buda, M., and Chouvet, G. (1994). Subthalamic nucleus modulates burst firing of nigral dopamine neurones via NMDA receptors. Neuroreport *5*, 1185-1188.

Chergui, K., Charlety, P.J., Akaoka, H., Saunier, C.F., Brunet, J.L., Buda, M., Svensson, T.H., and Chouvet, G. (1993). Tonic activation of NMDA receptors causes spontaneous burst discharge of rat midbrain dopamine neurons in vivo. Eur J Neurosci *5*, 137-144.

Chevaleyre, V., and Castillo, P.E. (2004). Endocannabinoid-mediated metaplasticity in the hippocampus. Neuron *43*, 871-881.

Chevaleyre, V., Takahashi, K.A., and Castillo, P.E. (2006). Endocannabinoid-mediated synaptic plasticity in the CNS. Annu Rev Neurosci *29*, 37-76.

Christoffersen, C.L., and Meltzer, L.T. (1995). Evidence for N-methyl-D-aspartate and AMPA subtypes of the glutamate receptor on substantia nigra dopamine neurons: possible preferential role for N-methyl-D-aspartate receptors. Neuroscience *67*, 373-381.

Coesmans, M., Weber, J.T., De Zeeuw, C.I., and Hansel, C. (2004). Bidirectional parallel fiber plasticity in the cerebellum under climbing fiber control. Neuron *44*, 691-700.

Coizet, V., Comoli, E., Westby, G.W., and Redgrave, P. (2003). Phasic activation of substantia nigra and the ventral tegmental area by chemical stimulation of the superior colliculus: an electrophysiological investigation in the rat. Eur J Neurosci *17*, 28-40.

Comoli, E., Coizet, V., Boyes, J., Bolam, J.P., Canteras, N.S., Quirk, R.H., Overton, P.G., and Redgrave, P. (2003). A direct projection from superior colliculus to substantia nigra for detecting salient visual events. Nat Neurosci *6*, 974-980.

Constantinidis, C., and Wang, X.J. (2004). A neural circuit basis for spatial working memory. Neuroscientist *10*, 553-565.

Contreras-Vidal, J.L., and Schultz, W. (1999). A predictive reinforcement model of dopamine neurons for learning approach behavior. J Comput Neurosci *6*, 191-214.

Costa, R.M. (2007). Plastic corticostriatal circuits for action learning: what's dopamine got to do with it? Ann N Y Acad Sci *1104*, 172-191.

Cui, G., Bernier, B.E., Harnett, M.T., and Morikawa, H. (2007). Differential regulation of action potential- and metabotropic glutamate receptor-induced Ca2+ signals by inositol 1,4,5-trisphosphate in dopaminergic neurons. J Neurosci *27*, 4776-4785.

D'Ardenne, K., McClure, S.M., Nystrom, L.E., and Cohen, J.D. (2008). BOLD responses reflecting dopaminergic signals in the human ventral tegmental area. Science *319*, 1264-1267.

Dan, Y., and Poo, M.M. (2004). Spike timing-dependent plasticity of neural circuits. Neuron *44*, 23-30.

Daoudal, G., and Debanne, D. (2003). Long-term plasticity of intrinsic excitability: learning rules and mechanisms. Learn Mem *10*, 456-465.

Dayan, P., and Niv, Y. (2008). Reinforcement learning: the good, the bad and the ugly. Curr Opin Neurobiol *18*, 185-196.

Debanne, D., Daoudal, G., Sourdet, V., and Russier, M. (2003). Brain plasticity and ion channels. J Physiol Paris *97*, 403-414.

Denys, D., Zohar, J., and Westenberg, H.G. (2004). The role of dopamine in obsessive-compulsive disorder: preclinical and clinical evidence. J Clin Psychiatry *65 Suppl 14*, 11-17.

Dommett, E., Coizet, V., Blaha, C.D., Martindale, J., Lefebvre, V., Walton, N., Mayhew, J.E., Overton, P.G., and Redgrave, P. (2005). How visual stimuli activate dopaminergic neurons at short latency. Science *307*, 1476-1479.

Doya, K. (2008). Modulators of decision making. Nat Neurosci *11*, 410-416.

Dragoi, G., and Buzsaki, G. (2006). Temporal encoding of place sequences by hippocampal cell assemblies. Neuron *50*, 145-157.

Drew, P.J., and Abbott, L.F. (2006). Extending the effects of spike-timing-dependent plasticity to behavioral timescales. Proc Natl Acad Sci U S A *103*, 8876-8881.

Dumont, E.C., and Williams, J.T. (2004). Noradrenaline triggers GABAA inhibition of bed nucleus of the stria terminalis neurons projecting to the ventral tegmental area. J Neurosci *24*, 8198-8204.

Durstewitz, D., Seamans, J.K., and Sejnowski, T.J. (2000). Neurocomputational models of working memory. Nat Neurosci *3 Suppl*, 1184-1191.

Edwards, D.A., Zhang, L., and Alger, B.E. (2008). Metaplastic control of the endocannabinoid system at inhibitory synapses in hippocampus. Proc Natl Acad Sci U S A *105*, 8142-8147.

Egorov, A.V., Hamam, B.N., Fransen, E., Hasselmo, M.E., and Alonso, A.A. (2002). Graded persistent activity in entorhinal cortex neurons. Nature *420*, 173-178.

Engblom, D., Bilbao, A., Sanchis-Segura, C., Dahan, L., Perreau-Lenz, S., Balland, B., Parkitna, J.R., Lujan, R., Halbout, B., Mameli, M.*, et al.* (2008). Glutamate receptors on dopamine neurons control the persistence of cocaine seeking. Neuron *59*, 497-508.

Erhardt, S., Mathe, J.M., Chergui, K., Engberg, G., and Svensson, T.H. (2002). GABA(B) receptor-mediated modulation of the firing pattern of ventral tegmental area dopamine neurons in vivo. Naunyn Schmiedebergs Arch Pharmacol *365*, 173-180.

Everitt, B.J., Cardinal, R.N., Parkinson, J.A., and Robbins, T.W. (2003). Appetitive behavior: impact of amygdala-dependent mechanisms of emotional learning. Ann N Y Acad Sci *985*, 233-250.

Fellous, J.M., Tiesinga, P.H., Thomas, P.J., and Sejnowski, T.J. (2004). Discovering spike patterns in neuronal responses. J Neurosci *24*, 2989-3001.

Fernandez de Sevilla, D., Nunez, A., Borde, M., Malinow, R., and Buno, W. (2008). Cholinergic-mediated IP3-receptor activation induces long-lasting synaptic enhancement in CA1 pyramidal neurons. J Neurosci *28*, 1469-1478.

Floresco, S.B., and Magyar, O. (2006). Mesocortical dopamine modulation of executive functions: beyond working memory. Psychopharmacology (Berl) *188*, 567-585.

Floresco, S.B., Tse, M.T., and Ghods-Sharifi, S. (2008). Dopaminergic and glutamatergic regulation of effort- and delay-based decision making. Neuropsychopharmacology *33*, 1966-1979.

Floresco, S.B., West, A.R., Ash, B., Moore, H., and Grace, A.A. (2003). Afferent modulation of dopamine neuron firing differentially regulates tonic and phasic dopamine transmission. Nat Neurosci *6*, 968-973.

Ford, C.P., Mark, G.P., and Williams, J.T. (2006). Properties and opioid inhibition of mesolimbic dopamine neurons vary according to target location. J Neurosci *26*, 2788-2797.

Fransen, E., Tahvildari, B., Egorov, A.V., Hasselmo, M.E., and Alonso, A.A. (2006). Mechanism of graded persistent cellular activity of entorhinal cortex layer v neurons. Neuron *49*, 735-746.

Froemke, R.C., and Dan, Y. (2002). Spike-timing-dependent synaptic modification induced by natural spike trains. Nature *416*, 433-438.

Gasbarri, A., Sulli, A., Innocenzi, R., Pacitti, C., and Brioni, J.D. (1996). Spatial memory impairment induced by lesion of the mesohippocampal dopaminergic system in the rat. Neuroscience *74*, 1037-1044.

Gentet, L.J., and Williams, S.R. (2007). Dopamine gates action potential backpropagation in midbrain dopaminergic neurons. J Neurosci *27*, 1892-1901.

Georges, F., and Aston-Jones, G. (2001). Potent regulation of midbrain dopamine neurons by the bed nucleus of the stria terminalis. J Neurosci *21*, RC160.

Georges, F., and Aston-Jones, G. (2002). Activation of ventral tegmental area cells by the bed nucleus of the stria terminalis: a novel excitatory amino acid input to midbrain dopamine neurons. J Neurosci *22*, 5173-5187.

Goldman-Rakic, P.S. (1995). Cellular basis of working memory. Neuron *14*, 477-485.

Gonzalez-Islas, C., and Hablitz, J.J. (2003). Dopamine enhances EPSCs in layer II-III pyramidal neurons in rat prefrontal cortex. J Neurosci *23*, 867-875.

Grace, A.A., and Bunney, B.S. (1979). Paradoxical GABA excitation of nigral dopaminergic cells: indirect mediation through reticulata inhibitory neurons. Eur J Pharmacol *59*, 211-218.

Grace, A.A., and Bunney, B.S. (1984). The control of firing pattern in nigral dopamine neurons: burst firing. J Neurosci *4*, 2877-2890.

Grace, A.A., Floresco, S.B., Goto, Y., and Lodge, D.J. (2007). Regulation of firing of dopaminergic neurons and control of goal-directed behaviors. Trends Neurosci *30*, 220-227.

Gurden, H., Tassin, J.P., and Jay, T.M. (1999). Integrity of the mesocortical dopaminergic system is necessary for complete expression of in vivo hippocampal-prefrontal cortex long-term potentiation. Neuroscience *94*, 1019-1027.

Hammer, M. (1997). The neural basis of associative reward learning in honeybees. Trends Neurosci *20*, 245-252.

Hammer, M., and Menzel, R. (1995). Learning and memory in the honeybee. J Neurosci *15*, 1617-1630.

Harney, S.C., Jane, D.E., and Anwyl, R. (2008). Extrasynaptic NR2D-containing NMDARs are recruited to the synapse during LTP of NMDAR-EPSCs. J Neurosci *28*, 11685-11694.

Harney, S.C., Rowan, M., and Anwyl, R. (2006). Long-term depression of NMDA receptor-mediated synaptic transmission is dependent on activation of metabotropic glutamate receptors and is altered to long-term potentiation by low intracellular calcium buffering. J Neurosci *26*, 1128-1132.

Harris, K.D., Csicsvari, J., Hirase, H., Dragoi, G., and Buzsaki, G. (2003). Organization of cell assemblies in the hippocampus. Nature *424*, 552-556.

Hassani, O.K., Cromwell, H.C., and Schultz, W. (2001). Influence of expectation of different rewards on behavior-related neuronal activity in the striatum. J Neurophysiol *85*, 2477-2489.

Hausser, M., Stuart, G., Racca, C., and Sakmann, B. (1995). Axonal initiation and active dendritic propagation of action potentials in substantia nigra neurons. Neuron *15*, 637-647.

Hersi, A.I., Rowe, W., Gaudreau, P., and Quirion, R. (1995). Dopamine D1 receptor ligands modulate cognitive performance and hippocampal acetylcholine release in memory-impaired aged rats. Neuroscience *69*, 1067-1074.

Hikosaka, O., Sesack, S.R., Lecourtier, L., and Shepard, P.D. (2008). Habenula: crossroad between the basal ganglia and the limbic system. J Neurosci *28*, 11825-11829.

Hong, S., and Hikosaka, O. (2008). The globus pallidus sends reward-related signals to the lateral habenula. Neuron *60*, 720-729.

Horvitz, J.C., Stewart, T., and Jacobs, B.L. (1997). Burst activity of ventral tegmental dopamine neurons is elicited by sensory stimuli in the awake cat. Brain Res *759*, 251-258.

Houk, J., Adams, J., and Barto, A. (1995). A model of how the basal ganglia generate and use neural signals that predict reinforcement. In Models of information processing in the basal ganglia, J. Houk, J. Davis, and D. Beiser, eds. (Cambridge, MA: MIT Press), pp. 249-270.

Houweling, A.R., and Brecht, M. (2008). Behavioural report of single neuron stimulation in somatosensory cortex. Nature *451*, 65-68.

Huang, Y.Y., Simpson, E., Kellendonk, C., and Kandel, E.R. (2004). Genetic evidence for the bidirectional modulation of synaptic plasticity in the prefrontal cortex by D1 receptors. Proc Natl Acad Sci U S A *101*, 3236-3241.

Huber, D., Petreanu, L., Ghitani, N., Ranade, S., Hromadka, T., Mainen, Z., and Svoboda, K. (2008). Sparse optical microstimulation in barrel cortex drives learned behaviour in freely moving mice. Nature *451*, 61-64.

Hyman, S.E. (2005). Addiction: a disease of learning and memory. Am J Psychiatry *162*, 1414-1422.

Hyman, S.E., Malenka, R.C., and Nestler, E.J. (2006). Neural mechanisms of addiction: the role of reward-related learning and memory. Annu Rev Neurosci *29*, 565-598.

Iribe, Y., Moore, K., Pang, K.C., and Tepper, J.M. (1999). Subthalamic stimulation-induced synaptic responses in substantia nigra pars compacta dopaminergic neurons in vitro. J Neurophysiol *82*, 925-933.

Ito, R., Dalley, J.W., Robbins, T.W., and Everitt, B.J. (2002). Dopamine release in the dorsal striatum during cocaine-seeking behavior under the control of a drug-associated cue. J Neurosci *22*, 6247-6253.

Johnston, D., and Narayanan, R. (2008). Active dendrites: colorful wings of the mysterious butterflies. Trends Neurosci *31*, 309-316.

Jones, S., and Bonci, A. (2005). Synaptic plasticity and drug addiction. Curr Opin Pharmacol *5*, 20-25.

Jones, S., Kornblum, J.L., and Kauer, J.A. (2000). Amphetamine blocks long-term synaptic depression in the ventral tegmental area. J Neurosci *20*, 5575-5580.

Jung, S.C., Kim, J., and Hoffman, D.A. (2008). Rapid, bidirectional remodeling of synaptic NMDA receptor subunit composition by A-type K+ channel activity in hippocampal CA1 pyramidal neurons. Neuron *60*, 657-671.

Kauer, J.A. (2004). Learning mechanisms in addiction: synaptic plasticity in the ventral tegmental area as a result of exposure to drugs of abuse. Annu Rev Physiol *66*, 447-475.

Kauer, J.A., and Malenka, R.C. (2007). Synaptic plasticity and addiction. Nat Rev Neurosci *8*, 844-858.

Kitai, S.T., Shepard, P.D., Callaway, J.C., and Scroggs, R. (1999). Afferent modulation of dopamine neuron firing patterns. Curr Opin Neurobiol *9*, 690-697.

Kroner, S., Rosenkranz, J.A., Grace, A.A., and Barrionuevo, G. (2005). Dopamine modulates excitability of basolateral amygdala neurons in vitro. J Neurophysiol *93*, 1598-1610.

Kwon, H.B., and Castillo, P.E. (2008). Long-term potentiation selectively expressed by NMDA receptors at hippocampal mossy fiber synapses. Neuron *57*, 108-120.

Lapish, C.C., Kroener, S., Durstewitz, D., Lavin, A., and Seamans, J.K. (2007). The ability of the mesocortical dopamine system to operate in distinct temporal modes. Psychopharmacology (Berl) *191*, 609-625.

Legault, M., and Wise, R.A. (2001). Novelty-evoked elevations of nucleus accumbens dopamine: dependence on impulse flow from the ventral subiculum and glutamatergic neurotransmission in the ventral tegmental area. Eur J Neurosci *13*, 819-828.

Li, S., Cullen, W.K., Anwyl, R., and Rowan, M.J. (2003). Dopamine-dependent facilitation of LTP induction in hippocampal CA1 by exposure to spatial novelty. Nat Neurosci *6*, 526-531.

Lisman, J.E., and Grace, A.A. (2005). The hippocampal-VTA loop: controlling the entry of information into long-term memory. Neuron *46*, 703-713.

Liu, Q.S., Pu, L., and Poo, M.M. (2005). Repeated cocaine exposure in vivo facilitates LTP induction in midbrain dopamine neurons. Nature *437*, 1027-1031.

Ljungberg, T., Apicella, P., and Schultz, W. (1992). Responses of monkey dopamine neurons during learning of behavioral reactions. J Neurophysiol *67*, 145-163.

Lorenzetti, F.D., Baxter, D.A., and Byrne, J.H. (2008). Molecular mechanisms underlying a cellular analog of operant reward learning. Neuron *59*, 815-828.

Mameli, M., Balland, B., Lujan, R., and Luscher, C. (2007). Rapid synthesis and synaptic insertion of GluR2 for mGluR-LTD in the ventral tegmental area. Science *317*, 530-533.

Mao, L.M., Wang, W., Chu, X.P., Zhang, G.C., Liu, X.Y., Yang, Y.J., Haines, M., Papasian, C.J., Fibuch, E.E., Buch, S.*, et al.* (2009). Stability of surface NMDA receptors controls synaptic and behavioral adaptations to amphetamine. Nat Neurosci.

Matsumoto, M., and Hikosaka, O. (2007). Lateral habenula as a source of negative reward signals in dopamine neurons. Nature.

Matsumoto, M., and Hikosaka, O. (2009). Representation of negative motivational value in the primate lateral habenula. Nat Neurosci *12*, 77-84.

McHaffie, J.G., Jiang, H., May, P.J., Coizet, V., Overton, P.G., Stein, B.E., and Redgrave, P. (2006). A direct projection from superior colliculus to substantia nigra pars compacta in the cat. Neuroscience *138*, 221-234.

Melis, M., Camarini, R., Ungless, M.A., and Bonci, A. (2002). Long-lasting potentiation of GABAergic synapses in dopamine neurons after a single in vivo ethanol exposure. J Neurosci *22*, 2074-2082.

Mirenowicz, J., and Schultz, W. (1996). Preferential activation of midbrain dopamine neurons by appetitive rather than aversive stimuli. Nature *379*, 449-451.

Montague, P.R. (2007). Neuroeconomics: a view from neuroscience. Funct Neurol *22*, 219-234.

Montague, P.R., and Berns, G.S. (2002). Neural economics and the biological substrates of valuation. Neuron *36*, 265-284.

Montague, P.R., Dayan, P., and Sejnowski, T.J. (1996). A framework for mesencephalic dopamine systems based on predictive Hebbian learning. J Neurosci *16*, 1936-1947.

Montague, P.R., Hyman, S.E., and Cohen, J.D. (2004). Computational roles for dopamine in behavioural control. Nature *431*, 760-767.

Montague, P.R., King-Casas, B., and Cohen, J.D. (2006). Imaging valuation models in human choice. Annu Rev Neurosci *29*, 417-448.

Montgomery, J.M., and Madison, D.V. (2002). State-dependent heterogeneity in synaptic depression between pyramidal cell pairs. Neuron *33*, 765-777.

Montgomery, J.M., Pavlidis, P., and Madison, D.V. (2001). Pair recordings reveal all-silent synaptic connections and the postsynaptic expression of long-term potentiation. Neuron *29*, 691-701.

Montgomery, J.M., Selcher, J.C., Hanson, J.E., and Madison, D.V. (2005). Dynamin-dependent NMDAR endocytosis during LTD and its dependence on synaptic state. BMC Neurosci *6*, 48.

Morishita, W., Marie, H., and Malenka, R.C. (2005). Distinct triggering and expression mechanisms underlie LTD of AMPA and NMDA synaptic responses. Nat Neurosci *8*, 1043-1050.

Morris, G., Arkadir, D., Nevet, A., Vaadia, E., and Bergman, H. (2004). Coincident but distinct messages of midbrain dopamine and striatal tonically active neurons. Neuron *43*, 133-143.

Nakahara, H., Itoh, H., Kawagoe, R., Takikawa, Y., and Hikosaka, O. (2004). Dopamine neurons can represent context-dependent prediction error. Neuron *41*, 269-280.

Nakamura, T., Barbara, J.G., Nakamura, K., and Ross, W.N. (1999). Synergistic release of Ca2+ from IP3-sensitive stores evoked by synaptic activation of mGluRs paired with backpropagating action potentials. Neuron *24*, 727-737.

Narayanan, R., and Johnston, D. (2007). Long-term potentiation in rat hippocampal neurons is accompanied by spatially widespread changes in intrinsic oscillatory dynamics and excitability. Neuron *56*, 1061-1075.

Narayanan, R., and Johnston, D. (2008). The ascent of channels with memory. Neuron *60*, 735-738.

Neher, E., and Sakaba, T. (2008). Multiple roles of calcium ions in the regulation of neurotransmitter release. Neuron *59*, 861-872.

Nelson, A.B., Gittis, A.H., and du Lac, S. (2005). Decreases in CaMKII activity trigger persistent potentiation of intrinsic excitability in spontaneously firing vestibular nucleus neurons. Neuron *46*, 623-631.

Nicola, S.M., Surmeier, J., and Malenka, R.C. (2000). Dopaminergic modulation of neuronal excitability in the striatum and nucleus accumbens. Annu Rev Neurosci *23*, 185-215.

Niv, Y. (2007). Cost, benefit, tonic, phasic: what do response rates tell us about dopamine and motivation? Ann N Y Acad Sci *1104*, 357-376.

Niv, Y., Daw, N.D., and Dayan, P. (2006). Choice values. Nat Neurosci *9*, 987-988.

Niv, Y., Daw, N.D., Joel, D., and Dayan, P. (2007). Tonic dopamine: opportunity costs and the control of response vigor. Psychopharmacology (Berl) *191*, 507-520.

Nowak, L., Bregestovski, P., Ascher, P., Herbet, A., and Prochiantz, A. (1984). Magnesium gates glutamate-activated channels in mouse central neurones. Nature *307*, 462-465.

Nugent, F.S., Penick, E.C., and Kauer, J.A. (2007). Opioids block long-term potentiation of inhibitory synapses. Nature *446*, 1086-1090.

O'Connor, J.J., Rowan, M.J., and Anwyl, R. (1994). Long-lasting enhancement of NMDA receptor-mediated synaptic transmission by metabotropic glutamate receptor activation. Nature *367*, 557-559.

Okamoto, T., Harnett, M.T., and Morikawa, H. (2006). Hyperpolarization-activated cation current (Ih) is an ethanol target in midbrain dopamine neurons of mice. J Neurophysiol *95*, 619-626.

Otani, S., Blond, O., Desce, J.M., and Crepel, F. (1998). Dopamine facilitates long-term depression of glutamatergic transmission in rat prefrontal cortex. Neuroscience *85*, 669-676.

Otani, S., Daniel, H., Roisin, M.P., and Crepel, F. (2003). Dopaminergic modulation of long-term synaptic plasticity in rat prefrontal neurons. Cereb Cortex *13*, 1251-1256.

Overton, P., and Clark, D. (1992). Iontophoretically administered drugs acting at the N-methyl-D-aspartate receptor modulate burst firing in A9 dopamine neurons in the rat. Synapse *10*, 131-140.

Overton, P.G., and Clark, D. (1997). Burst firing in midbrain dopaminergic neurons. Brain Res Brain Res Rev *25*, 312-334.

Pan, W.X., and Hyland, B.I. (2005). Pedunculopontine tegmental nucleus controls conditioned responses of midbrain dopamine neurons in behaving rats. J Neurosci *25*, 4725-4732.

Pan, W.X., Schmidt, R., Wickens, J.R., and Hyland, B.I. (2005). Dopamine cells respond to predicted events during classical conditioning: evidence for eligibility traces in the reward-learning network. J Neurosci *25*, 6235-6242.

Pan, W.X., Schmidt, R., Wickens, J.R., and Hyland, B.I. (2008). Tripartite mechanism of extinction suggested by dopamine neuron activity and temporal difference model. J Neurosci *28*, 9619-9631.

Pelkey, K.A., Topolnik, L., Yuan, X.Q., Lacaille, J.C., and McBain, C.J. (2008). State-dependent cAMP sensitivity of presynaptic function underlies metaplasticity in a hippocampal feedforward inhibitory circuit. Neuron *60*, 980-987.

Phillips, P.E., Stuber, G.D., Heien, M.L., Wightman, R.M., and Carelli, R.M. (2003). Subsecond dopamine release promotes cocaine seeking. Nature *422*, 614-618.

Philpot, B.D., Cho, K.K., and Bear, M.F. (2007). Obligatory role of NR2A for metaplasticity in visual cortex. Neuron *53*, 495-502.

Philpot, B.D., Espinosa, J.S., and Bear, M.F. (2003). Evidence for altered NMDA receptor function as a basis for metaplasticity in visual cortex. J Neurosci *23*, 5583-5588.

Philpot, B.D., Sekhar, A.K., Shouval, H.Z., and Bear, M.F. (2001). Visual experience and deprivation bidirectionally modify the composition and function of NMDA receptors in visual cortex. Neuron *29*, 157-169.

Prensa, L., and Parent, A. (2001). The nigrostriatal pathway in the rat: A single-axon study of the relationship between dorsal and ventral tier nigral neurons and the striosome/matrix striatal compartments. J Neurosci *21*, 7247-7260.

Pu, L., Liu, Q.S., and Poo, M.M. (2006). BDNF-dependent synaptic sensitization in midbrain dopamine neurons after cocaine withdrawal. Nat Neurosci *9*, 605-607.

Puopolo, M., Raviola, E., and Bean, B.P. (2007). Roles of subthreshold calcium current and sodium current in spontaneous firing of mouse midbrain dopamine neurons. J Neurosci *27*, 645-656.

Quinlan, E.M., Philpot, B.D., Huganir, R.L., and Bear, M.F. (1999). Rapid, experience-dependent expression of synaptic NMDA receptors in visual cortex in vivo. Nat Neurosci *2*, 352-357.

Rangel, A., Camerer, C., and Montague, P.R. (2008). A framework for studying the neurobiology of value-based decision making. Nat Rev Neurosci *9*, 545-556.

Raymond, C.R., and Redman, S.J. (2002). Different calcium sources are narrowly tuned to the induction of different forms of LTP. J Neurophysiol *88*, 249-255.

Raymond, C.R., and Redman, S.J. (2006). Spatial segregation of neuronal calcium signals encodes different forms of LTP in rat hippocampus. J Physiol *570*, 97-111.

Rebola, N., Lujan, R., Cunha, R.A., and Mulle, C. (2008). Adenosine A2A receptors are essential for long-term potentiation of NMDA-EPSCs at hippocampal mossy fiber synapses. Neuron *57*, 121-134.

Redgrave, P., Gurney, K., and Reynolds, J. (2008). What is reinforced by phasic dopamine signals? Brain Res Rev *58*, 322-339.

Redish, A.D. (2004). Addiction as a computational process gone awry. Science *306*, 1944-1947.

Reynolds, J.N., Hyland, B.I., and Wickens, J.R. (2001). A cellular mechanism of reward-related learning. Nature *413*, 67-70.

Reynolds, J.N., and Wickens, J.R. (2000). Substantia nigra dopamine regulates synaptic plasticity and membrane potential fluctuations in the rat neostriatum, in vivo. Neuroscience *99*, 199-203.

Reynolds, J.N., and Wickens, J.R. (2002). Dopamine-dependent plasticity of corticostriatal synapses. Neural Netw *15*, 507-521.

Robinson, R.B., and Siegelbaum, S.A. (2003). Hyperpolarization-activated cation currents: from molecules to physiological function. Annu Rev Physiol *65*, 453-480.

Roesch, M.R., Calu, D.J., and Schoenbaum, G. (2007). Dopamine neurons encode the better option in rats deciding between differently delayed or sized rewards. Nat Neurosci *10*, 1615-1624.

Roitman, M.F., Stuber, G.D., Phillips, P.E., Wightman, R.M., and Carelli, R.M. (2004). Dopamine operates as a subsecond modulator of food seeking. J Neurosci *24*, 1265-1271.

Rosenkranz, J.A., and Grace, A.A. (2002). Dopamine-mediated modulation of odour-evoked amygdala potentials during pavlovian conditioning. Nature *417*, 282-287.

Saal, D., Dong, Y., Bonci, A., and Malenka, R.C. (2003). Drugs of abuse and stress trigger a common synaptic adaptation in dopamine neurons. Neuron *37*, 577-582.

Sarkisov, D.V., and Wang, S.S. (2008). Order-dependent coincidence detection in cerebellar Purkinje neurons at the inositol trisphosphate receptor. J Neurosci *28*, 133-142.

Sawaguchi, T., and Goldman-Rakic, P.S. (1991). D1 dopamine receptors in prefrontal cortex: involvement in working memory. Science *251*, 947-950.

Schilstrom, B., Yaka, R., Argilli, E., Suvarna, N., Schumann, J., Chen, B.T., Carman, M., Singh, V., Mailliard, W.S., Ron, D., and Bonci, A. (2006). Cocaine enhances NMDA receptor-mediated currents in ventral tegmental area cells via dopamine D5 receptor-dependent redistribution of NMDA receptors. J Neurosci *26*, 8549-8558.

Schultz, W. (1998). Predictive reward signal of dopamine neurons. J Neurophysiol *80*, 1-27.

Schultz, W. (2006). Behavioral theories and the neurophysiology of reward. Annu Rev Psychol *57*, 87-115.

Schultz, W. (2007). Multiple dopamine functions at different time courses. Annu Rev Neurosci *30*, 259-288.

Schultz, W., Dayan, P., and Montague, P.R. (1997). A neural substrate of prediction and reward. Science *275*, 1593-1599.

Schwartz, B., Wasserman, E.A., and Robbins, S.J. (2002). Psychology of learning and behavior, 5th edn (New York, NY: W. W. Norton & Company).

Selig, D.K., Hjelmstad, G.O., Herron, C., Nicoll, R.A., and Malenka, R.C. (1995). Independent mechanisms for long-term depression of AMPA and NMDA responses. Neuron *15*, 417-426.

Shin, N., Soh, H., Chang, S., Kim, D.H., and Park, C.S. (2005). Sodium permeability of a cloned small-conductance calcium-activated potassium channel. Biophys J *89*, 3111-3119.

Smith, I.D., and Grace, A.A. (1992). Role of the subthalamic nucleus in the regulation of nigral dopamine neuron activity. Synapse *12*, 287-303.

Snyder, E.M., Philpot, B.D., Huber, K.M., Dong, X., Fallon, J.R., and Bear, M.F. (2001). Internalization of ionotropic glutamate receptors in response to mGluR activation. Nat Neurosci *4*, 1079-1085.

St Onge, J.R., and Floresco, S.B. (2009). Dopaminergic modulation of risk-based decision making. Neuropsychopharmacology *34*, 681-697.

Stuber, G.D., Klanker, M., de Ridder, B., Bowers, M.S., Joosten, R.N., Feenstra, M.G., and Bonci, A. (2008). Reward-predictive cues enhance excitatory synaptic strength onto midbrain dopamine neurons. Science *321*, 1690-1692.

Talwar, S.K., Xu, S., Hawley, E.S., Weiss, S.A., Moxon, K.A., and Chapin, J.K. (2002). Rat navigation guided by remote control. Nature *417*, 37-38.

Tepper, J.M., and Lee, C.R. (2007). GABAergic control of substantia nigra dopaminergic neurons. Prog Brain Res *160*, 189-208.

Tepper, J.M., Martin, L.P., and Anderson, D.R. (1995). GABAA receptor-mediated inhibition of rat substantia nigra dopaminergic neurons by pars reticulata projection neurons. J Neurosci *15*, 3092-3103.

Tepper, J.M., Paladini, C.A., and Celada, P. (1998). GABAergic control of the firing pattern of substantia nigra dopaminergic neurons. Adv Pharmacol *42*, 694-699.

Tepper, J.M., Sawyer, S.F., and Groves, P.M. (1987). Electrophysiologically identified nigral dopaminergic neurons intracellularly labeled with HRP: light-microscopic analysis. J Neurosci *7*, 2794-2806.

Thiagarajan, T.C., Lindskog, M., Malgaroli, A., and Tsien, R.W. (2007). LTP and adaptation to inactivity: overlapping mechanisms and implications for metaplasticity. Neuropharmacology *52*, 156-175.

Thiagarajan, T.C., Lindskog, M., and Tsien, R.W. (2005). Adaptation to synaptic inactivity in hippocampal neurons. Neuron *47*, 725-737.

Thomas, M.J., Beurrier, C., Bonci, A., and Malenka, R.C. (2001). Long-term depression in the nucleus accumbens: a neural correlate of behavioral sensitization to cocaine. Nat Neurosci *4*, 1217-1223.

Thomas, M.J., and Malenka, R.C. (2003). Synaptic plasticity in the mesolimbic dopamine system. Philos Trans R Soc Lond B Biol Sci *358*, 815-819.

Thomas, M.J., Malenka, R.C., and Bonci, A. (2000). Modulation of long-term depression by dopamine in the mesolimbic system. J Neurosci *20*, 5581-5586.

Tiesinga, P., Fellous, J.M., and Sejnowski, T.J. (2008). Regulation of spike timing in visual cortical circuits. Nat Rev Neurosci *9*, 97-107.

Tong, Z.Y., Overton, P.G., and Clark, D. (1996a). Antagonism of NMDA receptors but not AMPA/kainate receptors blocks bursting in dopaminergic neurons induced by electrical stimulation of the prefrontal cortex. J Neural Transm *103*, 889-904.

Tong, Z.Y., Overton, P.G., and Clark, D. (1996b). Stimulation of the prefrontal cortex in the rat induces patterns of activity in midbrain dopaminergic neurons which resemble natural burst events. Synapse *22*, 195-208.

Tovar, K.R., and Westbrook, G.L. (2002). Mobile NMDA receptors at hippocampal synapses. Neuron *34*, 255-264.

Tsai, H.C., Zhang, F., Adamantidis, A., Stuber, G.D., Bonci, A., de Lecea, L., and Deisseroth, K. (2009). Phasic Firing in Dopaminergic Neurons Is Sufficient for Behavioral Conditioning. Science.

Ungless, M.A., Singh, V., Crowder, T.L., Yaka, R., Ron, D., and Bonci, A. (2003). Corticotropin-releasing factor requires CRF binding protein to potentiate NMDA receptors via CRF receptor 2 in dopamine neurons. Neuron *39*, 401-407.

Ungless, M.A., Whistler, J.L., Malenka, R.C., and Bonci, A. (2001). Single cocaine exposure in vivo induces long-term potentiation in dopamine neurons. Nature *411*, 583-587.

Vetter, P., Roth, A., and Hausser, M. (2001). Propagation of action potentials in dendrites depends on dendritic morphology. J Neurophysiol *85*, 926-937.

Vijayraghavan, S., Wang, M., Birnbaum, S.G., Williams, G.V., and Arnsten, A.F. (2007). Inverted-U dopamine D1 receptor actions on prefrontal neurons engaged in working memory. Nat Neurosci *10*, 376-384.

Voigt, B.C., Brecht, M., and Houweling, A.R. (2008). Behavioral detectability of single-cell stimulation in the ventral posterior medial nucleus of the thalamus. J Neurosci *28*, 12362-12367.

Wang, H., Hu, Y., and Tsien, J.Z. (2006). Molecular and systems mechanisms of memory consolidation and storage. Prog Neurobiol *79*, 123-135.

Wang, H.X., Gerkin, R.C., Nauen, D.W., and Bi, G.Q. (2005). Coactivation and timing-dependent integration of synaptic potentiation and depression. Nat Neurosci *8*, 187-193.

Wang, M., Vijayraghavan, S., and Goldman-Rakic, P.S. (2004). Selective D2 receptor actions on the functional circuitry of working memory. Science *303*, 853-856.

Wang, X.J. (1999). Synaptic basis of cortical persistent activity: the importance of NMDA receptors to working memory. J Neurosci *19*, 9587-9603.

Wickens, J.R., Horvitz, J.C., Costa, R.M., and Killcross, S. (2007). Dopaminergic mechanisms in actions and habits. J Neurosci *27*, 8181-8183.

Wierzynski, C.M., Lubenov, E.V., Gu, M., and Siapas, A.G. (2009). State-dependent spike-timing relationships between hippocampal and prefrontal circuits during sleep. Neuron *61*, 587-596.

Wittmann, B.C., Schott, B.H., Guderian, S., Frey, J.U., Heinze, H.J., and Duzel, E. (2005). Reward-related FMRI activation of dopaminergic midbrain is associated with enhanced hippocampus-dependent long-term memory formation. Neuron *45*, 459-467.

Zaghloul, K.A., Blanco, J.A., Weidemann, C.T., McGill, K., Jaggi, J.L., Baltuch, G.H., and Kahana, M.J. (2009). Human substantia nigra neurons encode unexpected financial rewards. Science *323*, 1496-1499.

Zhang, F., Wang, L.P., Boyden, E.S., and Deisseroth, K. (2006). Channelrhodopsin-2 and optical control of excitable cells. Nat Methods *3*, 785-792.

Zhang, F., Wang, L.P., Brauner, M., Liewald, J.F., Kay, K., Watzke, N., Wood, P.G., Bamberg, E., Nagel, G., Gottschalk, A., and Deisseroth, K. (2007). Multimodal fast optical interrogation of neural circuitry. Nature *446*, 633-639.

Zhou, Q., and Poo, M.M. (2004). Reversal and consolidation of activity-induced synaptic modifications. Trends Neurosci *27*, 378-383.

Zweifel, L.S., Argilli, E., Bonci, A., and Palmiter, R.D. (2008). Role of NMDA receptors in dopamine neurons for plasticity and addictive behaviors. Neuron *59*, 486-496.

Zweifel, L.S., Parker, J.G., Lobb, C.J., Rainwater, A., Wall, V.Z., Fadok, J.P., Darvas, M., Kim, M.J., Mizumori, S.J., Paladini, C.A.*, et al.* (2009). Feature Article: Disruption

of NMDAR-dependent burst firing by dopamine neurons provides selective assessment of phasic dopamine-dependent behavior. Proc Natl Acad Sci U S A.

Vita

Mark Thomas Harnett was born in Morristown, New Jersey in 1977, eldest son of John Thomas and Irene Anne Harnett. He attended Reed College in Portland, OR where he earned a Bachelor of the Arts in Biology and developed an interest in the neural substrates of the mind, furthered by the research for his senior thesis at the Vollum Institute at Oregon Health & Science University with Professor Laurence O. Trussell. After graduating in 2000, he pursued neuroscience research as a post-baccalaureate: first at the University of Minnesota, studying K^+ channel physiology with Professor Linda Boland, and then back at Oregon Health & Science University, investigating ion channel regulation of synaptic transmission with Professor Stephen M. Smith for two years. He matriculated to the University of Texas at Austin's Institute for Neuroscience Ph.D. program in August 2003 and joined the lab of Professor Hitoshi Morikawa in the summer of 2004. He received an Institute for Neuroscience Fellowship for his first year of graduate school, a National Science Foundation Graduate Research Fellowship from 2004-2007, an Outstanding Teaching Assistant Award in 2005, a University Continuing Fellowship in 2007, and a Bruce and Jones Endowed Fellowship for Addiction Biology in 2008. He is the first author of a paper in the journal *Neuron* on synaptic plasticity of NMDA receptors in midbrain dopamine neurons, and has co-authored 4 additional papers with the Morikawa lab during his Ph.D. He will join the laboratory of Jeffery Magee at the Howard Hughes Medical Institute's Janelia Farm Research Campus in Ashburn, VA in the Fall of 2009 as a Postdoctoral Associate.

Permanent address: 8006 Camden Drive, Austin TX 78757

This dissertation was typed by the author.